THE UNIVERSITY OF QUEENSLAND

AUSTRALIA

Site-directed mutagenesis of the membrane-proximal (MPER) α-helical E2 region of DENV E to characterise structural and viral fusion significance of individual residues

Melissa Christine Shanks

B.Sc.

A thesis submitted for the degree of Master of Philosophy at

The University of Queensland in 2014

School of Chemistry and Molecular Biosciences

Abstract

Dengue (DENV) virus is a positive-strand RNA flavivirus that affects 100-200 million people worldwide annually. It is currently the most important arbovirus with 2.5 billion people at risk of disease. The envelope protein (E) of DENV is comprised of three domains, I, II, and III. The stem-anchor region connected to DIII contains two helices (membrane proximal and membrane distal) separated by a CS (conserved sequence) and followed by two membrane-spanning domains. It is believed that the two helices comprising the stem constrain monomeric E to lie flat against the viral envelope in the mature virion. Upon a low pH-induced conformational change, E shifts vertically away from the viral envelope, exposing the class II fusion peptide in domain II allowing it to interact with the target host cell membrane. Within the membrane-proximal helix there are a series of highly conserved, hydrophobic aromatic residues at positions F422, F429, F440, Y444 and F448, which all lie on one side of the helix. We examined whether these residues play a role in structural changes of E and localisation within the cell by mutagenesis. Recombinant constructs of prM and E containing the mutants F422A/Y, F429A/Y, F440A/Y, Y444A/F and F448A/Y were generated and, following transfection were tested for expression, heterodimeric association with prM, and cytoplasmic and cell surface expression via immunofluorescence. All constructs expressed protein and retained antibody specificity. The F422A resulted in reduced expression seen with immunofluorescence while the other mutants did not. Ultimately, fusion assays should be performed on these constructs to determine whether or not these mutants are capable of mediating membrane fusion.

Declaration by author

This thesis is composed of my original work, and contains no material previously published or written by another person except where due reference has been made in the text. I have clearly stated the contribution by others to jointly-authored works that I have included in my thesis.

I have clearly stated the contribution of others to my thesis as a whole, including statistical assistance, survey design, data analysis, significant technical procedures, professional editorial advice, and any other original research work used or reported in my thesis. The content of my thesis is the result of work I have carried out since the commencement of my research higher degree candidature and does not include a substantial part of work that has been submitted to qualify for the award of any other degree or diploma in any university or other tertiary institution. I have clearly stated which parts of my thesis, if any, have been submitted to qualify for another award.

I acknowledge that an electronic copy of my thesis must be lodged with the University Library and, subject to the General Award Rules of The University of Queensland, immediately made available for research and study in accordance with the *Copyright Act 1968*.

I acknowledge that copyright of all material contained in my thesis resides with the copyright holder(s) of that material. Where appropriate I have obtained copyright permission from the copyright holder to reproduce material in this thesis.

Publications during candidature

No publications.

Publications included in this thesis

No publications included.

Contributions by others to the thesis

No contributions by others

Statement of parts of the thesis submitted to qualify for the award of another degree

None

Acknowledgements

This research was funded by the ANZ Trustees Medical Research Scholarship.
I greatly appreciate their support.
I would like to thank my principal supervisor Professor Paul Young and my co-supervisor Associate Professor Stuart Kellie of the School of Chemistry and Molecular Sciences at the University of Queensland. Their support and guidance throughout my research project has been greatly appreciated.
I would also like to thank the members of the Young laboratory, past and present, for their support and friendship, in particular Jodie Robinson, Catriona McElnea, Michelle Meyer, and Patrick duPreez. The members of the Hall and Khromykh laboratories at the School of Chemistry and Molecular Sciences at the University of Queensland deserve appreciation for sharing their expertise and equipment. I would also like to thank Steve Mason for his help with the microscopy work and the QBI FACS lab and staff for their assistance with the FACS analysis. Thanks to Dr. Nigel MacMillan and his staff for his assistance on lentiviruses.
Finally, I would like to acknowledge my family and friends for their support and advice throughout the project, especially Aaron M. Graham for his inexhaustible support and encouragement.
This thesis is dedicated to my mother and father, Harlan Lee and Julie Christine Shanks.

Keywords

Dengue fever, DENV-2, flavivirus, viral fusion, structural protein, envelope protein

Australian and New Zealand Standard Research Classifications (ANZSRC)

ANZSRC code: 060506 Virology, 80%

ANZSRC code: 060112 Structural Biology, 10%

ANZSRC code: 060108 Protein Trafficking, 10%

Fields of Research (FoR) Classification

FoR code: 0605 Microbiology, 80%

FoR code: 0601 Biochemistry and Cell Biology, 20%

Table of Contents:

CHAPTER 2
MATERIALS and METHODS

- 2.1. Vectors
  - 2.1.1. pCI_NGCprME_opt_neo
  - 2.1.2. pSFV and pSFVprME
  - 2.1.3. Lentiviral Plasmids: pREV, pRRE, pMD.G, pLL3.7
    - 2.1.3.1. pLL3.7, pGL-3, and pLL3.7_luc+
- 2.2. Prokaryotic cell culture
  - 2.2.1. Culture
  - 2.2.2. Transformation
  - 2.2.3. DNA purification
- 2.3. DNA Engineering
  - 2.3.1. Restriction endonuclease digests
  - 2.3.2. Ligation
  - 2.3.3. Gel electrophoresis
  - 2.3.4. Gel Extraction
  - 2.3.5. Site-directed mutagenesis
  - 2.3.6. Colony Diagnostic PCR
  - 2.3.7. Sequencing
- 2.4. RNA Engineering
  - 2.4.1. Plasmid linearisation and transcription
  - 2.4.2. RNA transcription
  - 2.4.3. RNA transfection
- 2.5. Eukaryotic cell culture
  - 2.5.1. Maintenance of mammalian and insect cells
  - 2.5.2. Cell line storage and rescue
  - 2.5.3. Transfection
  - 2.5.4. Infection
  - 2.5.5. Virus stock production
    - 2.5.5.1. Plaque assay
- 2.6. Lentiviral expression system
  - 2.6.1. Transfection
  - 2.6.2. Transduction
  - 2.6.3. Luciferase assay
    - 2.6.3.1. Transfection with control plasmids
    - 2.6.3.2. Transfection to generate pseudotyped particles
  - 2.6.4. MTT assay
- 2.7. Protein Expression
  - 2.7.1. Cell lysate preparation
  - 2.7.2. SDS polyacrylamide gel electrophoresis
  - 2.7.3. Western transfer and immunoblotting
  - 2.7.4. Immunofluorescence: Antibodies and Molecular Probes

List of Figures:

List of Tables:

Abbreviations:

ADE	Antibody Enhancement
bp	Basepair
C	Capsid glycoprotein
C6/36	*Aedes albopictus* cell line
CDC	Centers for Disease Control, USA
CO_2	Carbon Dioxide
CPE	Cytopathic effects
CS	Conserved Sequence
DENV-2	Dengue Virus subtype 2
DF	Dengue Fever
DHF	Dengue Haemorrhagic Fever
dH_2O	Distilled Water
DI,II,III	Domains I, II, III of Dengue E protein
DMEM	Dulbecco's Modification of Eagles Medium
DMSO	Dimethyl Sulfoxide
DNA	Deoxyribonucleic Acid
DSS	Dengue Shock Syndrome
E	Envelope glycoprotein
EDTA	Ethylene Diamine Tetra-acetic Acid
eGFP	Green Fluorescent Protein
ER	Endoplasmic Reticulum
FACS	Fluorescent Activated Cell Sorting
FCS	Fetal Calf Serum
FFWI	Fusion From Within
FFWO	Fusion from Without
g	Gravity
GAG	Glycosaminoglycan
GFP	Green Fluorescent Protein
HCV	Hepatitis C Virus
HEK 293T	Human Embryonic Kidney cell line
HIV	Human Immunodeficiency Virus
HS	Heparan Sulphate
IF	Immunofluorescence
IRES	Internal Ribosome Entry Site
JEV	Japanese encephalitis
kB	Kilobase
kDA	Kilo dalton
LB	Luria Broth
M	Membrane glycoprotein
m.o.i.	Multiplicity Of Infection
mAb	Monoclonal Antibody
MCS	Multi-Cloning Site
ml	Milliliters
mM	Milimolar
NC	Nucleocapsid
NCG	New Guinea C strain of dengue-2
nm	Nanometers

NP40	Nonidet p40
NS1-5	Nonstructural glycoprotein 1, 2, 2B, etc.
OPTI-MEM	Optimised Modification of Eagles Medium
PAGE	Polyacrylamide Gel Electrophoresis
PBS	Phosphate Buffered Saline
PCR	Polymerase Chain Reaction
PFA	Paraformaldehyde
Phe	Phenylalanine
PI	Propidium Iodide
prM	Precursor of Membrane Protein
PS-EK	Porcine Stable-Equine Kidney cell line
RdRp	RNA-dependent RNA polymerases
RNA	Ribonucleic Acid
rpm	Revolutions Per Minute
RSP	Recombinant Subviral Particle
RT-PCR	Reverse Transcriptase Polymerase Chain Reaction
SAP	Shrimp Alkaline Phosphatase
SD	Standard Deviation
SDS	Sodium dodecyl sulfate
sE	Soluble fragment of E protein
SF	Serum Free Media
TBEV	Tick Borne Encephalitis Virus
TM	Transmembrane
TGN	Trans Golgi Network
Tyr	Tyrosine
UTR	Untranslated Region
UV	Ultraviolet
VP	Vesicle Packets
VSV	Vesicular Stomatitis Virus
WGA	Wheat Germ Agglutinin
WHO	World Health Organization
WNV	West Nile Virus
w/v	Weight to volume ratio
µg	micrograms
µl	microliters
Vero	African Green Monkey Kidney cell line
YF	Yellow Fever

CHAPTER 1

INTRODUCTION

1.1. Dengue Fever and Global Prevalence

Dengue virus belongs to the family *Flaviviridae*, a group of positive-strand RNA viruses, which are primarily spread through arthropod vectors. It is closely related to at least 70 other species such as Hepatitis C, West Nile, Yellow Fever, Japanese and Tick-Borne Encephalitis [1]. Dengue Fever (DF) and the associated syndromes Dengue Haemorrhagic Fever (DHF) and Dengue Shock Syndrome (DSS) are second only to malaria in terms of the number of people that become infected annually. Carried by *Aedes aegypti,* there is an estimated 50-100 million cases of which, 250,000-500,000 are DHF resulting in 30,000 to 50,000 deaths per year [2, 3]. Two and a half billion people are exposed annually and dengue infection is the leading cause for hospitalization in at least eight South-East Asia countries [4]. Infection rates have increased in the last few decades because of the geographical expansion of *Aedes agypti* and *Aedes albopictus* [5]. This situation is likely to become worse with the effects of global warming increasing the territorial spread of these mosquitoes. In 1970 there were seven countries that had endemic Dengue fever, now there are 60 [6]. Australia has seen infections since 1873 and is interdependent on the infection rate in Asia and the Pacific [7]. In December 2007, warnings were reported in Australia of the spread of mosquito-borne diseases, specifically of Dengue, Ross River fever and Malaria because the tropical zone has increased two degrees of latitude in the last 25 years [8]. In February 2011, there were 39 cases of DENV-2 in East Innisfail, QLD [9].

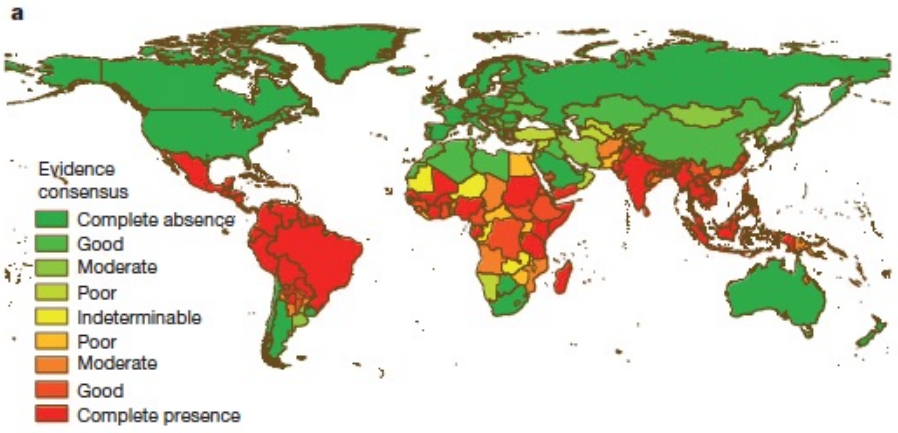

Figure 1. Distribution of Dengue Fever globally as of 2011 [10]. Global evidence consensus of risk and burden of dengue from complete absence to complete presence.

While DF is a mild, febrile illness, it can cause large-scale societal hardship when periodic epidemics break out in equatorial regions. In 2007, Brazil reported 560,000 cases (with 82,000 in Sao Paulo), Indonesia 134,847 and 80,000 in Vietnam [6]. Dengue fever causes severe headache and eye pain, joint pain (it is often called “bone break fever”), rash, mild bleeding manifestations and low white cell count. DHF and Dengue Shock Syndrome (DSS) on the other hand can be severe and has a 2.5% chance of fatality, usually in children and immuno-compromised adults and, if survived, can take weeks to recover from. If modern health care is not provided, case fatality can reach 20% [8]. Historically children have borne the brunt of the disease burden but this age profile is changing in Asia and Latin America where adults are increasingly being affected [11]. DENV has 4 serotypes 1-4 and multiple genotypes. If a patient has been affected by one serotype, this will most likely not confer immunity to another and in fact may lead to more severe antibody-enhancement induced DHF or DSS, as does co-infection with one or more serotypes [5, 12].

Due to the geographic spread, the global number of infections and ignorance of the disease, dengue has become an important re-emerging virus [13]. There are currently no vaccines or therapeutics for dengue infections; however, there are currently five in clinical trials [14]. Our laboratory is engaged in research to accurately elucidate the structural relationships between the viral proteins and the cellular host receptors. By increasing our knowledge of this relationship we hope to design anti-viral therapies that can combat Dengue infection and/or prevent transmission.

1.2. Antibody-Dependent Enhancement and Vaccine development

One of the most successful vaccines in providing immunity is for Yellow Fever (YF), which has a highly related genome and antigenic structure to Dengue. The diversity and pathogenesis is very different as there are four serotypes (1-4) for dengue [7]. For reasons yet unknown, when one has been infected with a previous serotype and is co-infected or subsequently infected with a different serotype, the severity of the disease may be higher. This is called antibody-dependent enhancement (ADE), as the primary antibodies do not neutralize the subsequent virus. Cross-reactive memory T cells appear to increase cytokine production when exposed to the secondary serotype [15]. In contrast to the “reassuring dogma that infectious diseases evolve inexorably toward commensalism and reduced virulence” [16], Dengue offers no cross-reactive immunity

and re-infection is more severe. This feature has hindered vaccine development. A vaccine has been a WHO priority for three decades now to control dengue [11]. There are several types of vaccines in development including a YF-DF chimera, a DNA vaccine, a recombinant viral vector and subviral particles with Dengue envelope proteins [6]. Sanofi-Pasteur has created a tetravalent vaccine called ChimeriVax™, which has a YF backbone (C and NS proteins) and prME of all four serotypes, which is in Phase III clinical trials [14, 17]. Unfortunately, ADE events may only present in phase IV clinical trials or post-market.

1.3. Dengue virus structure

DENV is a positive strand RNA virus, 10.7 kB in length with the following genome organization: 5' UTR-C-prM-E-NS1-NS2B-NS3-NS4A-NS4B-NS5-UTR-3'. The dengue genome translates to a single 3391 amino acid polypeptide, which is co-translationally processed by viral and cellular proteases, generating three structural and 7 non-structural proteins (figure 2) [18].

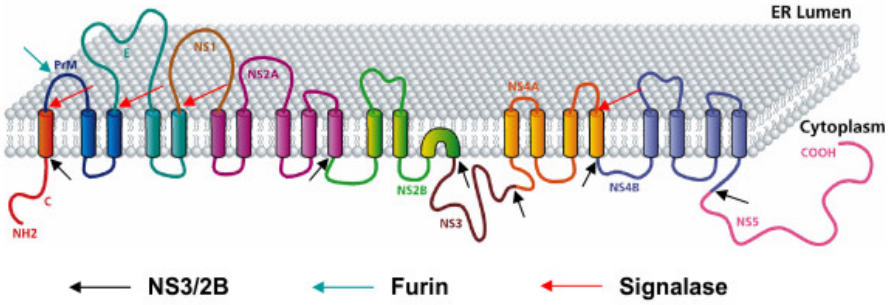

Figure 2. Dengue genome and polyprotein structure. Dengue genome structure is a single open reading frame, 10.7kB in length displaying the three structural and seven non-structural proteins. The positive sense RNA strand has 5' cap and poly-A tail elements. The 3391 amino acid polypeptide is co- and post-translationally processed by viral and cellular proteases displayed. This figure displays the single polyprotein configuration in the endoplasmic reticulum before transcriptional cleavage by viral NS3/2B, cellular furin and signalase. [19].

The structural proteins are comprised of prM, the membrane precursor, M the membrane protein, C the capsid protein, and E the envelope protein. The C protein is 100 amino acids in length, M is 75 (8 kDa) and E is 495 (~50 kDa) [20]. The virion displays icosahedral symmetry with a spherical nucleocapsid 40-50 nM in diameter. The E glycoprotein is responsible for cell association and binding. DC-SIGN and heparin sulfate are considered to be binding candidates and are thought to adhere the virus to the cell before higher affinity receptors engage [21].

1.4. Dengue virus cellular pathway

The virus enters by cell surface binding by receptor-mediated endocytosis [22]. Cellular binding receptors have not been completely characterised but include attachment receptors DC-SIGN, heparin sulfate, and immunoglobulin F_c receptors as well as possibly integrin and CD14 or a similar molecule [1]. After uptake of the virion into the endosome following endocytosis, the acidic pH of the endosome induces structural alterations in E that lead to membrane fusion and the release of the nucleocapsid into the cytoplasm. After un-coating, the plus-stranded RNA genome is translated to initiate virus replication and subsequent polyprotein synthesis and processing. Virus assembly occurs in the endoplasmic reticulum (ER) and leads to the formation of immature (prM-containing) particles that are transported through the exocytic pathway (figure 3). The capsid protein assembles with RNA on the cystolic face of the ER membrane, which then buds through the membrane, acquiring an envelope of lipids along with prM and E proteins [23].

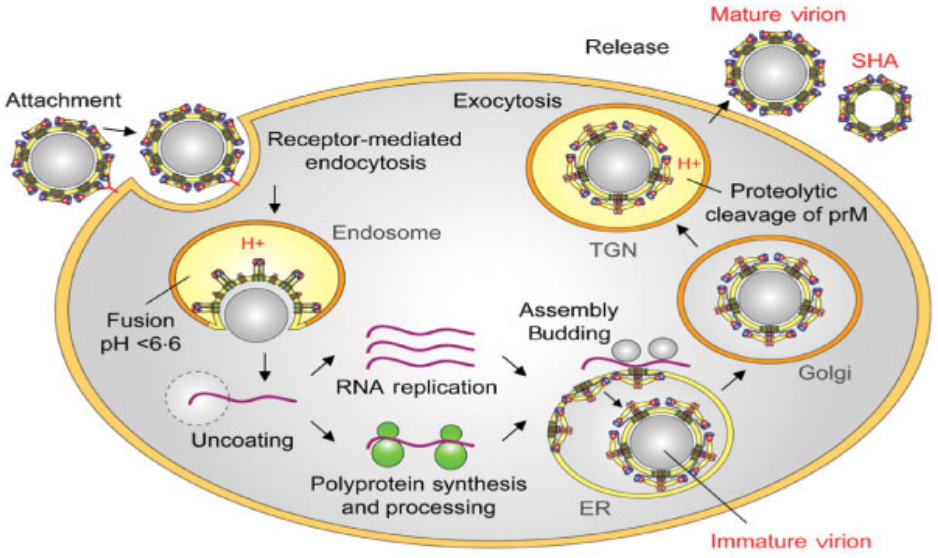

Figure 3. Dengue virus life cycle. Virus entry occurs by receptor-mediated endocytosis. The acidic pH in the endosome induces structural alterations in E that lead to membrane fusion and the release of the nucleocapsid into the cytoplasm. After uncoating, the plus-stranded RNA genome is translated to initiate virus replication. Virus assembly occurs in the endoplasmic reticulum (ER) and leads to the formation of immature (prM-containing) particles that are transported through the exocytic pathway. The acidic pH in the trans-Golgi network (TGN) causes an irreversible conformational change in the prM–E complex that is required for the maturation cleavage by cellular furin. Mature infectious particles are released by exocytosis [24].

The acidic pH of the trans-Golgi network (TGN) causes a low pH-induced irreversible conformational change with E protein subunits rearranging from homodimers to

monomers and then homotrimers in a three-fold axis of symmetry [25-27]. This conformational change in the prM-E complex is required for cleavage by cellular furin, maturation of the viral particle and subsequent release.

1.5. Immature versus mature viral particles: the envelope protein

Dengue virions transition between a number of structural forms during maturation and two of these forms have been imaged by cryo-EM; the immature and mature form of E. In immature fusion-incompetent viruses, E forms a stable heterodimeric complex with the chaperone prM approximately 15 minutes after synthesis, see figure 2 [21, 28]. These immature virions are non-infectious and are not capable of hemagglutination or fusion [29]. Subviral particles are also assembled on the ER and consist of only prM, E and lipids. They are routinely seen in flaviviral infections. Inefficient cleavage of prM by cellular furin occurs regularly resulting in extracellular, partially mature noninfectious particles. A recent study showed that as much as 40% of all extracellular DENV particles from C6/36 cells are partially immature, which shows that maturation during virus egress is rather inefficient [30].

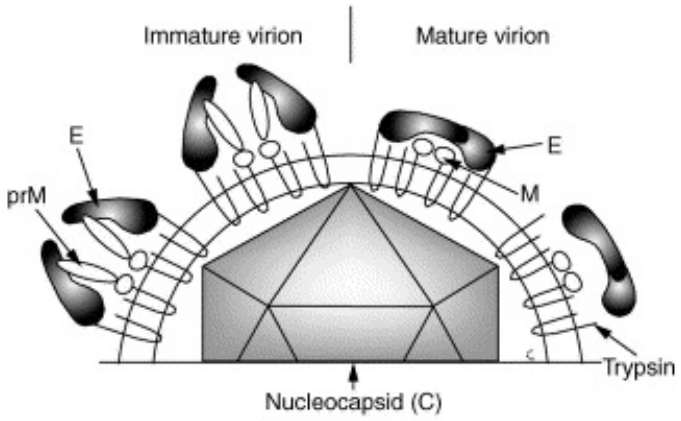

Figure 4. Mature versus immature prME protein. The heterodimers of prM and E displayed on DENV surfaces project in the immature virion; prM protects the fusion peptide (FP) region of E. During viral maturation, pr is cleaved from M and the homodimers of E rearrange to lie flat in an icosahedral formation. The FP is buried before the active fusion is triggered. M remains associated with the viral membrane [26].

The trans-Golgi network (TGN) is an acidic environment, in which prM functions to protect E's fusion loop from premature fusion. After processing through the endocytotic pathway, furin cleaves the N-terminal pr domain of prM in the late TGN (figure 4). One hundred amino acids of prM are released by furin [31]. The cleaved pr domain remains temporarily associated with E and is lost as the pH rises through the secretory pathway.

This generates fusion-competent mature virus particles [26]. In this mature form at neutral pH, E is arranged as homodimers that lie horizontally on the viral membrane in 30 “rafts” [27]. Each “raft” has three parallel dimers arranged in a herringbone pattern with icosahedral symmetry [24, 27, 29]. This scaffold of 90 E homodimers is arranged from head to tail and each monomer is anchored via two transmembrane segments [32]. The fusion peptide (FP) is embedded in a hydrophobic pocket of the neighboring monomer.

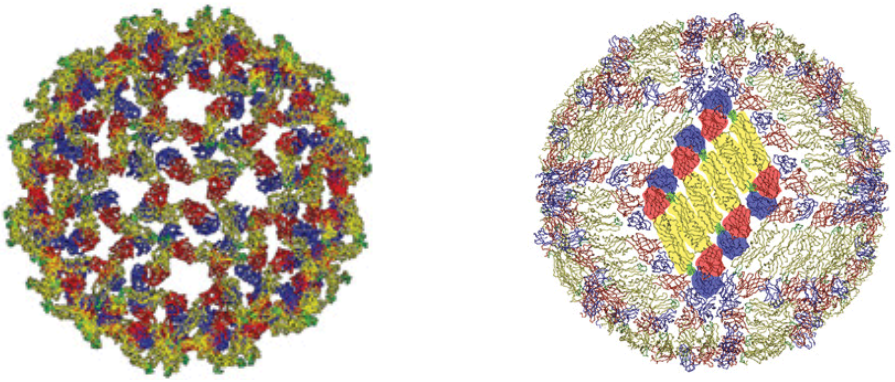

Figure 5. Immature to mature virion cryo-EM reconstruction. Immature flavivirus of Dengue-2 at 16-Å resolution (left) with heterodimer of prM (green) and E displayed. Domains I, II, and III are color-coded red, yellow, and blue respectively. prM protein that caps the trimeric spike is visible. Mature (right) homotrimer conformational change after disassociation of pr [29].

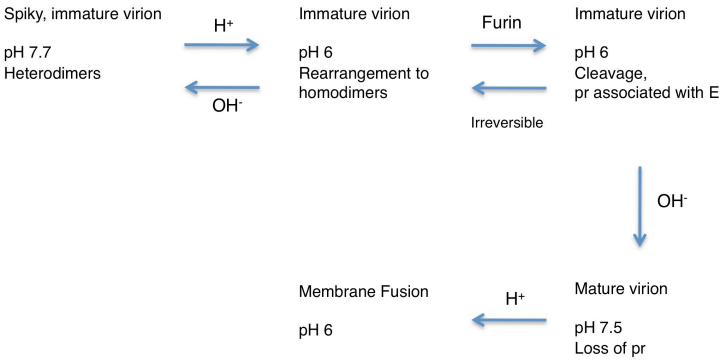

Figure 6. pH changes and E protein conformation. The spiky, immature virion at pH 7.7 as heterodimer pairs. As the protein matures, at pH 6, the protein rearranges to homodimers. Furin cleaves pr from E at pH 6 although pr stays associated with E to protect it from premature fusion. At pH 7, the mature virion loses its association with pr and membrane fusion occurs at pH 6.

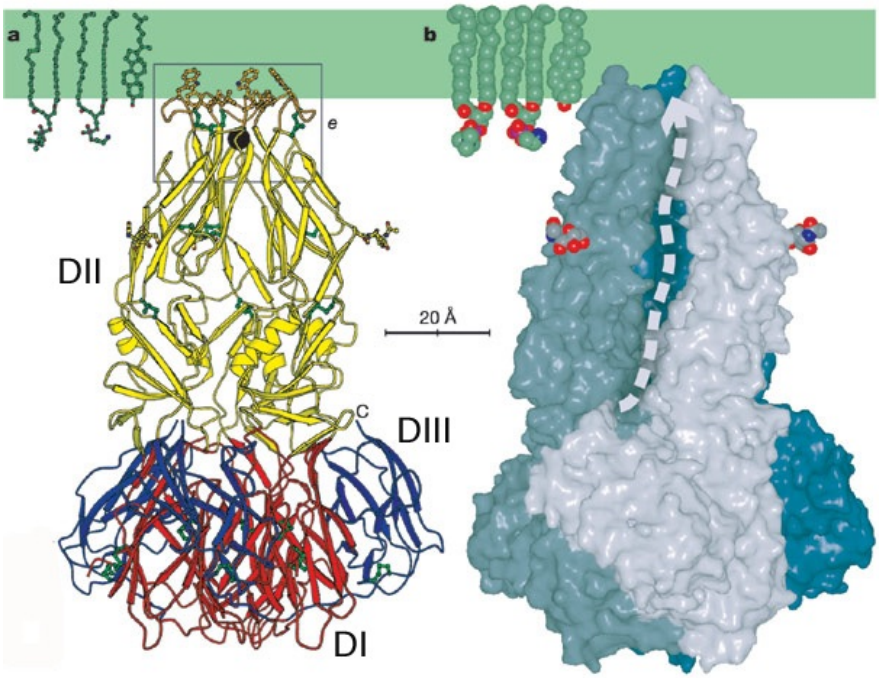

Figure 7. DENV envelope protein showing domains I, II, and III. Domain I is in red, domain III is in blue and domain II is in yellow. The perforated grey line shows the predicted α-helices, E2 (membrane proximal) and E1 (membrane distal) [21].

The X-ray crystallographic structure of E has been determined [23, 31, 33] and the cryo-EM structures are displayed in figure 5 [34]. E has twelve strictly conserved cysteines, which form six disulfide bridges. The E monomer has three domains referred to as domain I (amino acids 1-50, 136-194), domain II (51-135), and domain III (300-395) (figures 5 and 7) [5, 18]. Domain III is an immunoglobulin-like domain, domain I is termed "central" and domain II is the dimerisation domain [35]. These domains are rich in β-sheets, typical of all class II fusion proteins [36]. The "dimerisation" domain II of one dimer contacts with DI and DIII of its neighbours in a triangulation T=1 orientation [26, 34]. This involvement stabilizes the E protein dimer. DI and DII are connected by four polypeptide strands while DI and DIII are connected by only one [31]. DII also contains the internal fusion peptide (FP). Domain I is an eight-stranded β-barrel containing two large insertion loops that form the gated finger-like domain. Domain III forms a 10-stranded β-barrel with an immunoglobulin-like fold and contains the cellular receptor binding motifs [37]. Antigenic determinants that respond to neutralizing antibodies are also found in this domain [26].

As the E protein matures, it rearranges from a spiky, heterodimeric partnering with prM in the immature form to homotrimers in the mature form (figure 5). This pH-induced maturation begins at around pH 6, as E rearranges to homodimers. Furin cleaves pr from E at pH 6 although pr stays associated with E to protect it from premature fusion. At pH 7, the mature virion loses its association with pr and membrane fusion occurs at pH 6 (figure 6).

1.5. Non-Structural Proteins: NS1, NS2A, NS2B, NS3, NS4A/B, NS5

There are seven non-structural proteins for Dengue, some of which have known ribbon structures (figure 8) [38]. NS3 is a protease-helicase with a chymotrypsin-like serine protease as well as a RNA helicase and RTPase/NTPase. NS5, which is the largest protein at 104 kDa, is most conserved among serotypes 1-4. It has a methyl-transferase domain at its N-terminal end and a RNA-dependent RNA polymerase at its C-terminal end [38]. NS1 at 45 kDa is translocated into the lumen of the ER and secreted from the cell [39]. It is involved in the viral replication complex and acts in viral defense through inhibition of complement activation [40, 41]. NS2A (22 KDa) is part of the replication complex [42]. NS 4A/4B (16 KDa/27 KDa) are integral membrane proteins. NS4A induces membrane alterations, which are important for viral replication [43]. NS4B has been implicated in assisting viral RNA replication through direct interaction with NS3 [44]. NS4B is also an interferon α/β induced signal transduction blocker [45].

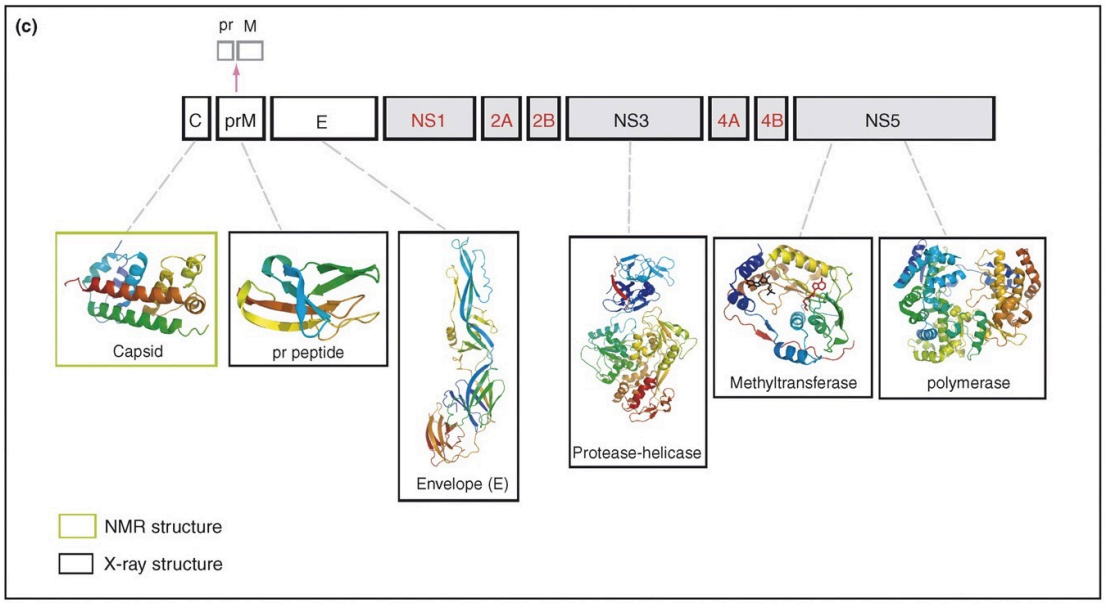

Figure 8. Known ribbon diagrams of Dengue structural and non-structural proteins [38].

1.6. Class I fusion

It is useful to review the well characterised class I fusion machinery of influenza hemagglutinin (HA) in comparison to Dengue class II fusion. Class I includes retro-, orthomyxo-, paramyxo-, corona- and filoviridae [46]. In class I fusion, exposure to the low-pH environment of the endosome or binding to a receptor alters the fusion protein conformation so that an N-terminally located fusion peptide (FP) extends into the host membrane. The protein then trimerizes, critically instigated by the stem region, resulting in a helical hairpin structure, which brings the two membranes into close proximity [12, 46]. This hairpin structure or hemifusion stalk forms a mixture of the outer leaflets of the lipid membranes [29]. Finally, the fusion peptide rearranges completely so that the FP and the transmembrane domains are anti-parallel to each other but in the same membrane (figure 9).

The trimeric post-fusion structure of HA is typical of class I and similar to class II DENV [47]. Numerous studies have shown that several regions are crucial for this fusion process including both membrane anchors, the FP, the transmembrane and membrane-proximal regions [46, 48-50]. Many class I viral envelope proteins have been characterised including HIVgp41, HCV, SIVgp41, Ebola G, HTLV-1, RSV, HRSV, VSV-G, SARS, and MoMuLV [46, 47, 51].

1.7. Class II fusion and dengue virus E

Class II fusion flaviviruses have one of the fastest and most efficient membrane fusion machineries of all enveloped viruses to date [20]. The dimeric E on the virus surface has the FP buried before binding. The E protein binds to one or more receptors and is internalised in the low-pH endosome. The acidic pH of the endosome causes dissociation of the E dimers, which allows DI and DII to flex relative to each other [23, 29, 52]. Histidine 146 and 323 are critical pH sensors for this large-scale conformational change of E [53-55]. H323 is at the interface between DI and III and its protonation leads to the dissolution of domain interactions and exposure of the fusion peptide [56]. These histidines then form salt bridges with negatively charged residues in the post-fusion conformation [57]. Fusion does not occur until the late endosome/lysosome even though the pH is low enough in the early endosome. This is thought to be controlled by compartment-specific lipid composition [58]. The hinge region between DI and DII helps direct the FP toward the host membrane. This is facilitated by the presence of conserved

glycines in three of the four peptides connecting DI and DII [31, 59]. DII of E swings outward towards the host cell membrane at the DI-DII hydrophobic hinge region. This movement destroys the tight packing interactions on the outer surface of the virion, enabling the trimerisation of E and insertion of the FP into the outer leaflet of the host cell membrane. DIII shifts, folding back onto itself and in the process brings the viral membrane towards the FP and the host cell membrane [60]. As DIII moves toward DII, hemifusion of the lipid membrane occurs. This hairpin structure or hemifusion stalk in the "active fusion" form of trimeric E has the transmembrane and FP regions in close proximity in the fused membrane [21, 29, 61] (figures 9 and 10). The fusion pore flicks open and the virus then gains entry [62].

1.8. Class III fusion

There is a third class of fusion proteins, newly termed Class III, which have features of both Class I and Class II [63]. They contain a central trimeric coiled-coil, typical of Class I in their post-fusion state while three of their domains are predominately β-sheets, which is typical of Class II. VSV-G, Baculovirus gp64, and Epstein-Barr Virus gB are in this class, which also includes HSV-1 (a DNA virus) [64].

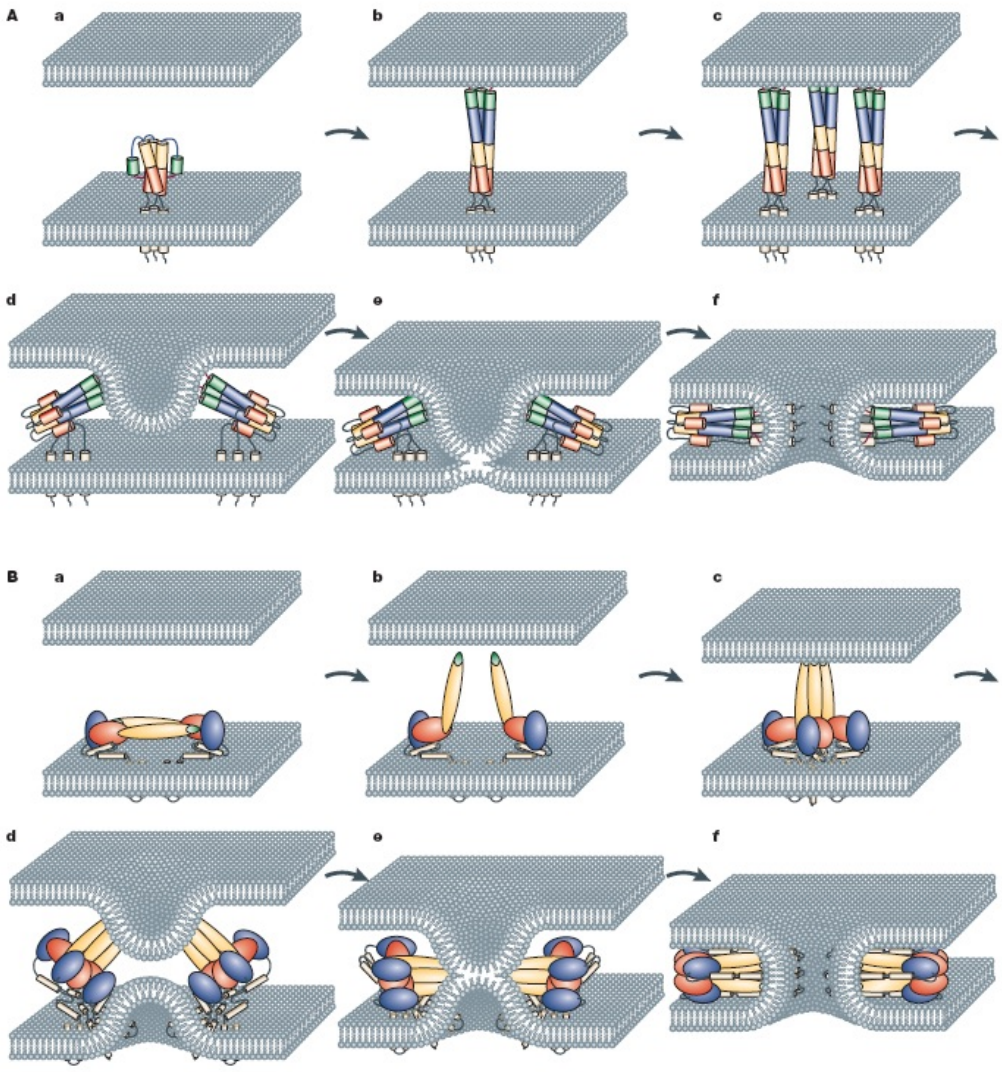

Figure 9. Proposed fusion process of homotrimer E showing Class I (A) and Class II (B).
[A] Class I fusion. (**a**). After binding to a receptor, or exposure to the low-pH conditions of the endosome, the fusion protein forms an extended conformation and the fusion peptide extends into the host membrane (**b**). Trimerisation of the protein (**c**) is followed by a conformational change of the fusion protein when the host cell and viral membranes fold towards each other (**d**). A restricted hemifusion stalk is formed, in which the outer leaflets of the lipid membranes mix (**e**), and finally the fusion peptide rearranges completely so that the fusion peptide and transmembrane domains are anti-parallel to each other, but in the same membrane (**f**).
[B] Class II fusion. The dimeric E protein is on the virus surface with the fusion peptide (shown in green) buried in the dimer (**a**). E binds to a receptor and is internalised in the endosome. Under low-pH conditions, domain II swings outward towards the host cell membrane, presumably at the domain I–II hinge region (**b**). This conformational change allows the E proteins to rearrange laterally. The fusion peptide inserts itself into the outer leaflet of the host cell membrane, enabling trimerisation of the E protein (**c**). Domain III of the E protein folds back onto itself, and in the process brings the viral membrane towards the fusion peptide and host cell membrane (**d**). As domain III moves towards domain II, hemifusion of the lipid membranes occurs (**e**), and finally a trimer forms where the transmembrane regions and the fusion peptide are in close proximity [29].

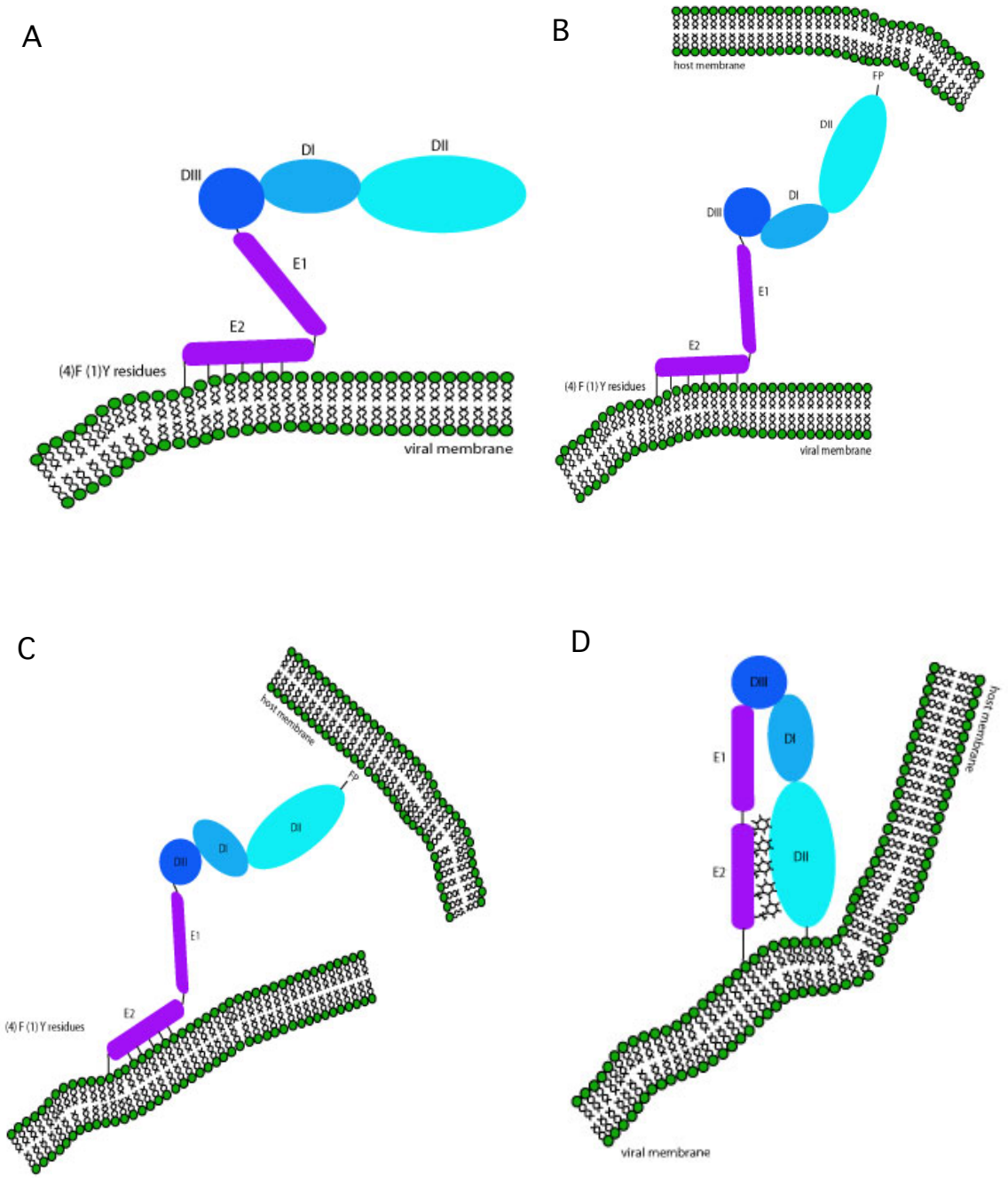

Figure 10. DENV pH-activated conformational change of E. E in monomeric form, from inactivated to "active fusion".
[A, B] The hinge between DI and DII allows rotation of DII from a horizontal to vertical position.
[C, D] DIII shifts and rotates, directing DII to expose the FP region towards the host membrane for embedding. The hydrophobic residues of E2 pull the viral membrane in close proximity to the host membrane to allow for fusion pore formation and then re-orient into a hydrophobic trough formed by adjacent DII domains of the final trimeric E.

1.9. E stem and anchor region

The stem or membrane-proximal external region (MPER) of E is composed of a membrane distal α-helix E1 (residues 398-420), a conserved region CS, and a membrane proximal α-helix E2 (426-448) [29, 34] (figure 11). There are two anchoring transmembrane regions, TM1 and TM2.

Stiansy, et al. (1996) proposed that the E2 membrane proximal alpha helix between TM1 and E1 of DIII is crucial for prME association and fusion [37, 65]. It is also thought to be fundamental in instigating curvature in the lipid bilayer, which is crucial for fission and fusion [66]. This may promote virus release by inducing membrane curvature at sites where virus budding occurs. The stem domain of E is rich in aromatic, hydrophobic residues and is highly conserved among flaviviruses [21] (figure 11). In DENV-2, E2 contains four phenylalanine and one tyrosine residues (figure 12 and 13). E1 and E2 are both amphipathic with one face positively charged, which may help alleviate electrostatic repulsion between the membrane-facing surfaces of E (figure 14). During fusion, the charge interactions between the membrane, ectodomain and stem regions of E change, which leads to a rearrangement of E1 and E2 [31].

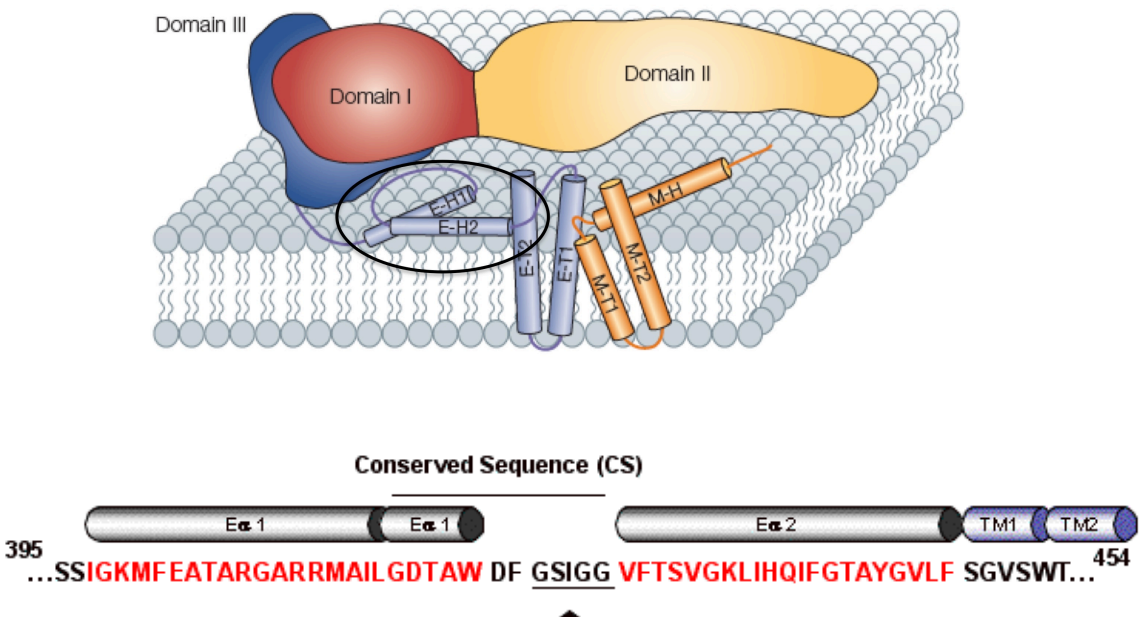

Figure 11. Diagram of the dengue virus E stem region. **[Top]** DI-DIII of DENV E with helices of membrane (yellow), transmembrane (middle blue), E1 and E2 (circled). **[Bottom]** Predicted E1 and E2 α-helices are shown as cylinders (red). The "activation hinge" between DI and DII is underlined.

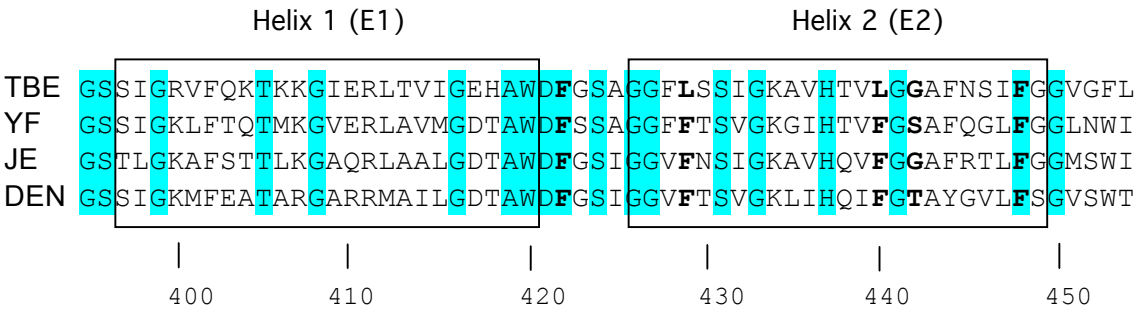

Figure 12. Multiple sequence alignment of stem helical domains. The four major Flaviviruses are aligned, TBE (tick-borne encephalitis, YF (yellow fever), JE (Japanese encephalitis) and DEN (dengue). DEN refers to DENV-1 subtype. Helix 1 (E1) contains amino acids 398-420, helix 2 (E2) corresponds to residues 426-448 [65].

F_{422}G S L GG * VF_{429}T S I G K A L H Q VF_{440}GG IY_{444}GAAF_{448}

Figure 13. MPER α-helix E2 peptide sequence 422 to 488. In bold, green are nonpolar, hydrophobic residues. The remaining residues are all polar (either uncharged or basic). * proposed activation hinge

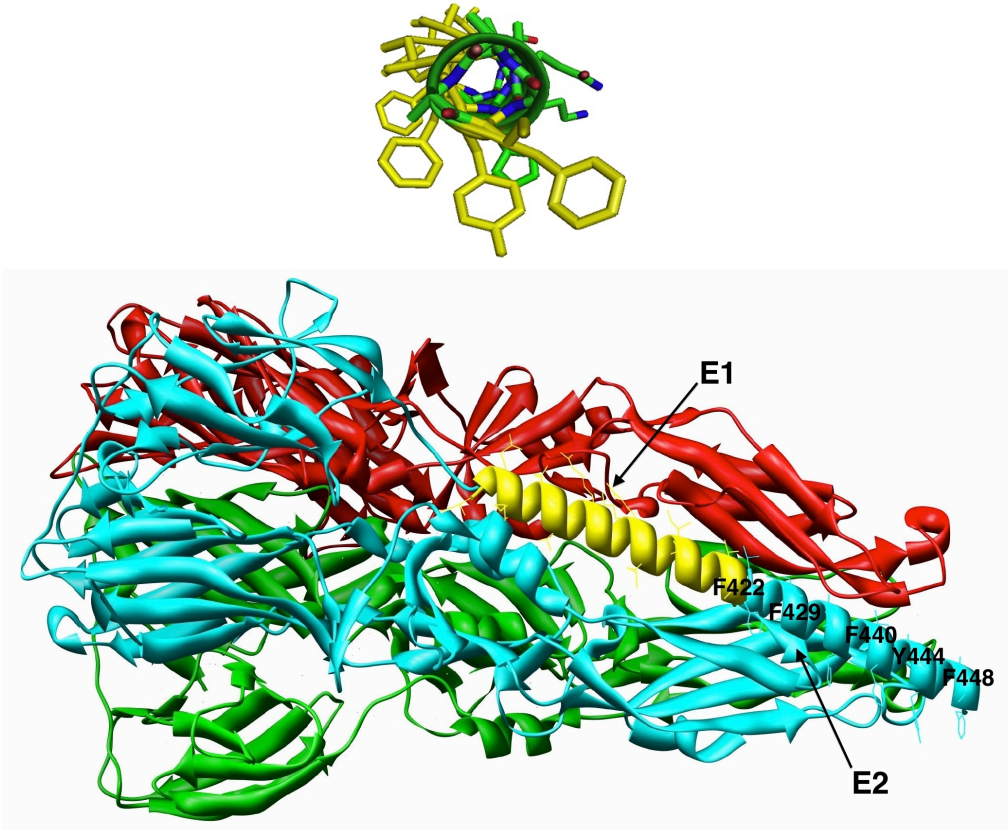

Figure 14. Stem α-helices E1 and E2 location in the envelope glycoprotein**. [Top]** Diagram of the top-down display of phenylalanine and tyrosine residues spiraling out of the α-E2 helix. The aromatic, hydrophobic side groups map to one side of the amphipathic helix. **[Bottom]** Stem α-helices E1 and E2 location in the envelope glycoprotein. (Modified from P.R. Young)

The structural significance of this region has been previously investigated by the Young laboratory through mutation of the phe/tyr residues to non-conservative alanines as in figure 15. Three mutant constructs were created with either the first two (F422, F429), last two (Y444, F448) or all five phe/tyr residues mutated to alanines. Mutant prME constructs were transfected into mammalian cells and the expressed proteins prM and E were immunoprecipitated from ^{35}S met-cys labeled cell lysates. The mutant heterodimers could be co-precipitated with monoclonal antibodies (MAb) against either the prM (2H2) or E (3H5) components, indicating that none of these aromatic residues were critical to prME heterodimerisation [67]. However, none of these mutants led to fusion indicating that they were crucial for the conformational changes leading to fusion peptide display. Theoretically, these substitutions were thought to have been enough to disrupt the E2 α-helix configuration so that the conformational changes required for exposure of the FP could not occur [67]. These membrane-anchoring residues may be essential for maintenance of structural integrity, providing stability for DII to be move vertically, exposing the FP region and thus initiating fusion (figure 10). It is known that seven hydrophobic residues, one of which is F448, interact with the M protein for possible pre-fusion stability in E's heterodimeric state. These residues do not interact in homodimeric E [35]. F429 has been proven to be crucial in the formation of virus-like particles (VLPs), heterodimerisation and protein production. When mutated to proline in a pSFV replicon system, a lower rate of infectivity occurred, as well as low levels of protein expression and viral RNA production [68]. F422 has also been mutated to proline, resulting in decreased viral assembly and membrane binding. Peptides corresponding to this stem region (419 to 447) target a late-stage fusion intermediate resulting in loss of association with the lipid bilayer and inhibiting entry [69, 70]. There appears to be a specific interaction with DII, which inhibits the movement of DII in relation to DI, preventing the two membranes from pinching together. A stem-derived peptide appears to bind the post-fusion, trimeric form of E competing for binding to the stem, which blocks DII from "zipping" along the stem to create hemifusion of the membranes [71].

The Young laboratory has previously tested truncated versions of the stem and transmembrane domains of E and prM. The prM constructs generated included pr by itself, prM with no TM, prM with one TM domain only, and full-length prM (figure 16). Full-length E and prM expressed singly were located on the cell surface. Without prM as

a chaperone, E was not expected to migrate to the cell surface but this may be a fusion-incompetent version [67]. PrM truncation constructs were co-expressed with full-length E. The only prM truncation to be expressed on the cell surface was prM with one TM segment. Stable heterodimer associations were formed with prM full-length and pr with at least one TM segment. PrM lacking a TM anchor was only partially successful in formation of the heterodimer. No fusion occurred with any of these truncated products, clarifying that the transmembrane and stem regions are crucial for heterodimerisation and consequently, fusion.

	wild type	mutant 1	mutant 2	mutant 3
422	F	**A**	F	**A**
429	F	**A**	F	**A**
440	F	F	F	**A**
444	Y	Y	**A**	**A**
448	F	F	**A**	**A**

Figure 15. Amino acid substitutions of the E2 α-helix. The four phenylalanine and one tyrosine residue substitutions were previously made by the Young laboratory (P.R. Young personal communication).

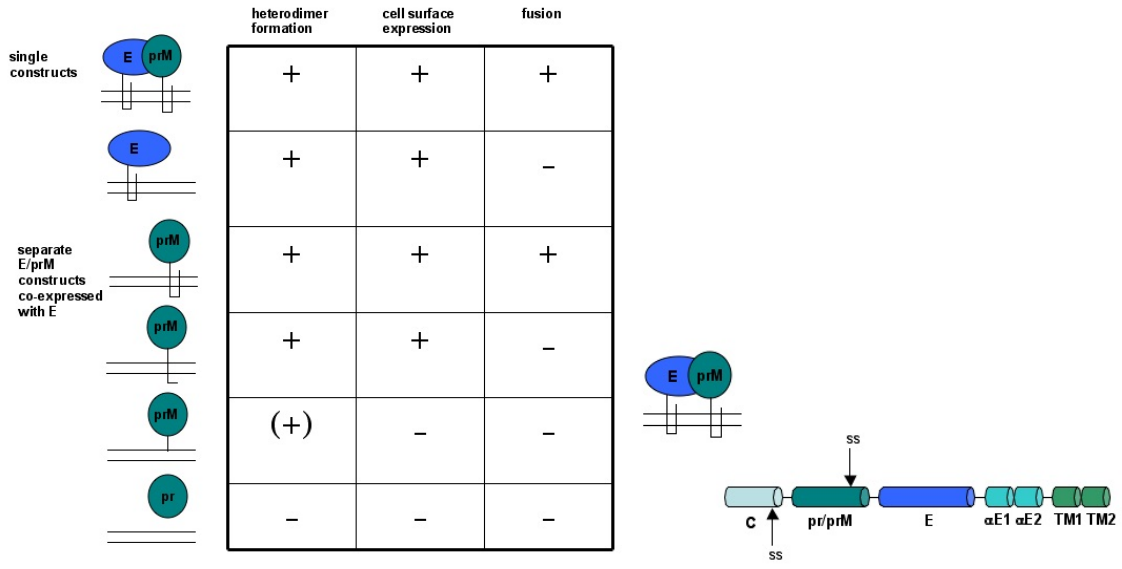

Figure 16. PrM and E truncations of the stem region previously tested. Full-length pr and E, E and pr singly, pr with one TM segment deleted, both TM segments deleted and pr without the stem region. "Ss" represents signal sequence; the N-terminus cleavage site for C and prM. The parentheses corresponds to partial formation.

This study will further this research by mutating independently each phe or tyr to either non-conservative alanine or conservative, hydrophobic residues (tyrosine or phenylalanine), instead of group substitutions, (figure 17). The substitution with tyr or phe is expected to retain E anchored to the viral membrane so as not to disrupt the conformational change and bar fusion.

	wild type	mutant 1	mutant 2	mutant 3	mutant 4	mutant 5
422	F	**A/Y**	F	F	F	F
429	F	F	**A/Y**	F	F	F
440	F	F	F	**A/Y**	F	F
444	Y	Y	Y	Y	**A/F**	Y
448	F	F	F	F	F	**A/Y**

Figure 17. Amino acid substitutions of the E2 α-helix. Shown are the four phenylalanine and one tyrosine residues that will be mutated.

1.10. Lentiviral pseudotyped particle expression system

One of the problems associated with flavivirus fusion studies has been the quantification of fusion phenotypes for selected mutants of prM and E. Standard approaches for establishing quantitative fusion assays for dengue have been unsuccessful. An alternative approach is the use of pseudotyped retroviruses that could provide a measure of successful entry into target cells and therefore a measure of fusion. Lentiviral pseudotype vectors have been created for the expression of a variety of virus envelope proteins such as Hepatitis C [72, 73], Ebola [74], SIV-1 [75] and SARS [76]. Lentiviruses are primarily used in gene therapy although they have been proven useful in pantropic transduction [77, 78]. Lentiviral vector constructs have proven to be very productive in terms of transduction due to their ability to infect both replicating and non-replicating cells. A lentiviral expression system was developed to test fusion of MPER E2 mutants determined by wild-type prME results.

The third generation, HIV-1 based system to be used in this project is noninfectious, as the replicative genes have been deleted and the minimal essential components have been separated onto independent plasmids (see figures 25-28, Appendix I). The four plasmids used in this system are: an “expression” construct containing gag and pol viral proteins, a “transfer” construct, which has the production and packaging elements, a “packaging” plasmid containing the viral envelope gene, and a fourth “reporter” vector containing luciferase or eGFP to analyze infectivity and transduction. The commonly

used Vesicular Stomatitis Virus (VSV-G) envelope protein is recognised by a broad spectrum of cells and forms highly stable particles [79, 80]. The lentivirus is capable of transferring the reporter gene to infected cells but incapable of replicating (see figure 15).

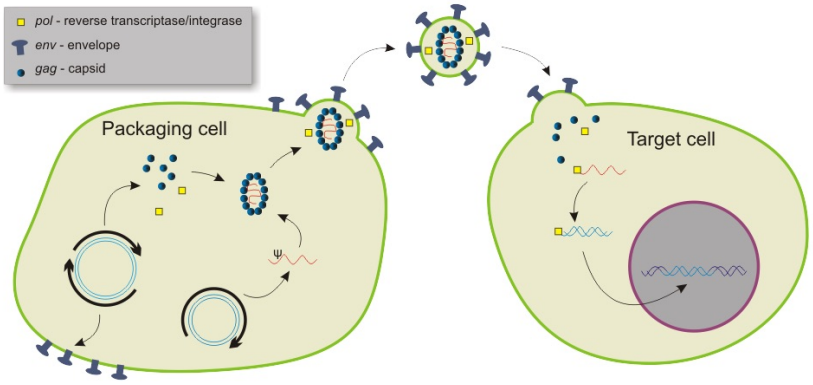

Figure 18. The lentiviral development pathway. Transfection of HEK 293Ts with the 3rd generation four plasmid system (pLL3.7, pRRE, pREV, NGC_prME) is followed by harvest of lentiviral supernatant. Cells are then transduced and analyzed to determine infectious units via FACS analysis [81].

1.12. Aim of Research Project

The aim of this research project is to determine the structural significance of the membrane-proximal (MPER) E2 α-helix in Dengue's E protein in pH-activated conformational change and its role in membrane fusion. Site-directed mutagenesis of the α-helix E2 will be carried out to determine the role of five individual residues in viral fusion (F422A/Y, F429A/Y, F440A/Y, Y444A/F and F448A/Y). A lentiviral expression system will be developed to assay fusion of E2 mutants. This expression system is a method of studying viral fusion of these mutants, which can be problematic. Structural characterisation of the mutants will be investigated by cell surface expression including co-immunoprecipitation to confirm protein expression and prME heterodimerisation. Immunofluorescence will be used to view protein expression, co-localisation of prM and E and cell surface trafficking. Fluorescent activated cell sorting and flow cytometry will be used to determine cell surface expression. The elucidation of host-viral fusion of wild-type and mutant prME viral particles ideally would be studied by alternative pathways such as a fusion assay.

1.12.1. Specific Aims

1. Site-directed mutagenesis of the membrane-proximal (MPER) α-helical E2 domain of DENV E to obtain full-length prM and E mutant plasmids that will be used in all subsequent research (Chapter 3).

2. Develop a lentiviral expression system to assay fusion of these E2 mutants (Chapter 4).

3. Investigate and characterise the structure of prM and E mutants by cell surface expression and host-viral fusion in a mammalian cell line by:

a. FACS analysis to detect and quantify cell surface expression.
b. Protein expression confirmed by SDS-PAGE and Western immunoblot.
c. Immunofluorescence to confirm in-cell prM and E expression, co-localisation, and cell surface trafficking (Chapter 5).

4. Investigate the structure of prM and E mutants in a pSFV-based vector. Characterise these mutants for cell surface expression and host-viral fusion in an insect cell line by:

a. FACS analysis to detect and quantify cell surface expression.
b. Protein expression confirmed by SDS-PAGE and Western immunoblot.
c. Immunofluorescence to confirm in-cell prM and E expression, co-localisation, and cell surface trafficking (Chapter 6).

CHAPTER 2

MATERIALS AND METHODS

2.1. Vectors

2.1.1. pCI_NGCprME_opt_neo plasmid

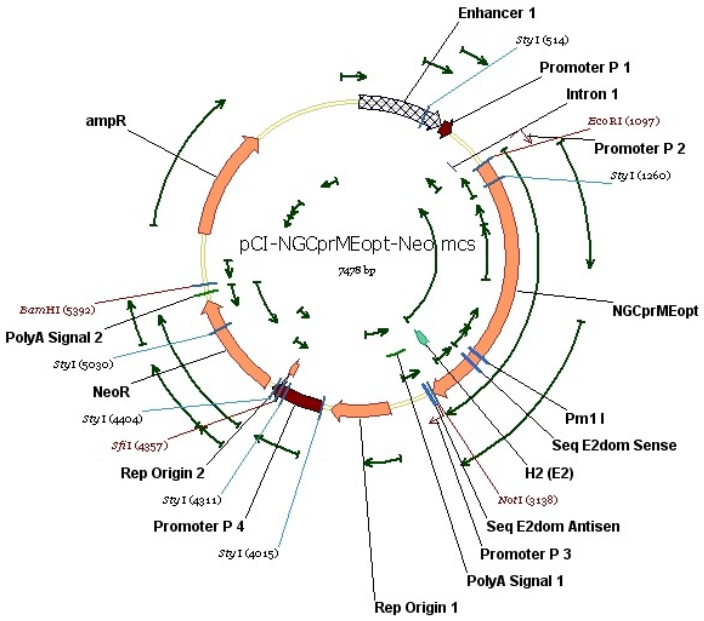

Figure 19. Plasmid map of pCI_NGCprME_opt_neo (New Guinea DENV 2, optimized, neomyocin). The vector contains the prME genes (E2 domain noted), NeoR and ampR genes.

Geneart designed pCI_NGCprME_opt_neo. The vector has a chimeric intron after the CMV promoter/enhancer to promote high levels of gene expression and a SV40 late polyadenylation signal to enhance RNA stability and translation. It has an ampicillin resistance gene as well as an additional gene for neomycin phosphotransferase, which confers resistance to the antibiotic G-418. A LacZ gene facilitates blue-white screening.

2.1.2. pSFV plasmids

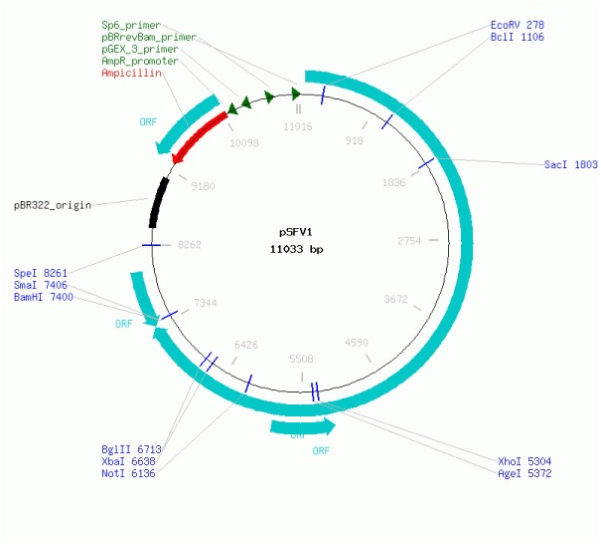

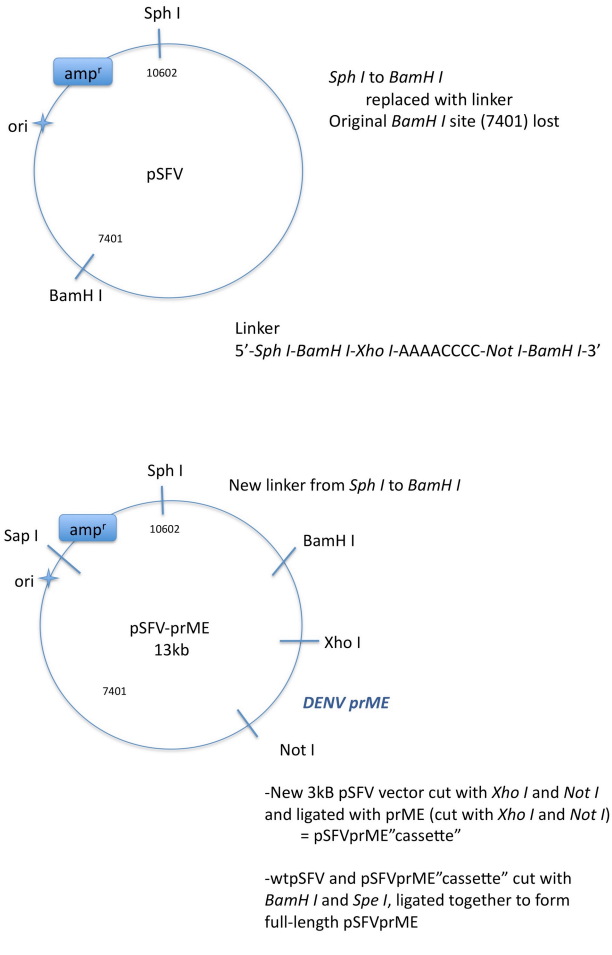

Figure 20. Plasmid map of pSFVprME. Displayed are the prME genes inserted into wild-type pSFV plasmid.

The pSFV replicon (Semliki Forest Virus) was acquired from Invitrogen. It is a full cDNA clone of SFV, with the genes encoding the structural proteins removed. The non-structural proteins, 26S subgenomic RNA promoter, 5' and 3' untranslated elements required for replication remain, and the vector system can be used to express genes in both mammalian and insect cells. The region between restriction sites *Sph I* and *BamH I* was replaced with a linker designed as follows: *Sph I* – *BamH I* – *Xho I* – AAAACCCC – *Not I* –*BamH I*. The original *BamH I* site was lost. This allowed for digestion with *Xho I* and *Not I* to insert prME, which was named the pSFVprME "cassette" vector. This was then digested with *BamH I* and *Spe I* and ligated with a digested full-length pSFV to make a vector that is full-length pSFV with prME cloned in.

The plasmid is linearised with *Spe I* and transcribed in vitro to produce RNA transcripts for transfection into C6/36 cells. Primers were designed to check insertion of prME and correct cloning direction as follows:

To sequence 5' end of prME in pSFVprME "cassette" vector:

PDP R1 (Rev)	GTACTGCACGCGGATCACGAT
prME_Seq_Rev_5'end	TGTCCTCGCACAGCTCG

To sequence 3' end of prME and check mutations in pSFVprME "cassette" vector:

PDP R1 (Rev)	GTACTGCACGCGGATCACGAT
prME_SeqMut_Fwd_3'end	TGCAGTACGAGGGCGAC

To sequence pSFV to check prME insertion and correct orientation:

PDP R1 (Rev)	GTACTGCACGCGGATCACGAT
prME_InsCheck_Fwd	TCGTGTGTGTAAGCACTCTATG

2.3.1. Lentiviral plasmids: pRRE, pREV, pLL3.7, and pMD.G

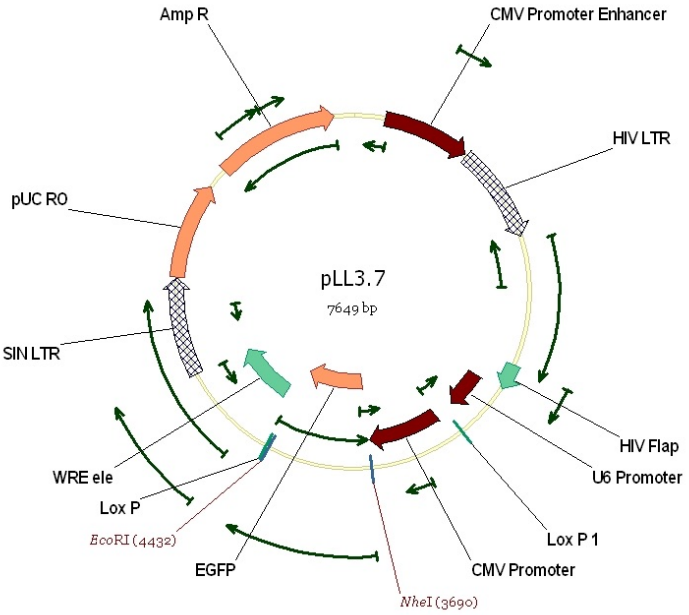

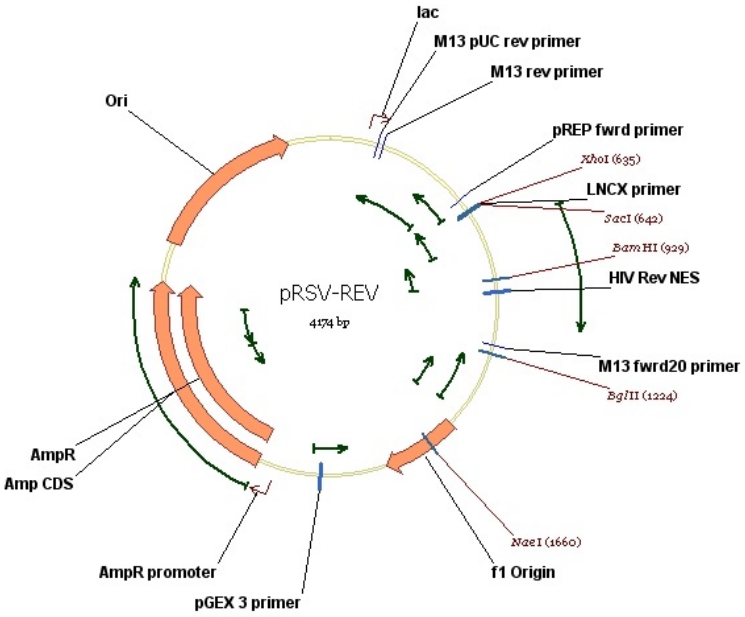

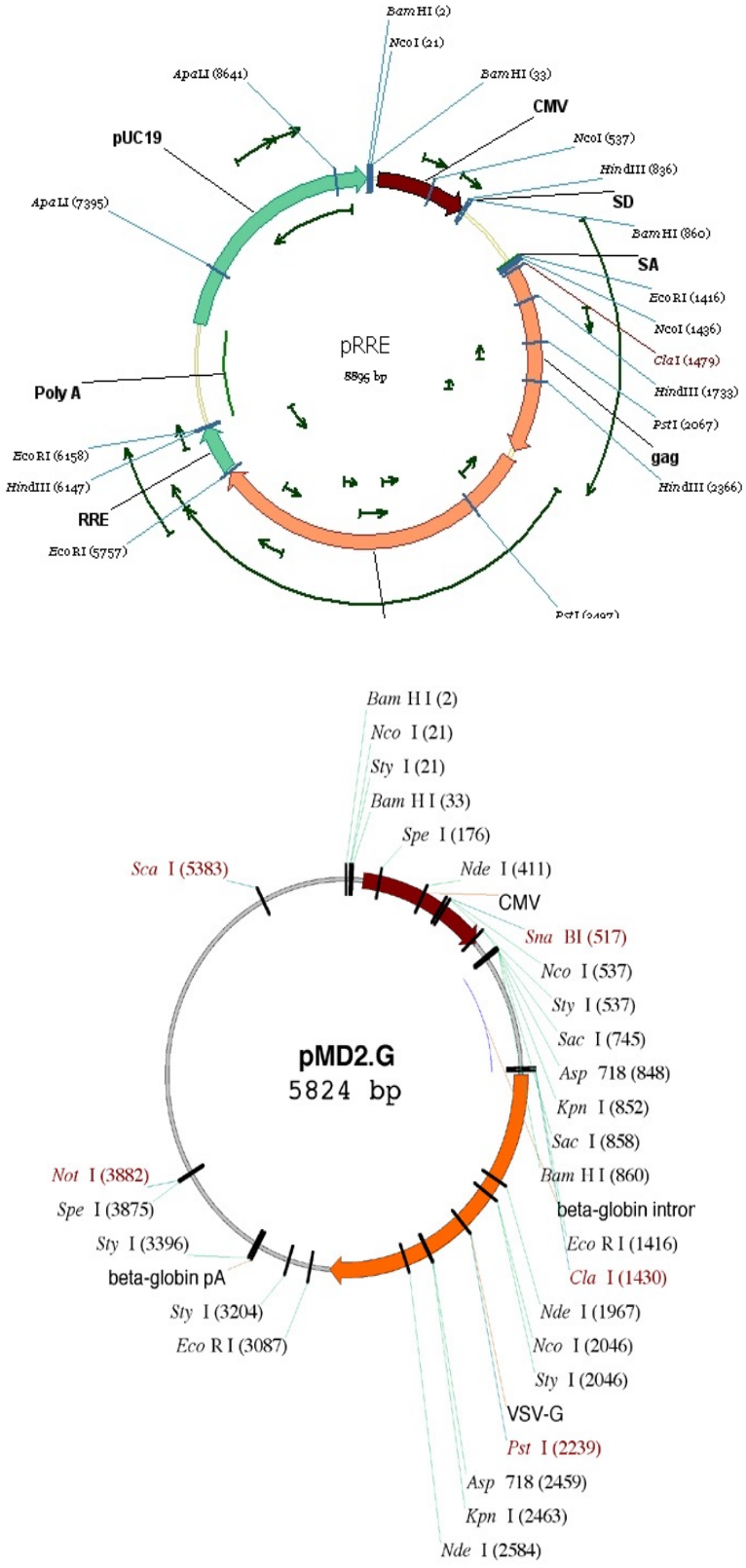

Figure 21. Lentiviral plasmids pLL3.7 (luc+), pRRE, pREV, and pMD2.G (VSV-G).

Lentiviral vector constructs have proven to be very productive in terms of transduction due to their ability to infect both replicating and non-replicating cells. A four-plasmid vector system is used in the third generation lentiviral expression system (figure 21). The accessory proteins such as tat, vrf, vpr and nef are deleted from the original plasmid. Also, the env gene is replaced with a VSV-G (Vesicular Stomatitis Virus Envelope Protein) and is placed on a third helper plasmid. By splitting the vector system into four plasmids, the number of recombination events required to form a complete replicative competent virus increases yet this system is safer to use. The four-plasmid system consists of pRRE (gag, pol), pREV (production and packaging), pLL3.7 (GFP fluorescent protein), and pMD.G (VSV-G envelope protein). pMD.G can also be replaced with pCI_NGCprME_opt_neo to use prME envelope protein in lieu of VSV-G. Dr. Nigel MacMillan generously provided the plasmids.

2.3.1.1. pLL3.7, pGL-3, and pLL3.7_luc+

Luciferase was cloned into pLL3.7 in lieu of GFP. This was to test the expression system via a luciferase assay instead of FACS. pLL3.7 vector was digested with *Nhe I* and *EcoR I,* which results in a 6907 bp vector and a 742 bp insert containing eGFP. pGL-3 (IMB/Invitrogen) was digested with *Xba I* and *Bgl II* resulting in a 1706 bp insert containing the luciferase gene. These plasmids were digested overnight with Klenow fragment in the presence of dNTPs and the correct sized bands (6907 bp for pLL3.7 and 1706 bp for pGL-3) were gel extracted. The two bands were then ligated together to form pLL3.7_luc+.

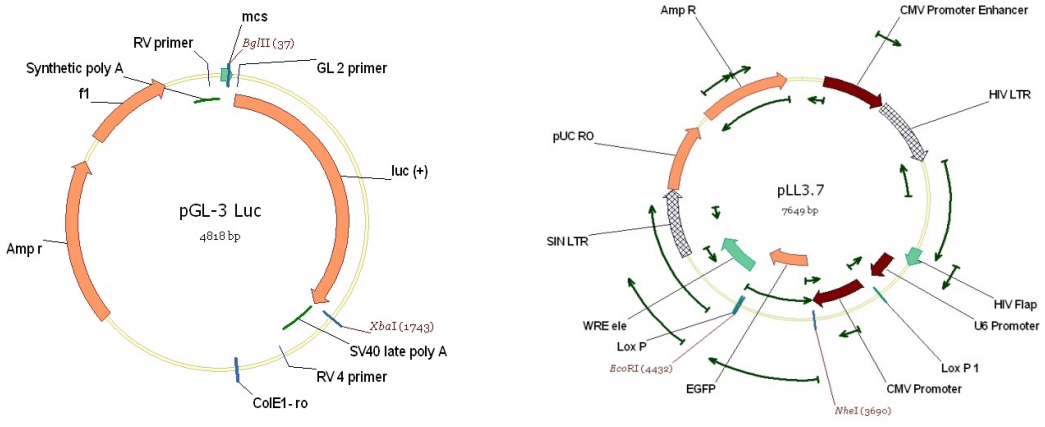

Figure 22. Plasmid maps for cloning of the luciferase gene. pGL-3 (right) and pLL3.7 (left). pGL-3 was cut with *Bgl II* and *Xba I* and pLL3.7 was cut with *Nhe I* and *EcoR I*. The luc+ region from pGL-3 was ligated into the GFP region in pLL3.7 via blunt-end cloning. The luciferase assay can then be used in lieu of FACS.

2.2. Prokaryotic cell culture

2.2.1. Culture

Escherichia coli strains used for routine culture work were either XL-10 Gold or H5-α cells. Chemically competent cells were routinely made and stored at –80ºC until required. Bacteria were cultured in Luria-Broth (LB; 10 g/L tryptone or peptone, 5 g/L sodium chloride, 10 g/L yeast extract) with 100 μg/ml ampicillin. Agar plates were prepared by addition of 16 g/L bactoagar to LB media prior to autoclaving, and 100 μg/ml ampicillin prior to plating. Bacterial plates were grown at 37ºC for 16-24 hours.

2.2.2. Transformation

Competent cells were thawed on ice, and 1 μl of plasmid DNA was added to a 100 μl aliquot of cells. The mixture was flicked gently to mix, and incubated for 15 minutes on ice before being heat shocked at 42 ºC for 2 minutes. After recovering on ice for a further 3 minutes 900 μl LB media at room temperature (RT) was added and cells incubated at 37 ºC with shaking for 30 minutes. Approximately 100 μl cells was plated and grown overnight. Cells were plated on ampicillin agar plates and grown overnight.

2.2.3. DNA purification

Miniprep cultures of 3-5 ml were inoculated with a single colony from a fresh ampicillin plate and grown overnight at 37 °C at 200 rpm in an environmental shaker. DNA was extracted using a Invitrogen's Purelink Plasmid Miniprep kit according to the manufacturer's instructions. Maxiprep cultures of 50-100 ml were used to grow up large amounts of DNA for transfection experiments. Maxipreps were inoculated from a miniprep grown for 8 hours. Maxiprep cultures were grown for 16 hr at 37 °C at 200 rpm in an environmental shaker and purified using Purelink Plasmid Maxiprep kits (Invitrogen) to make sure endonucleases were removed.

2.3. DNA Engineering

2.3.1. Restriction endonuclease digests

Plasmid DNA was digested using approximately 1 μg of enzyme to 1 μg DNA. Restriction reactions were carried out in the appropriate buffers supplied with the enzymes (New England Biolabs) and bovine serum albumin (BSA) where appropriate. All digests were carried out at the recommended temperature for 2 hours to overnight.

2.3.2. Ligation

Ligations were performed using 100 ng of vector and a vector to insert molar ratio ranging from 1:1 for blunt end ligations to 1:3 for cohesive end ligations, although a range of ratios were sometimes used to optimise cloning. Ligations were performed using Quick T4 DNA Ligase Kit (NEB, New England Biolabs) using the recommended amount of buffer and ligase. Reactions were incubated for 10 minutes at RT and transformed immediately.

2.3.3. Gel electrophoresis

Agarose gels were 1 % agarose in 50 or 100 ml TAE buffer (0.014 M Tris-acetate and 0.001 M EDTA pH 8.0) and contained 2 or 4 μl ethidium bromide. Separation was performed by electrophoresis in submerged horizontal trays with TAE buffer at 100
Volts for one hr. Prior to loading, the DNA samples were mixed with 2 μl loading buffer (10mM Tris-HCl, 1 mM EDTA, 3 % Ficoll, 0.5 % bromophenol blue, 0.5 % xylene cyanol). Generuler 1kB Mix DNA marker was used (Fermentas). DNA was visualised using an ultraviolet transilluminator and photographed.

2.3.4. Gel Extraction

DNA fragments were extracted from agarose gel blocks using Purelink Quick Gel Extraction kit (Invitrogen) or Zymoclean Gel DNA Recovery kit (Zymo) according to the manufacturer's instructions.

2.3.5. Site Directed mutagenesis

PCR mutagenesis was performed with complimentary oligonucleotides in a touchdown, two-step PCR with 1 Unit of *Phusion* polymerase (Finnzyme), using Buffer GC, 0.5 μM primers, 50 ng NGC_prME_opt_neo template, 0.5 mM dNTPs, 1.5 mM $MgCl_2$ and 5% DMSO in a 50 μl reaction. Oligonucleotides were ordered through Sigma-Genosys and stored at 100 μM concentrations in 1X TE. The following cycling conditions were used in an ABI GeneAmp PCR System 2400 or Eppendorf Thermocycler Personal: 98ºC for 1 minute, 2 cycles of 98ºC for 10 seconds, 60ºC for 30 seconds, and 72ºC for 10 minutes after which, the primer solutions are added to the reactions. The second stage PCR begins with 98ºC for 2 minutes, followed by 30 cycles of 98ºC for 20 seconds and 72ºC for 6 minutes with a final extension of 72ºC for 10 minutes and a 4ºC hold. PCR

amplicon was purified with PureLink PCR Purification kit (Invitrogen), treated with *Dpn I* (New England Biolabs), purified again and transformed as above. Primers designed for site-directed mutagenesis of the α-E2 helix are listed in table 1.

Mut.	Forward Primer	Reverse Primer
F440A	5'-CACCAGGTG*GCC*GGAGCCATCTACGGA-3'	5'-GATGGCTCC*GGC*CACCTGGTGCAG-3'
F440Y	5'- CTGCACCAGGTG*TAC*GGAGCCATCTACGGA-3'	5'-TGGCTCC*GTA*CACCTGGTGCAGGGCCTT-3'
F448A	5'-GAGCCGCC*GCC*TCCGGCGTGT-3'	5'-GACACGCCGGA*GGC*GGCGG-3'
F448Y	5'-GCC*TAC*TCCGGCGTGTCCTGGACC-3'	5'-CGGA*GTA*GGCGGCTCCGTAGATGGCTC-3'
F422A	5'-GCAGCCTGGGCGGCGTG*GCC*ACCTCCATCGG-3'	5'-CCGATGGAGGT*GGC*CACGCCGCCCAGGCTGC-3'
F422Y	5'-GCAGCTGGGCGGCGTG*TAC*ACCTCCATCGG-3'	5'-CCGATGGAGGT*GTA*CACGCCGCCCAGGCTGC-3'
F429A	5'-GACACCGCCTGGGAC*GCC*GGCAGCCTGGGC-3'	5'-GCCCAGGCTGCC*GGC*GTCCCAGGCGGTGTC-3'
F429Y	5'-GACACCGCCTGGGAC*TAC*GGCAGCCTGGGC-3'	5'-GCCCAGGCTGCC*GTA*GTCCCAGGCGGTGTC-3'
Y444A	5'-GTGTTCGGAGCCATC*GCC*GGAGCCGCCTTCTCCG-3'	5'-CGGAGAAGGCGGCTCC*GGC*GATGGCTCCGAACAC-3'
Y444F	5'-GTGTTCGGAGCCATC*TTC*GGAGCCGCCTTCTCCG-3'	5'-CGGAGAAGGCGGCTCC*GAA*GATGGCTCCGAACAC-3'

Table 1. pCI_NGCprME_opt_neo oligonucleotides. These primers were used for site-directed mutagenesis of the α-E2 helix. Residues F440A/Y, F448A/Y, Y444A/F, F429A/Y, F422A/Y were mutated. The mutated codon is in italics.

2.3.6. Colony diagnostic PCR

Colony screening of mutants to confirm insertion of prME or linkers was performed with 1 colony diluted in 100 μl of water, of which, 1 μl was added to each PCR reaction. Colony diagnostic PCR was performed with 0.05 U/μl *Taq* polymerase (NEB), using 25 mM Tris pH 8.3, 50 mM KCl, 2.5 mM $MgCl_2$ and 20 μM primers. Oligonucleotides were ordered through Sigma-Genosys and stored at 100 μM concentrations in 1X TE.

The following cycling conditions were used in an ABI GeneAmp PCR System 2400 or Eppendorf Thermocycler Personal: 95ºC for 4 min, 30 cycles of 95ºC for 15 sec, 50ºC for 15 sec, 72ºC for 60 sec, a final extension of 72ºC for 5 min and a 4ºC hold. Non-purified

amplicon was digested with appropriate diagnostic restriction endonucleases and run against vector controls.

2.3.7. Sequencing

Plasmid DNA and sequencing oligonucleotides were submitted to the Australian Genomic Research Facility (AGRF). Sequences were analysed using Vector NTI version 10 (Invitrogen).

2.4. RNA Engineering

2.4.1. Plasmid precipitation and linearisation

RNA was precipitated with 1/10th volume of 3M Na acetate and three volumes of 100% EtOH. Samples were incubated on ice for 20 minutes or overnight at -20°C. Tubes were then centrifuged at top speed for 15-30 min at RT. Pellets were washed with 1 ml 70% EtOH then chilled in an ice bath for 10 minutes. Tubes were centrifuged at top speed for 5 minutes. EtOH was carefully removed and RNA was re-suspended in TE. RNA was linearised with *Spe I* in buffer # for 2 hours at 37°C.

2.4.2. RNA Transcription

In vitro transcription was performed in a 20 μl reaction containing 1 mg linearised cDNA, 80 mM Hepes – KOH (pH 7.5), 32 mM MgCl2, 2 mM spermidine, 40 mM dithio- threitol, 5 mM each of GTP, CTP and UTP, 1.5 mM ATP, 3.5 mM m7G(57)ppp(57)A cap analog (New England Biolabs) and 20–40 U SP6 RNA polymerase (Gibco BRL) or 2 ml SP6 RNA polymerase – pyrophosphatase mix (SP6 Ribomax kit, Promega). Following incubation at 40°C for four to six hours, the reaction mixture was either used directly for transfection or stored overnight.

2.4.3. RNA Transfection

RNA was transfected in C6/36 cells in 96-well plates. 0.4 μl of RNA and 0.8 μl of lipofectamine-2000 (Invitrogen) were added into 25 μl of SF media. After four to six hours, 50 μl of media was added to wells. At sixteen hours, media was taken off and cells were fixed. If a pH drop was tested, media was taken off and low pH media was added (5.5, 6 or 7.5 HCl adjusted pH, RPMI Hepes free, 15 mM MES). Samples were

incubated for three hours at 40°C. Cells were then fixed and stained with Hoechst and appropriate antibodies.

2.5. Eukaryotic cell culture

2.5.1. Maintenance of mammalian cell lines

Cell lines used were Vero (African Green Monkey Kidney), HEK 293T (Human Embryonic Kidney), PS-EK (Porcine Stable-Equine Kidney) and C6/36 (*Aedes Albopictus*), all of which were provided from Young laboratory stocks. Media was removed from the flasks and cells were washed with 1X PBS (Phosphate buffered saline solution). Trypsin was added (2 ml for a T_{75} flask) and incubated at 37º C for five (Vero) or seven minutes for PS-EK cells. Flask was tapped gently to loosen cells and media added at a 1:4 trypsin:media ratio. Cells were then split (e.g. 1:10 split uses 1 ml of cells and 9 ml of fresh media into a new T_{75} flask). Generally, Opti-mem I media was used with 10% fetal calf serum (FCS) for Vero cells, DMEM media + 10% FCS was used for HEK 293T and PS-EK cells. Flasks were incubated overnight at 37ºC and checked for confluency daily.

2.5.2. Cell line rescue and storage

Cell stocks were partially defrosted and 20 ml of appropriate media was used to wash them. Cells were centrifuged for 5 minutes at 120 x g, 4ºC. Supernatant was poured off and cells were re-suspended in 10 ml growth media. Cell solution was added to a T_{25} flask and incubated overnight. After confluent, cells were split into a T_{75} or T_{175} flask. To store cells, media was removed from the flasks and cells were rinsed 2x with 1X PBS. Flasks were trypsinised as above. Cells were resuspended in 10 ml fresh media and moved to a 25 ml Falcon tube. Cells were centrifuged for five minutes at 200 x g, 4ºC. Supernatant was poured off and cells were resuspended in ice-cold freezing media (40% Media, 10% DMSO, 50% FCS), (i.e. three ml for one T_{75} flask). Cells were stored at -80ºC overnight in an EtOH bath and then transferred to a liquid nitrogen dewer the following day.

2.5.3. Transfection

PS-EK, HEK 293T, or Vero cells were seeded (2 x 10^5 cells/ml) onto sterile coverslips in 24-well Falcon plates and grown overnight at 37ºC + 5% CO_2. 1 μg of DNA was added to 3 μl of Lipofectamine-2000 (Invitrogen). 50 μl of serum-free Opti-Mem I was added to a Falcon tissue culture tube with DNA or Lipofectamine. Solutions were incubated for five minutes and then added together and incubated a further twenty minutes. Mixtures were added to cells drop-wise and incubated for four to six hours at 37ºC + 5% CO_2. Media was then changed and cells were incubated for another 24 hours. Cells were then washed 1x in 1X PBS and fixed in 4% PFA (in PBS) for fifteen minutes at 4°C. If cells were permeabilised, PFA was discarded and 4% PFA + 0.2% TX100 added. Plates were incubated for fifteen minutes at 4°C and cells were washed with 1X PBS.

2.5.4. Infection

Cells were seeded (2 x 10^5 cells/ml) in six-well plates with 1.5 – 2 ml media and grown overnight at 37ºC + 5% CO_2. Media was removed and 1 ml serum-free (SF) media was added with virus neat and in dilutions (i.e. 5-fold) with a starting m.o.i. = 0.1 to 10 generally used. Cells were incubated for two hours and 3 ml complete media was added and incubated overnight. Cells were then washed and fixed as above.

2.5.5. Virus stock production

C6/36 (*Aedes albopictus*) cells were used to generate DENV-2 viral stocks. Sealed T_{175} flasks with 25 ml RPMI media (15 mM Hepes pH 7.3 and saturated sodium
Hydroxide) were incubated at 28°C. Cells were cultured to approximately 80% confluency and virus stock added at 1:10 dilution in SF media. Flasks were incubated at 28°C until cytophatic effects (CPE) such as synctial formation and irregular growth were observed. Supernatant was removed from the cells and clarified by centrifugation at 500 rpm for 5 minutes and stored at -80°C in 1 ml aliquots.

2.5.5.1. Plaque Assay

Viral stock titre was determined by plaque assay. Vero cells were seeded in 96-well plates at 200 μl, 1 x 10^5 cells/ml and cells were grown overnight. Cells were then washed with 1X PBS and virus stocks were diluted in series from 10^{-2} to 10^{-8} in SF media. Dilutions were transferred to the cells and incubated for two hours at 37C. Cells were

then overlayed with 1.5% carboxymethylcellulose (CMC) in Medium 199 (Life Technologies) with 2.5% FCS and incubated for four days at 37ºC. On the fourth day, the overlay was removed and cells were washed with 1X PBS. Cells were fixed in 200 μl ice cold 80% acetone in PBS for twenty minutes at -20°C and the plate was dried overnight. The plates were developed with 200 μl 9% MeOH/10%H2O2 for twenty minutes. Cells were then washed with PBS/0.1% BSA on a shaker. The plate was then blocked with 200 μl PBS/0.1% BSA. A 1:200 dilution (50 μl) of rabbit anti-NS1 polyclonal serum in PBS/0.1 % BSA was added and incubated for one hour at RT. The cells were then washed twice with 1X PBS/0.1 % BSA. A 1:500 dilution of secondary antibody, goat anti-rabbit peroxidase-conjugated) was added and cells were incubated for one hour at RT. The plate was washed with 1X PBS/0.1 % BSA. Plaques were visualised with 100 μl SIGMAFAST™ DAB by dissolving 2 DAB tablets and 2 H_20_2 tablets in 10 ml dH_20. The plate was incubated in the dark and when plaques were seen, the reaction was stopped by washing with dH_20. Plates were then scanned and plaques were counted. Viral titre was estimated.

2.6. Lentiviral expression system

2.6.1. Transfection

HEK 293Ts cells were seeded in twelve T_{75} flasks in DMEM + 10% FCS at low passage number (>15). Four plasmids were transiently co-transfected with 270 μg of pLL3.7 (eGFP), 176 μg of pRRE, 68 μg of pREV and 95 μg of pMD.G (VSV-G) (figure 21). Plasmids were mixed with 13.5 ml of 0.25M $CaCl_2$ and 13.5 ml 2X BBS solution. After a 15 minute incubation, the transfection mix was gently added to flasks drop-wise and incubated at 37°C overnight. The following day, cells were tested for visible GFP marker under fluorescent microscopy. Media was removed and 15 ml DMEM + 2% FCS was added to the flasks, which were incubated overnight at 37°C. Supernatant was pooled the following day for a total of 180 ml. Fresh DMEM + 2% FCS was added to the flasks, which were re-incubated overnight. A second pool was obtained the following day and added to the primary pool. Supernatant was filtered through a 0.45-μm filter. This supernatant should have had a viral titer of ~10^6 viral particles/ml. When a concentration step was performed, supernatant was centrifuged in Vivaspin columns (100,000 mwco) at 4°C, 3000 rpm. Ultracentrifugation was also performed where supernatant was

centrifuged at 70,000 x g and 20°C for 15-30 minutes. Supernatant was stored at 4°C if used immediately or at -20°C for less than a month or -80°C for periods over a month in 20 μl aliquots.

2.6.2. Transduction

HEK 293T cells were then seeded in 24 well plates (1 x 10^5 cells/500 μl) in PBS + 0.02% EDTA. A ten-fold serial dilution of lentiviral supernatant was prepared from undiluted to 50 μl diluted to 10^{-6} in 1X PBS. Viral dilutions were added to the cells, mixed and incubated at 37°C overnight. GFP fluorescence was visible 24 hours after transduction. Cells were further incubated for 24 hours, then washed twice with 1X PBS and re-suspended in 500 μl 1X PBS + 0.02% EDTA by vigorously pipetting up and down. Percentage of viable cells and fluorescent cells was determined by FACS analysis and a mock transduction was subtracted from sample numbers. The biological titer (BT = TU/ml) was calculated according to the formula: TU/μl = P X N / 100 x V) x 1/DF where P = % GFP+ cells, N = number of cells at time of transfection = 10^5, V = volume of dilution added to each well = 20 μl and DF = dilution factor = 1 (undiluted), 10^{-1} diluted 1/10, 10^{-2} dilution 1/100, and so on.

2.6.3. Luciferase assay

2.6.3.1. Transfection with control plasmids

Control plasmids pGL-3b ("basic", negative control), pCI (empty, negative control), pGL3c (positive "control", which contains *Photinus pyralis* firefly gene), and the engineered pLL3.7_luc+ were tested in a luciferase assay. Vero cells were seeded at 2.5 x 10^5 cells/100 μl in a 96-well plate and grown overnight. DNA was transfected at 0.2 μg with 0.5 μl of Lipofectamine-2000 in serum and phenol-red free media. Solutions were incubated for 5 minutes at room temperature, mixed and incubated again for twenty minutes. Solutions were added drop-wise to cells and incubated at 37°C for five hours. Solutions were taken off and 100 μl of serum and phenol-red free media was added. After overnight incubation, 100 μl of Bright Glo Luciferase substrate (Promega) was added to wells and immediately assayed on a luminometer (Althos Lucy).

2.6.3.2. Transfection to generate pseudotyped particles

The lentiviral plasmids were used to generate pseudotyped particles with pLL3.7_luc+ instead of the GFP version. HEK 293T cells were transiently co-infected with the four lentiviral expression constructs pRRE (packaging), pREV (Rev-expression), pMD.G (VSV-G envelope), and the luciferase expressing pLL3.7 luc+ reporter plasmid. Cells were seeded in 6-well plates at 2.5 x 10^5 cells/2 ml and transfected the following morning in the presence of Hepes-buffered H_20, 0.5M $CaCl_2$, and 2X BES buffer. Concentrations of plasmids were as follows: 2.5 μg pMD.G, 3.75 μg pRRE, 3.75 μg pREV, and 10 μg pLL3.7_luc+ per plate or per 12 ml. Two other controls were prepared with pGL-3b (basic, no luciferase activity) or pGL-3c (control, positive luciferase activity) used in lieu of pLL3.7_luc+. Media was changed one hour prior to transfection and 16 hours post-transfection. Supernatant was collected two days post-transfection and then again on day three, pooled, centrifuged and filtered through a 0.45 μm Millipore cartridge.

For infection, Vero cells were seeded at 2.5 x 10^5 cells/100 μl in a 96-well plate and grown overnight. Lentiviral supernatant was added in serum and phenol-red free media at 2.5-fold dilutions from 50 μl to 0 and incubated at 37°C for two hours, after which infection solutions were taken off and 100 μl of serum and phenol-red free media was added. After overnight incubation, 100 μl of Bright Glo Luciferase substrate (Promega) was added to wells and immediately assayed on a luminometer (Althos Lucy).

2.6.4. Cell viability assay

To confirm lentiviral particles were not cytotoxic to cells, a cell viability assay was carried out with luciferase lentivirus stocks (3-(4,5-Dimethylthiazol-2-yl)-2,5-diphenyltetrazolium bromide, a yellow tetrazole (MTT)). A 96-well plate was seeded with HEK 293T cells (2.5 x 10^5 cells/100 μl) and incubated overnight. The following day, cells were washed with 1X PBS and 100 μl of SF media was added. A serial dilution of lentivirus stock was prepared in SF media. Dilutions were added to the cells and incubated for the stated time. After incubation, media was replaced with the addition of 10 μl MTT (5 mg/ml in PBS, Sigma). Cells were incubated for 3 hours at 37°C in the dark. The dye was solubilized with 100 μl acidic isopropanol (0.04 M hydrocholoric acid in isopropanol) and the plate was incubated on an orbital shaker in the dark for four hours. The absorbance was read at 550 nm on a spectrofluorometer.

2.7. Protein Expression

2.7.1. Cell Lysate preparation

The day following transfection, six-well plates were incubated on ice and supernatants were removed. The supernatants were spun at 4500 rpm, 4°C for ten minutes and then frozen at -20°C. Plates were washed with 1 ml 1X cold PBS and cells were lysed with 200-500 μl cold 1X RIPA buffer (50 mM Tris-1 mM EDTA, 150 mM NaCl, 1% Triton-X, 1% Na-deoxycholate, and 0.1% SDS) + protease inhibitor cocktail (Roche). Cells were incubated on ice for five minutes and plate bottoms were scraped. Lysed cells were transferred to 1.5 ml eppendorf tubes and sheared with a 26cc needle and syringe. Cells were spun at 14,000 rpm, 4°C for ten minutes and supernatants were stored at -20°C in 25 μl aliquots. Alternatively, total cell lysates were prepared by solubilising cells in a sodium dodecyl-sulfate (SDS) hot lysis buffer. After PBS wash, 100 μl 2% SDS/66 mM Tris pH 7.4 (heated to near boiling) was added to the cells. Plate bottoms were then scraped and transferred to 1.5 ml eppendorf tubes. Lysates were sheared with a 26cc needle and syringe and boiled for two to three minutes. Cells were then centrifuged at 14,000 rpm for ten minutes at 4°C and stored as above.

2.7.2. SDS Polyacrylamide gel electrophoresis

To separate protein by electrophoresis, 12% resolving/4% stacking polyacrylamide gels were used. 5X SDS-PAGE sample buffer (with or without 1 μl 1M DTT) was added to the samples, which were then boiled for five minutes. Samples were loaded with 7 μl BioRad Dual Stain Precision Plus Protein marker and gels run at 110V for ten minutes until samples were at the end of the stacking gel and then run at 200V for 40-42 minutes.

2.7.3. Western transfer and Immunoblotting

Gels were removed from their cassettes and equilibrated in 1X Transfer buffer (25 mM Tris-HCl pH 8.3, 192 mM glycine, 20% (v:v) MeOH) along with blotting paper, nitrocellulose membrane and sponges for two to three minutes. Transfer cassettes were then assembled with four papers on either side of gels. Gels were transferred to nitrocellulose membranes under submerged conditions at 100V for one hour. Cassettes were disassembled and the membrane was placed in blocking solution (5% skim-milk powder (MP) in PBS or 1% BSA) overnight at 4°C or for one hour at RT. Membranes were blocked in 5% MP, 1X PBS for one hour at 4°C. Membranes were then incubated

with primary antibody at 37°C for one hour (or overnight at 4°C) at 1:1000 dilution (6 mg/ml stock) in 3 ml in a sealed bag, which was gently shaken every fifteen minutes. Membranes were washed with 3X PBS + 0.1% Tween for five to ten minutes and membranes were incubated for one hour at RT with conjugated secondary antibody (IR 800) at 1:10,000 in 5 ml. Membranes were then washed 3X PBS + 0.1% Tween for five to ten minutes and dried for five minutes under the biohazard hood. Membranes were then scanned on a Bio-RAD GS™-700 densitometer.

2.7.4. Immunofluorescence: Antibodies and Molecular Probes

After cells were fixed (4% paraformaldehyde (PFA) for 10 minutes at 4ºC) or fixed and permeabilised (4% PFA + 0.2% Triton-X for 10 minutes at 4ºC), cells were washed (1 ml PBS, 3X five minutes), air dried and stored at 4ºC. Cells were then stained with 30 μl of diluted DENV anti-E mAb 3H5 or 4G2 in PBS + 0.1% BSA. A 1:200 to 1:400 dilution was generally used. After incubation for one hour in the dark, coverslips were washed with 1 ml PBS, 3X for five minutes. Cells were dually labeled with 30 μl, 1:400 dilution of 0.5mg/ml Alexa-Flour 488 (Molecular Probes goat anti-mouse IgG conjugate) in PBS + 0.1% BSA and then washed as before. Coverslips were briefly dried on top of filter paper and mounted to microscope slides with Vectashield™ (Vector Labs). Cells were also stained with 30 μl, 1:10,000 dilution of Hoechst or propidium iodide where indicated. Dye-tracking studies were carried out with organelle dyes CMAC, CM DiI, WGA (Wheat Germ Agglutinin), and ER-Tracker, (Molecular Probes) at various concentrations. Cells were viewed with the Zeiss LSM 510 Meta Confocal Microscope, captured at 40-160X magnification with the provided Zeiss software.

2.7.5. Immunofluorescence: Flow Cytometry

Plate wells were washed with 1 ml 1X PBS and incubated with 200 μl Trypsin for 5 minutes at 37ºC. Cells were gently removed from the wells with 1 ml media and transferred to 15 ml Falcon tubes. Cells were then centrifuged at 300 x g for 5 minutes and washed 3X with 1 ml 1X PBS. Cells were fixed (1% paraformaldehyde (PFA) for 10 minutes at 4ºC), centrifuged and cell pellets were re-suspended in 500 μl 0.5% PFA. FACS data was acquired within three days, usually the following day (FACS BD LSRII and BD FACSDiva software).

CHAPTER 3

RESULTS: DESIGN of pClprME_opt_neo MUTANT PLASMIDS

3.1. Introduction

PCR mutagenesis was performed in a touchdown, two-stage PCR with *Phusion* polymerase and NGC_prME_opt_neo template [82]. All ten MPER E2 mutants were produced with single-point mutation oligonucleotides. The first PCR stage cycling conditions were as follows: 98ºC for one minute, two cycles of 98ºC for ten seconds, 60ºC for thirty seconds, and 72ºC for ten minutes after which, the primer solutions are added to the reactions. This decreases primer-dimer formation and thus increases affinity for the template. The second stage PCR begins with a 98ºC melt for two minutes, followed by thirty cycles of 98ºC for twenty seconds and 72ºC for six minutes with a final extension of 72ºC for ten minutes and a 4ºC hold. With *Phusion* polymerase, it is possible to mutate one amino acid while maintaining a high degree of fidelity throughout the 7.4 kB plasmid. Following cloning, the mutated plasmids were sequenced for the full 7400 base pairs. Samples were submitted to the Australian Genomic Research Facility (AGRF) and sequences were analysed using Vector NTI version 10 (Invitrogen).

3.2. Results

The touchdown, two-stage PCR with *Phusion* polymerase was optimised to increase specific amplicon and reduce non-specific product. To optimise this long PCR, additional enzyme was added halfway through the reaction to prevent enzyme-deficiency, DMSO was increased to 5%, $MgCl_2$ was increased to 3.0 mM, annealing temperatures were lowered from 65 to 60ºC and the master mix buffer was changed from Buffer HF (high fidelity) to GC (high GC content in template). Although there was a large amount of non-specific product, the amplicon was sufficiently identifiable to continue with cloning (Mutants F422A/Y and F448Y/A shown in figure 23).

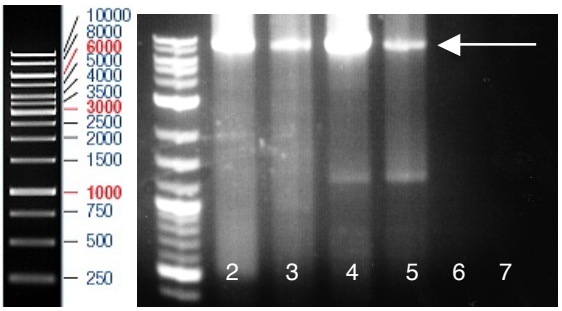

Figure 23. Two stage PCR amplicon with *Phusion*. Pooled amplicon (arrow) F440A, F440Y, F448A, and F448Y, Lanes 6 and 7 are no primer controls. This amplicon was subsequently digested with *Dpn I* and then transformed. (MassRuler DNA Ladder Mix, Thermo Scientific)

PCR amplicon was then pooled and purified, treated with *Dpn I* to render inert any remaining supercoiled plasmid and then purified again. Mutated plasmids were then transformed into TopTen competent cells. Four or more colonies were chosen and DNA minipreps were made (figure 24).

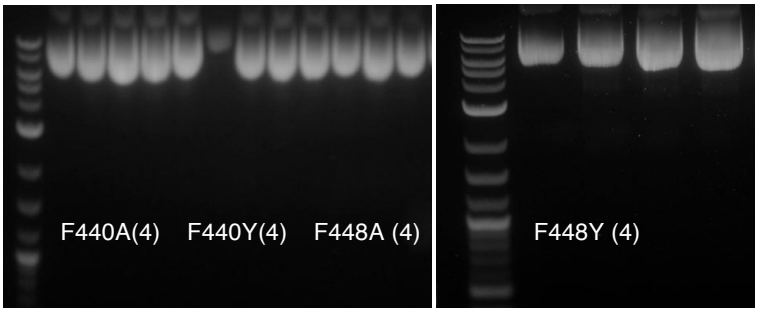

Figure 24. Mutant plasmid minipreps. **[Left]** F440A DNA plasmid minipreps 1-4, F440Y 1-4 and F448A 1-4. These mutated plasmids were from transformed competent cells after PCR, *Dpn I* treatment and purification. **[Right]** Mutant plasmids F448Y 1-4.

Plasmids were then sequenced and results confirmed the single point mutation with 1.5 kB sequenced (Table 2). Using primers outside the prME region, the complete plasmid was then sequenced to confirm no other mutations, deletions or insertions occurred (see Appendix). Maxipreps were then made with Invitrogen Pure-link plasmid kit to ensure a high degree of purity without any endonuclease activity.

420

F422A

W	D	**A**	G	S	L	G	G	V	**F**	T	S	I	G	K	A	L	H	Q	V	**F**	G
CTG	GGA	**GCC**	CGG	CAG	CCT	GGG	CGG	CGT	GTT	CAC	CTC	CAT	CGG	AAA	GGC	CCT	GCA	CCA	GGT	GTT	CGG

A	I	**Y**	G	A	A	**F**	S	G	V	S
AGC	CAT	CTA	CGG	AGC	CGC	CTT	CTC	CGG	CGT	GTC	C

F429A

W	D	**F**	G	S	L	G	G	V	**A**	T	S	I	G	K	A	L	H	Q	V	**F**	G
CTG	GGA	CTT	CGG	CAG	CCT	GGG	CGG	CGT	**GCC**	CAC	CTC	CAT	CGG	AAA	GGC	CCT	GCA	CCA	GGT	GTT	CGG

A	I	**Y**	G	A	A	**F**	S	G	V	S
AGC	CAT	CTA	CGG	AGC	CGC	CTT	CTC	CGG	CGT	GTC	C

F440A

W	D	**F**	G	S	L	G	G	V	**F**	T	S	I	G	K	A	L	H	Q	V	**A**	G
CTG	GGA	CTT	CGG	CAG	CCT	GGG	CGG	CGT	GTT	CAC	CTC	CAT	CGG	AAA	GGC	CCT	GCA	CCA	GGT	**GCC**	CGG

A	I	**Y**	G	A	A	**F**	S	G	V	S
AGC	CAT	CTA	CGG	AGC	CGC	CTT	CTC	CGG	CGT	GTC	C

Y444A

W	D	**F**	G	S	L	G	G	V	**F**	T	S	I	G	K	A	L	H	Q	V	**F**	G
CTG	GGA	CTT	CGG	CAG	CCT	GGG	CGG	CGT	GTT	CAC	CTC	CAT	CGG	AAA	GGC	CCT	GCA	CCA	GGT	GTT	CGG

A	I	**A**	G	A	A	**F**	S	G	V	S
AGC	CAT	**GCC**	CGG	AGC	CGC	CTT	CTC	CGG	CGT	GTC	C

F448A

W	D	**F**	G	S	L	G	G	V	**F**	T	S	I	G	K	A	L	H	Q	V	**F**	G
CTG	GGA	CTT	CGG	CAG	CCT	GGG	CGG	CGT	GTT	CAC	CTC	CAT	CGG	AAA	GGC	CCT	GCA	CCA	GGT	GTT	CGG

A	I	**Y**	G	A	A	**A**	S	G	V	S
AGC	CAT	CTA	CGG	AGC	CGC	**GCC**	CTC	CGG	CGT	GTC	C

F422Y

W	D	**Y**	G	S	L	G	G	V	**F**	T	S	I	G	K	A	L	H	Q	V	**F**	G
CTG	GGA	**TAC**	CGG	CAG	CCT	GGG	CGG	CGT	GTT	CAC	CTC	CAT	CGG	AAA	GGC	CCT	GCA	CCA	GGT	GTT	CGG

A	I	**Y**	G	A	A	**F**	S	G	V	S
AGC	CAT	CTA	CGG	AGC	CGC	CTT	CTC	CGG	CGT	GTC	C

F429Y

W	D	**F**	G	S	L	G	G	V	**Y**	T	S	I	G	K	A	L	H	Q	V	**F**	G
CTG	GGA	CTT	CGG	CAG	CCT	GGG	CGG	CGT	**TAC**	CAC	CTC	CAT	CGG	AAA	GGC	CCT	GCA	CCA	GGT	GTT	CGG

A	I	**Y**	G	A	A	**F**	S	G	V	S
AGC	CAT	CTA	CGG	AGC	CGC	CTT	CTC	CGG	CGT	GTC	C

F440Y

W	D	**F**	G	S	L	G	G	V	**F**	T	S	I	G	K	A	L	H	Q	V	**Y**	G
CTG	GGA	CTT	CGG	CAG	CCT	GGG	CGG	CGT	GTT	CAC	CTC	CAT	CGG	AAA	GGC	CCT	GCA	CCA	GGT	**TAC**	CGG

A	I	**Y**	G	A	A	**F**	S	G	V	S
AGC	CAT	CTA	CGG	AGC	CGC	CTT	CTC	CGG	CGT	GTC	C

420

Y444F

W	D	**F**	G	S	L	G	G	V	**F**	T	S	I	G	K	A	L	H	Q	V	**F**	G
CTG	GGA	CTT	CGG	CAG	CCT	GGG	CGG	CGT	GTT	CAC	CTC	CAT	CGG	AAA	GGC	CCT	GCA	CCA	GGT	GTT	CGG

A	I	**F**	G	A	A	**F**	S	G	V	S
AGC	CAT	**TTC**	CGG	AGC	CGC	CTT	CTC	CGG	CGT	GTC	C

F448Y

W	D	**F**	G	S	L	G	G	V	**F**	T	S	I	G	K	A	L	H	Q	V	**F**	G
CTG	GGA	CTT	CGG	CAG	CCT	GGG	CGG	CGT	GTT	CAC	CTC	CAT	CGG	AAA	GGC	CCT	GCA	CCA	GGT	GTT	CGG

A	I	**Y**	G	A	A	**Y**	S	G	V	S
AGC	CAT	CTA	CGG	AGC	CGC	**TAC**	CTC	CGG	CGT	GTC	C

Table 2. Mutant plasmid sequences. Mutants F/Y → A showing the nucleotide change to GCC and the amino acid single point mutation. Mutants F/Y → Y showing the change to TAC.or TTC and the single point mutations. Mutants were then sequenced for the complete prME region (see Appendix A).

The single-point mutations (F422A/Y, F429A/Y, F440A/Y, Y444A/Y, F448A/Y) reside in ten separate NGC_prME_opt_neo plasmids, which allow for singular examination of the group substitutions previously made by the Young laboratory. The single amino acid changes were then examined for their role in structural changes of E, including prM heterodimeric formation and secretory pathway.

CHAPTER 4

RESULTS: CONSTRUCTION OF LENTIVIRAL PSEUDOTYPED PARTICLES

4.1. Introduction

For the second aim of this project, a lentiviral expression system was developed as an alternative fusion assay to test MPER E2 mutants. Two separate four-plasmid systems from Dr. Nigel MacMillan (Diamantina Institute, University of Queensland) and Dr. Rod Minchin (School of Biomedical Sciences, University of Queensland) were acquired and transiently co-transfected by calcium-phosphate precipitation into HEK 293T cells (refer to materials and methods section for description of this four-plasmid system). Transfection in HEK 203T cells results in lentivirus with the chosen envelope protein displayed (figure 25). These transduction-ready pseudotyped lentiviral particles infect target cells by fusion, which tests fusion capability. After uncoating and reverse transcription, the provirus is integrated, which results in the target cell stably expressing the reporter gene, eGFP. After viral RNA translation, assembly, and budding, mature lentivirus is released studded with the chosen envelope protein and expressing eGFP.

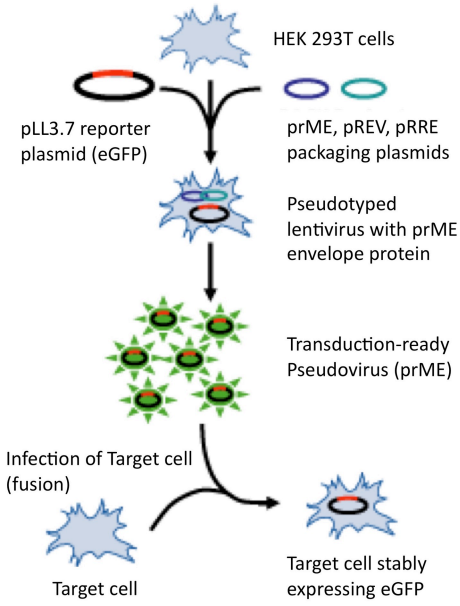

Figure 25. Development of lentiviral expression system. Pseudotyped lentiviral particles are made with the four-plasmid system containing either VSV-G or Dengue prME as the envelope protein. After these viral particles infect target cells (by fusion of pseudovirus to target cells), they then stably express the reporter plasmid eGFP.

Wild-type prME was tested, along with the control envelope protein VSV-G (Vesicular Stomatitis Virus). These lentiviral supernatants were titrated neat or concentrated (up to

60-fold) with either HEK 293T or Vero cells. Cells were then tested for positive eGFP (green fluorescent protein) expression by flow cytometry. Development of this expression system initially failed to result in a reproducible, efficient system to test fusion of E2 mutants determined by wild-type prME results. In an attempt to optimise expression, several variables were individually modified, including transfection with or without polybrene addition; different ratios of plasmids; or small (T_{75}) or large scale cultures (10+ T_{175} flasks) of HEK 293T cells. With these variables tested in conjunction or separately, GFP-expressing cells were, on average, less than 20% of the total cell population. The highest percentages were achieved with plasmids in the transfection ratio of (pREV: pRRE: pLL3.7: pMD.G) 1: 2.5: 4: 1.5, transduction with cells of low passage number (>15) and viral harvests that were relatively fresh (within 2 weeks). However, even after optimisation, repeat transductions resulted in large variations in the percentage of GFP positive cells. Twenty-five transfection trials were conducted to create the pseudotyped particles followed by transduction to test viral supernatants.

4.2. Results: Transfection of cells to generate pseudotyped viral particles and transduction of cells to test viral particles with VSV-G or DENV prME

Preliminary transductions with the VSV-G (positive control) pseudotyped particles were conducted on Vero cells and resulted in low percentages of cells taking up the virus (figure 26, A). The background level of fluorescence was 5.2%. Additions of viral supernatant ranging from 10^{-1} to $10^{2.8}$ μl resulted in positive fluorescence, after background subtraction, peaking at 4.5% with 10^{1} μl of virus supernatant. Samples should optimally have, at minimum, 10,000 viable cells to acquire a significant sample size for fluorescence versus background fluorescence. In this experiment, cells counted ("number of events") were low, ranging from 785 to 1924, which indicated that the cells did not survive the preparation, or were lost, prior to reading. There was no causal trend with a larger volume of virus added; the higher volume of virus added did not increase the number of cells fluorescing. Subsequent trials with VSV-G and Vero or HEK 293T cells produced negligible percentages of positive cells ranging from 0-0.4% even with 10,000 cells counted (data not shown). Without a stably fluorescing positive control in VSV-G, there is no comparative example for prME.

DENV prME viral supernatant was prepared and Vero cells transduced, which resulted in percentages of positive cells ranging from 1 to 13.4% for 10^1 μl with a possible best range of supernatant added from 10^1 to $10^{1.9}$ μl (13.4 to 10.1%), (figure 26, B). Cells counted were higher with an average of 6400. Unfortunately, subsequent trials with DENV prME and VSV-G, prepared in parallel, produced fluctuating and low positive percentages acquired (data not shown).

It was possible that the viral supernatants were too dilute, therefore, supernatants were concentrated in Vivaspin centrifugation columns (mwco 100,000) (N. Macmillan, personal communication). A concentrated VSV-G lentiviral supernatant was prepared and transduced into HEK 293T cells (figure 26, C). There was significant cell loss as depicted by the percentage of viable cells, which ranged from 2.3 to 3.6%, 0.4 to 1.3% of which were positively fluorescing. These low positive cell percentages were typical of many trials conducted with fresh or stored supernatant as well as secondary trials conducted immediately following promising results.

A concentrated stock of prME was prepared and after HEK 293T cell transduction, higher percentages of positive cells were seen, which peaked at 53.6% with 1 μl of 10^{-2} dilution (figure 26, D and E). The highest percentages were generally seen with the lowest amount of virus applied. This was repeated in three subsequent experiments with this stock of concentrated virus and results could not be replicated. This might indicate that the freshness of the supernatant is important or that the infective particles are unstable.

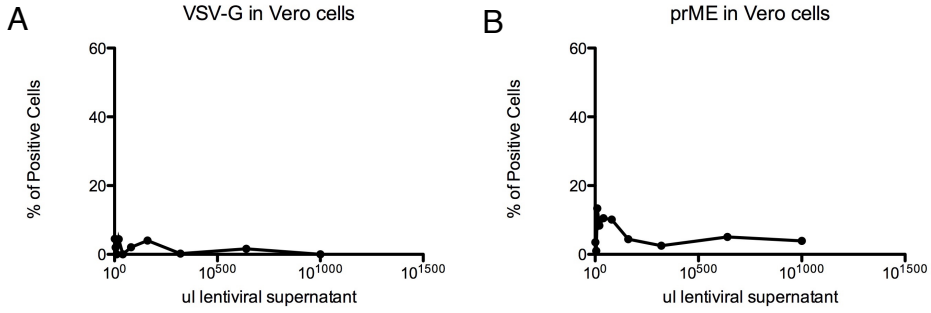

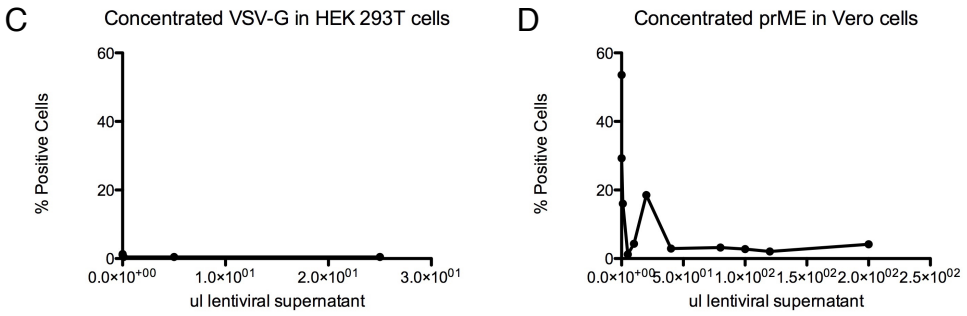

E

Sample	Description	Total %	% Positive cells
2-6	Mock	2.9	
1-1	10^{-2} dilution	56.5	53.6
1-2	10^{-1}	32.2	29.3
1-3	$10^{0.5}$ μl	18.9	16
1-4	$10^{0.7}$ μl	4.1	1.2
1-5	10^{1} μl	7.2	4.3
1-6	$10^{1.3}$ μl	21.4	18.5
2-1	$10^{1.6}$ μl	5.8	2.9
2-2	$10^{1.9}$ μl	6.1	3.2
2-3	10^{2} μl	5.7	2.8
2-4	1.2 x 10^{2} μl	5	2.1
2-5	2 x 10^{2} μl	7.1	4.2

Figure 26. Flow cytometry of Vero cells transduced with prME lentiviral pseudotyped particles. **[A]** Vero cells transduced with the control VSV-G. Cells were transduced with neat preparations of viral supernatant from 0 – 1 ml. The % Total is the percent of viable cells detected and fluorescing and % positive cells is percentages with background (mock) subtracted. Results were variable, with the highest percentage at 4.5% (Standard deviation (SD) = 1.86). **[B]** Vero cells transduced with prME. Cells were titrated with viral supernatant neat from 0 – 1 ml. Results were variable, with the highest percentage at 13.4% (SD = 4.06). **[C]** Vero cells transduced with concentrated VSV-G. Cells were transduced with neat preparations of viral supernatant from 0 – $10^{1.4}$ μl. Results varied from 1.3 to 0.4% with 10,000 cells counted (SD = 0.42). **[D + E]** Vero cells transduced with concentrated prME**.** Cells were transduced with viral supernatant 2 x 10^{2} μl neat to 10^{-2} dilutions. Results varied from 53.6 to 1.2%, with a trend towards the highest percentage of positive cells for the lowest amount of virus (10^{-2} dilution) with one exception at $10^{1.3}$ μl of supernatant (SD = 16.32).

Pseudotyped lentiviral particles of VSV-G and prME were tested together with supernatant titrated from neat to 125-fold dilutions (figure 27). VSV-G supernatant did not show any positive fluorescing cells while prME gave a low positive percent population from 0.1 to 1.6%. These results show, again, the low positive percentages often achieved even with fresh lentiviral supernatant.

Concentrated lentiviral supernatant of wild-type prME was then tested on Vero cells (figure 27). Supernatant was added at $10^{1.7}$ μl and in subsequent 5-fold dilutions to 2.4 x 10^{-4} μl. This transduction showed a clear trend with 2 and 5.2% positive cells at the highest volume added followed by a peak of 12.3% at the 25-fold dilution and a following

decline in positive percentages. This transduction was repeated with the supernatant but percentages were low or negligible.

A

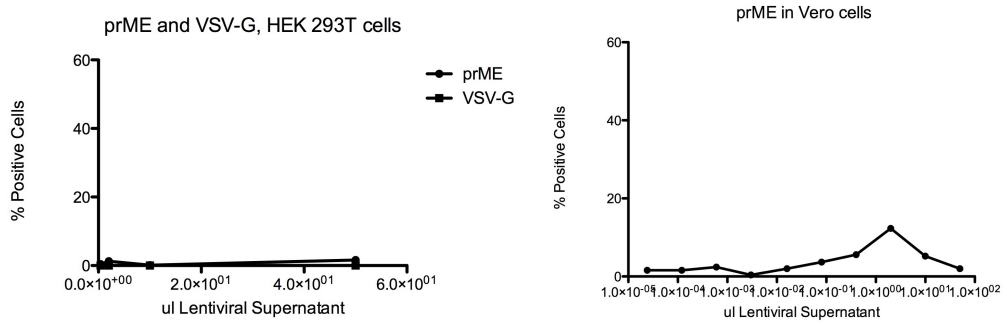

B

prME in Vero cells TU/ml calculated

μl added	% positive	No. of cells	No. of positive cells	per ul	TU/ml
5 x 10^{1}	2	1.28x10^{6}	25600	512	5.120x10^{5}
1 x 10^{1}	5.2	1.28x10^{6}	66560	6656	6.656x10^{6}
$10^{0.3}$	12.3	1.28x10^{6}	157440	78720	7.872x10^{7}
4x10-^{1}	5.6	1.28x10^{6}	71680	179200	1.792x10^{8}
8x10-^{2}	3.7	1.28x10^{6}	47360	592000	5.920x10^{8}
1.6x10-^{2}	2	1.28x10^{6}	25600	1600000	1.600x10^{9}
3.0x10-^{3}	0.4	1.28x10^{6}	5120	1706667	1.707x10^{9}
6.0x10-^{4}	2.4	1.28x10^{6}	30720	5.1E+07	5.120x10^{10}
1.2x10^{-4}	1.6	1.28x10^{6}	20480	1.7E+08	1.707x10^{11}
2.4x10^{-4}	1.6	1.28x10^{6}	20480	8.5E+08	8.533x10^{11}

Figure 27. Flow cytometry of HEK 293T cells transduced with lentiviral pseudotyped particles with VSV-G or prME. **[A Left]** Results for prME varied from 0.1% to 1.6% (SD = 0.71). There were no cells fluorescing with VSV-G. **[A Right]** Flow cytometry of Vero cells transduced with lentiviral pseudotyped particles with a concentrated stock of prME. Cells were transduced with 5-fold dilutions of concentrated supernatant. Results show a peak at the 25-fold dilution of 12.3% with a steady decline with subsequent dilutions (SD = 3.45). **[B]** The viral TU/ml was calculated by taking the percentage of positive cells, the number of cells processed and volume.

A concentrated stock of VSV-G lentiviral supernatant was prepared and tested with HEK 293T cells. When lentiviral dilutions were compared with the mock control, there was no population of cells fluorescing. Figure 28 shows the percentage of non-viable cells detected by the cytometer, which is designed to find viable cells that are the correct morphology, i.e. intact and spherical. The graph shows the mock sample with 15% non-viable cells but with lentiviral supernatant added, that percentage increases dramatically to 47.8 – 68.5% with the highest volume added, only decreasing at the 10^{-1} dilution. In all

experiments prior to this, the positive population was taken from the viable cell population count. This shows that with the addition of lentivirus, large populations of cells die, either by exocytosis of the virus or apoptosis after transduction.

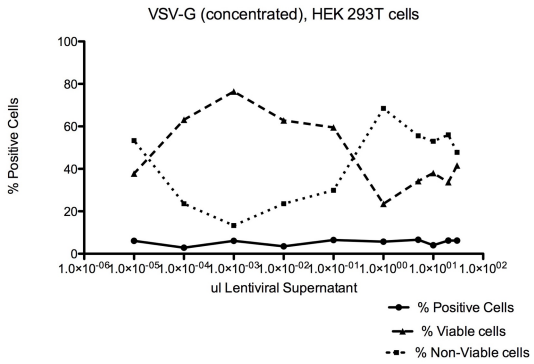

Figure 28. Flow cytometry of Vero cells transduced with a concentrated stock of VSV-G lentiviral pseudotyped particles. Cells were transduced with neat preparations of viral supernatant from 30 to 10^{-5} μl dilutions. Results show that there is no positive cell population with the addition of supernatant. With the addition of lentivirus, the non-viable cell count increases dramatically to 47.8 to 68.5%, which shows that large populations of cells do not survive transduction (SD = 1.33).

4.3. Results: Luciferase reporter system

4.3.1. Luciferase plasmid cloning

Since flow cytometry gave low and irreproducible results, an alternative system was developed by replacing eGFP with luciferase. This was an attempt to generate a more sensitive detection system. This could negate the deleterious handling effects that occur with FACS as well test an alternative reporter gene. This four plasmid system was developed by cloning luciferase (*Photinus pyralis,* pGL-3c, Invitrogen) into pLL3.7. Pseudotyped particles were produced and tested for luciferase activity on a luminometer. Harvests of lentivirus were tested for cell cytotoxicity with an MTT assay (data not shown).

To generate pLL3.7_luc+, pLL3.7 was digested with *Nhe I* and *Pci I*, which results in a 6925 bp vector and a 724 bp insert containing eGFP. Double-digested pGL-3 results in a 2239 (which contains the luciferase gene) and a 1683 bp band (figure 29). These two bands were gel extracted, ligated and transformed into TopTen competent cells. The new luciferase reporter plasmid is 9164 bp in length and was named pLL3.7_luc+.

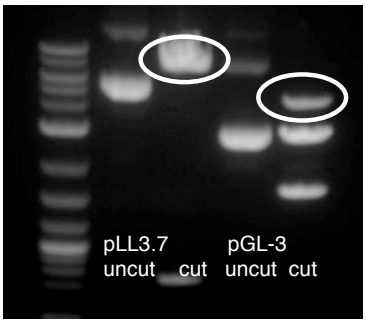

Figure 29. pLL3.7_luc+ cloning plasmids digested. The first band is pLL3.7 uncut, followed by pLL3.7 digested with *Nhe I* and *Pci I* resulting in 6925 and 724 bp bands. The third band is uncut pGL3c, followed by the plasmid digested with *Nhe I* and *Pci I*, which results in 2239 and 1683 bp bands. The 6925 bp and 2239 bp bands were gel extracted and ligated together to produce a 9164 bp vector (pLL3.7_luc+)

Twelve colonies were picked from this transformation and these colonies were digested with diagnostic restriction enzymes *BamH I* (which cuts only pLL3.7) and *Ava I* (which cuts inside the luciferase gene) (figure 30). *Ava I* cuts at 7075, 2311, 2951, and 4831 resulting in 4329, 650, 1862, and 2262 bp bands (without the luciferase gene there are only three bands 4329, 650, and 4124 bp in length). Two colonies had the correct products and were sent to sequencing, which resulted in a positive insertion of the luciferase gene for Clone 6.

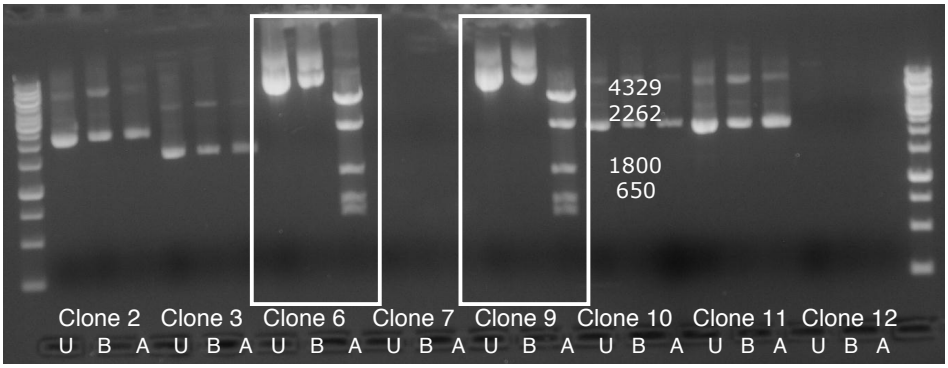

Figure 30. pLL3.7_luc+ cloning plasmids digested. Eight possible pLL3.7_luc+ clones digested with diagnostic restriction enzymes. The first band is uncut (U), the second band is *BamH I* digested (B) and third band is *Ava I* digested (A). There are two possible clones (6 and 9), which show the correct band sizes. Clones 6 and 9 do not have the 4124 bp band, which has been cut into 1800 and 2262 bp bands.

4.3.2. Luciferase substrate assay

To test this new pLL3.7_luc+ reporter plasmid, several plasmids were transfected in parallel into PS-EK cells: pGL-3b ("basic", negative control), pGL-3c ("control", positive

control containing the luciferase gene), pCI (empty, negative control) and pLL3.7_luc+. Luciferase activity was detected with pLL3.7_luc+ values ranging from 4-7 RLUs/ml (reflecting light units/ml) and pGL-3b (negative) at 0.2 (table 3). Repeating this experiment, higher values were detected with pLL3.7_luc+ ranging from 39 to 51, pGL-3c (positive control) from 14 to 20, significantly lower than the pLL3.7_luc+ clone while background levels were very low, ranging from 0.2 to 0.8 (table 4).

pGL-3b (neg)	pCIneo (neg)	pLL3.7_luc+ Clone 6	pLL3.7_luc+ Clone 9	Mock
0.272	0.938	4.110	4.871	0.515
0.287	1.135	7.451	4.598	1.026
0.267	1.023	5.598	3.515	0.742
0.244	0.564	4.617	5.724	1.312
Averages				
0.268	0.915	5.444	4.639	0.899

Table 3. Luciferase readings for the transfection trial of controls. The second trial in RLUs/ml shows four replicates for each sample. pCI and mock (lipofectamine with no DNA) samples were approximately the same. pGL-3 is clearly not expressing luciferase and appears to be a good negative DNA control. pLL3.7 luc+ clones number 6 and 9 have values that are reproducible.

pGL-3b (neg)	pGL-3c (pos)	pLL3.7_luc+ Clone 6	pCIneo (neg)	Mock + lipo	Mock (blank)
0.768	16.58	44.25	1.301	0.674	0.202
0.828	19.97	39.23	1.313	0.423	0.188
0.856	14.96	51.61	1.232	0.479	0.218
0.81	18.91	39.3	1.11	0.412	0.161
Averages					
0.82	17.61	43.60	1.24	0.50	0.19

Table 4. Luciferase readings for transfection trial of controls. Readings are in RLUs/ml showing four replicates for each sample. pGL-3b is the negative control plasmid. pGL3-b is the positive control plasmid. pLL3.7_luc+ is the lentiviral reporter vector containing luciferase in lieu of eGFP. pCI is the original cloning vector for the DENV NGC prME clones. Mock (+lipo) is no plasmid but with the lipofectamine transfection solution and mock (blank) is without. There is a 50-fold difference between pGL-3b and pLL3.7 luc+ and a 2.5-fold increase from the positive control pGL-3c to the clone.

This luciferase reporter plasmid was then tested in the lentiviral packaging system with the three other lentiviral plasmids. HEK 293T cells were transiently co-infected with the four lentiviral expression constructs pRRE (packaging), pREV (Rev-expression), pMD.G (VSV-G envelope), and the new luciferase expressing pLL3.7_luc+ reporter plasmid. Two controls were prepared with pGL-3b (basic, no luciferase activity) or pGL-3c (control, positive luciferase activity) used in lieu of pLL3.7_luc+. Two independent

preparations failed to give detectable luciferase activity, and time course and dose response did not improve this. After a longer incubation during transduction (from two hours to overnight) and activity tested later (from overnight to two days), no luciferase activity could be measured (table 5).

Replicate	$10^{1.7}$ µl	$10^{0.7}$ µl	1 x 10^{1} µl	2 x 10^{1} µl	5 x 10^{1} µl	0 µl
1	0.014	0.016	0.016	0.014	0.02	0.015
2	0.01	0.016	0.014	0.016	0.014	0.014
3	0.012	0.018	0.016	0.016	0.014	0.014
4	0.011	0.010	0.012	0.010	0.010	0.011
SD	0.0017	0.0035	0.0019	0.0028	0.0041	0.0017

Table 5. Luminometer readings for Vero cells infected with VSV-G lentiviral supernatant from 0 to 50 µl. There were no recordable levels of luciferase activity. The subsequent two trials of VSV-G with pLL3.7_luc+, pGL-3b or pGL-3c were also negative.

4.4. Discussion

4.4.2. Conclusions of the lentiviral expression system

There are several challenges when using lentiviral systems. At transfection, cells must take up all four lentiviral plasmids, and expression must be sufficient for infectious particles to assemble. The supernatant generally does not have enough lentivirus present for efficient transduction, it must be concentrated and be relatively fresh, within 1 or 2 days old. Cells must withstand transduction of lentivirus and remain intact through fixing and washing. When the same conditions were used in replicate transductions, percentages of fluorescing cells would vary. A concentrated stock of prME resulted in the highest percentage of cells fluorescing, peaking at 53.6% with 1 µl of the 10^{-2} dilution. Yet, when this experiment was repeated the percentage of cells fluorescing was low or negligible. The control protein, VSV-G was concentrated and tested in several transductions. These resulted in low percentages of cells fluorescing, from 0 to a maximum of 2%. Since the control protein would not make functional pseudotyped particles, there is no stock of lentivirus to compare wt prME, and subsequently, prME mutants to. It would be challenging to compare changes in protein expression and fluorescence between MPER E2 mutants, which may be relatively minor, given these inherent problems. It is possible that there is not enough lentivirus to survive even short-term storage, either at 4°C or -20/-80°C without a freezing buffer. This system would be best applied by maintaining a live positive cell population by cell sorting. As it is, a large-

scale, high-volume (ten T_{175} flasks) harvesting method must be used, which is cumbersome and costly. In total, 25 transfection trials were conducted to create the pseudotyped particles followed by transduction to test viral supernatants resulting in non-reproducible and inconsistent results. This system has proven successful with a related flaviviridae, Hepatitis C although it has been proposed that Hep C E1E2 glycoproteins are distinctly separate from other flaviviruses [36, 73, 83-88]. Hep C is phylogenetically related but not analogous to prME, as E1 has been compared to Class I fusion proteins, whereas E2 is classified as a Class II glycoprotein [36, 89, 90]. E1E2 has an ER retention signal, as does prME but a fraction of E1E2 is not retained and migrates to the cell surface. This protein is then available for pseudotype particle formation [91, 92]. E1E2 does not have a maturation pathway that involves proteolytic cleavage of pr from E that Dengue does. The maturation of E1E2 involves medial or *trans*-Golgi localised glycosylation and not enzymatic cleavage, also resulting in protein available for formation of HCVpp (Hepatitis C pseudotyped particles) [93]. Our theoretical design was based upon the Drummer laboratory's (Burnett Institute) success with HCVpp [personal communication]. There are a few key differences in this system, which has been shown to be detrimental to prME lentiviral generation. The HCVpp system involves a three-plasmid, luciferase reporter assay, which results in a higher amount of transfection efficiency (three versus four plasmids) and possibly a large difference in the amount of lentivirus generated [91]. Not being GFP-based, the luciferase assay is more sensitive, although it is level PC3. It is also possible to lyse the transduced cells to quantify lentiviral generation within the cell as well as cell-surface expressed protein. Thirdly, HCVpp was harvested at three days and not the following day [72, 91], which could be crucial in the level of virus produced. Our plasmid pLL3.7_luc+ was cloned, substituting the luciferase gene for GFP (level PC2). The clones produced fluorescing cells with the luciferase assay. The plasmid was then used in the four-plasmid lentiviral packaging system but when assayed, this transfection did not produce any luciferase activity, indicating that there were no lentiviral particles made. For future direction, the three-plasmid PC2 HCVpp system could be used to clone prME in place of VSV-G. Lentivral particles should be harvested after three days and concentrated. Generation of pseudotyped particles would then be tested with the luciferase assay. All ten MPER E2 mutants would then be cloned in place of wt prME and tested to compare their fusion ability.

CHAPTER 5

RESULTS: EXPRESSION OF prM AND E IN MAMMALIAN CELLS

5.1. Introduction

The third aim of this project was to investigate and characterise the structure of wild type and MPER E2 mutants in a mammalian cell line. Since the results for the lentiviral expression system were inadequate, the mutants were transfected into a mammalian cell line to compare expression and localisation. FACS analysis was used to detect and quantify cell surface expression (section 5.2). Two monoclonal antibodies, 4G2 (α-E fusion peptide) and 3H5 (α-E domain I and III linker) conjugated with Alexa Fluor 488 were used to probe transfected and infected cells. Protein expression of prME was confirmed by SDS-PAGE and Western immunoblot (section 5.3). All ten MPER E2 mutants (F422A/Y, F429A/Y, F440A/Y, Y444A/F, and F448A/Y) were transfected along with wild-type prME, negative pCI, and infected controls. To confirm in-cell prME expression, localisation, and cell surface trafficking, MPER E2 mutants were analysed by immunofluorescence with multiple trials of transfected and infected (NGC DENV-2) PS-EK, Vero and HEK 293T cells (section 5.4). Cells were visualised under confocal laser-scanning microscopy (Zeiss LSM 510 Meta Confocal Microscope). Several molecular probes were also examined to study prME expression and progression through the secretory pathway (section 5.5).

5.2. Results: Analysis of cellular and surface expressed prM and E

5.2.1. Flow cytometry of transfected cells to quantify cell surface expression

Plasmids containing prM and E wild type and mutants were transfected into PS-EK, HEK 293T and Vero cells as described in the Materials and Methods section. To determine whether these proteins were expressed, cells were assayed by flow cytometry using murine monoclonal 4G2 (against E fusion peptide) and 3H5 (which recognises the E domain I and III linker) followed by Alexa-488 conjugated goat anti-mouse IgG. All ten MPER E2 mutants were tested along with wild-type prME and negative pCI (empty vector) controls. Results showed positive fluorescence but were inconsistent, showing a lack of reproducibility similar to that found with the lentiviral pseudotype particle system.

Background levels were first tested with infected PS-EK cells and 3H5 or 4G2. The fluorescence levels with these two antibodies were significantly higher compared with minimal background levels of Alexa Fluor 488 or no conjugate (figure 31).

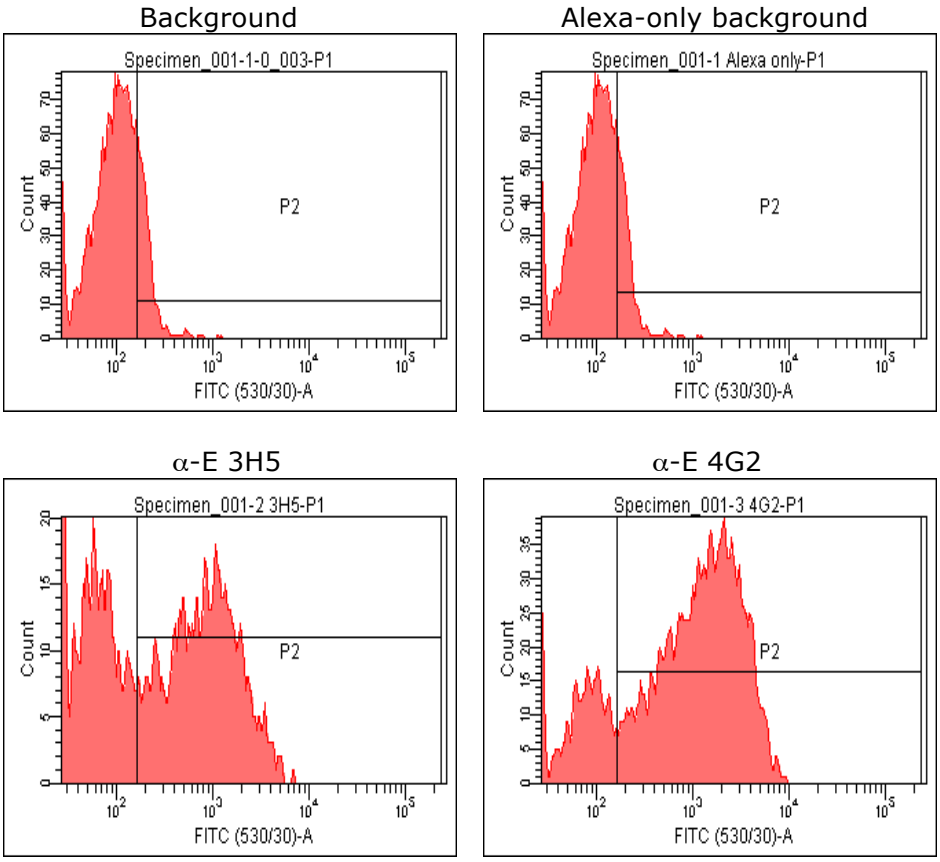

Figure 31. Flow cytometry analysis of infected PS-EK cells. Background controls to set thresholds for fluorescence. Top panel is background fluorescence with or without Alexa Fluor 488. The bottom two histograms show E protein monoclonal antibodies 3H5 (α-E domain I and III linker) and 4G2 (α-E fusion peptide), both of which show good levels of fluorescence compared to the background.

PS-EK cells were then transfected with pCI, wt prME and all ten E2 mutant plasmids (F422A/Y, F429A/Y, F440A/Y, F448A/Y, Y444A/F. Cells were seeded in six-well plates with 2 x 10^5 cells/ml and transfected with 1 μg of DNA and 3 μl of Lipofectamine-2000. Five hours post-transfection, transfection media was taken off and complete media was added. Cells were fixed the following day (24 hours post-transfection) and wells were probed with 3H5 and Alexa Fluor 488. Antibody 3H5 was chosen, as it has previously been shown to be a better antibody to use with FACS (table 6) [94]. Alen, et al. (2009) compared antibody 3H5 to 4G2 in flow cytometry experiments and 3H5 had a higher

mean fluorescence of intensity with DENV-2 NGC. Cells were counted to 10,000, viable cells determined by their spherical morphology, "% Positive cells" are the subset of viable cells that are fluorescing, and "Positive % Total" is the percent of total cell counts that were positive. Background (pCI) was around 1% and wt prME showed 6% positive fluorescence. The E2 mutants ranged from 1.7 to 9.2% positive fluorescence (background subtracted), in line with wild-type prME, which showed that E protein could be tracked through flow cytometry in transfected cells with this antibody. There was a loss of cell counts with the E2 mutant transfections but only minimal difference to cell viability. This may have skewed the results, especially when the viable cell percentage was low (i.e. E2 mutant F440Y).

Sample	% Viable Cells	% Positive Cells	Positive % Total	Cell Count
pCI	40.8	2.4	1	10000
prME	42.7	14.1	6	10000
F422A	28.2	10.6	3	10000
F422Y	25.4	12.2	4.3	3137
F429A	37.1	9.4	3.5	3377
F429Y	34.3	22.2	7.6	4013
F440A	33.7	27.1	9.2	3450
F440Y	14.4	11.8	1.7	1886*
Y444A	31.4	25.9	8.1	3140
Y444F	35.6	13.2	4.7	5537
F448A	38.6	14.1	5.4	4179
F448Y	37.3	10.3	3.8	7902

Table 6. FACS analysis of permeabilised PS-EK cells transfected and probed with 3H5. The controls pCI and wt prME and all ten E2 mutants and probed with 3H5. Background (pCI) was about 1% and wt prME was 6% positive fluorescence. The E2 mutants ranged from 1.7 to 9.2 % positive, which showed that E protein could be tracked through flow cytometry in transfected cells with monoclonal antibody 3H5. (SD = 2.43, mutants only)
*Low cell count for this sample

The cell counts were not all 10,000, therefore, this experiment was repeated to attain higher intact cell numbers. The results were consistent with the above data (table 7). Non-permeabilised cells, as expected, showed low levels of fluorescence (0 – 1.2%) whereas permeabilised cells ranged from wt prME at 4.7% positive fluorescence (similar to 6% previously seen) while the E2 mutants ranged from 0.2 to 16.2 % fluorescence, which was marginally higher. This experiment was repeated five times with fluctuating percentages of positive cells – either cell pellets were lost and cell count too low for detection or positive fluorescence levels too low to see any difference between

background, positive controls and E2 mutants (table 8). If there are any differences between wild-type and the E2 mutants, FACS analysis would be too inconsistent to allow for detection in non-permeabilised cells, as was the case with lentiviral infection. This method of quantification may benefit from harvesting cells at three days instead of one day post-transfection, again similar to lentiviruses. There appears to be a low, but detectable level of E expressed at the cell surface in non-permeabilised cells, whereas with permeabilised cells, E levels significantly higher. Fluorescence may increase if cells were harvested later to allow for E trafficking to the cell surface. Cell preparations for flow cytometry are very different than the procedure for confocal immunofluorescence and similar to the lentiviral pseudotype particle FACS analysis. After transfection, cells were scraped off the bottom of plates, centrifuged and fixed. Cell pellets were then blocked and probed by indirect fluorescence. There is usually a large amount of cell loss through this procedure due to multiple washing steps, which leads to variable results in comparison with immunofluorescence, which starts from fixed cells after infection or transfection. Results are therefore inherently variable; cell counts and fluorescence are positive in one experiment and then too low for detection in the following experiment.

Ideally, confocal immunofluorescence and FACS-prepared samples would be tested in parallel to confirm transfection efficiencies and to compare the two detection methods. Confocal immunofluorescence was conducted to confirm expression and localisation of prME (section 5.4). While confocal microscopy provides a good comparison of wild-type prME and MPER E2 mutants, it requires subjective quantification, which FACS does not.

	Sample	Viable Cells	Positive % Total	(-) Background
Non-perm	pCI	22.4	0.7	
	prME	20.4	0.7	0
	F422A	18.9	0.8	0.1
	F422Y	20.8	0.9	0.2
	F440A	20.2	0.8	0.1
	F440Y	17.7	1.4	0.7
	Y444A	18.9	1	0.3
	Y444F	21.5	0.9	0.2
	F429A	21.7	0.6	-0.1
	F429Y	20.5	0.6	-0.1
	F448A	23.8	1	0.3
	F448Y	26.1	1.9	1.2

Perm	pCI-perm	28.3	2.2	
	prME-perm	20.7	6.9	4.7
	F448A-perm	15.5	5.2	3
	F448Y-perm	25.6	18.4	16.2
	F422A-perm	15.7	2.4	0.2
	F422Y-perm	15.6	3.3	1.1
	F429A-perm	17.9	6.4	4.2
	F429Y-perm	18.4	5.7	3.5
	Y444A-perm	13.5	3.4	1.2
	Y444F-perm	17.5	5.4	3.2
	F440A-perm	20	6.7	4.5
	F440Y-perm	22.2	14	11.8

Table 7. FACS analysis of PS-EK cells transfected with the controls pCI and wt prME and all ten E2 mutants and probed with 3H5/488. Cell count was 10,000 for all samples. Wild-type prME, permeabilised cells showed 4.7% positive fluorescence (similar to 6% previously seen) while the E2 mutants ranged from 0.2 to 16.2 % fluorescence, which was marginally higher than seen previously (SD = 5.11, permeabilised mutants only).

Sample	Cell Count	Viable Cells	Positive % Total	(-) Background
pCI	6987	6.1	1.9	
prME	1054	6.9	2.7	0.8
F422A	10000	10.8	2.6	0.7
F422Y	10000	11.8	2.2	0.3
F429A	5909	7.9	2.8	0.9
F429Y	5959	7	2.6	0.7
F440A	10000	9.2	2.2	0.3
F440Y	4020	9.5	1.3	-0.6
Y444A	10000	13.1	2.7	0.8
Y444F	3781	5.2	1.5	-0.4
F448A	3878	7.3	2.8	0.9
F448Y	1178	8.8	1.9	0

Table 8. FACS analysis of non-permeabilised PS-EK cells transfected with the controls pCI and wt prME and all ten E2 mutants and probed with 3H5/488. Viable cell levels (and subsequently fluorescence) were very low and there appeared no differences between wt prME and E2 mutants. Cells should be permeabilised to reach minimal detection limits. (SD = 0.54, mutants only)

5.2.2. In-cell detection of prM and E

Due to the variable detected fluorescence with flow cytometry, another system for quantifying fluorescing cells was investigated. A GE in-cell analyser combines the visualisation of confocal microscopy with a quantifiable analysis of positive cells, similar to flow cytometry. A further advantage with this machine is its high-throughput capability to test multiple replicates at the same time with its 96-well plate format as well as the

ability to test live or fixed cells. Transfected PS-EK cells were tested on the GE in-cell analyser. All ten E2 mutants were individually transfected into PS-EK cells along with wild-type prME and pCI. Cells were seeded in 96-well plates with 1 x 10^5 cells/50 μl and transfected with 0.4 μg of DNA and 1 μl of Lipofectamine-2000. Five hours post-transfection, transfection media was taken off and complete media was added. Cells were fixed the following day (24 hours post-transfection) and wells were probed with Hoechst (1:10,000) and either 1:400 or 1:600 α-E 4G2 or 3H5 and Alexa Fluor 488. Cells displayed detectable fluorescence, with approximately half of cells positive (figure 32). With this imager, it is possible to automatically quantify fluorescence by subtracting cells that were not transfected (background). This can be accomplished only with an additional dye, such as DAPI or Wheat Germ Agglutinin (WGA). This method of detection appeared promising but experimentation was set aside to complete the other aims of the project.

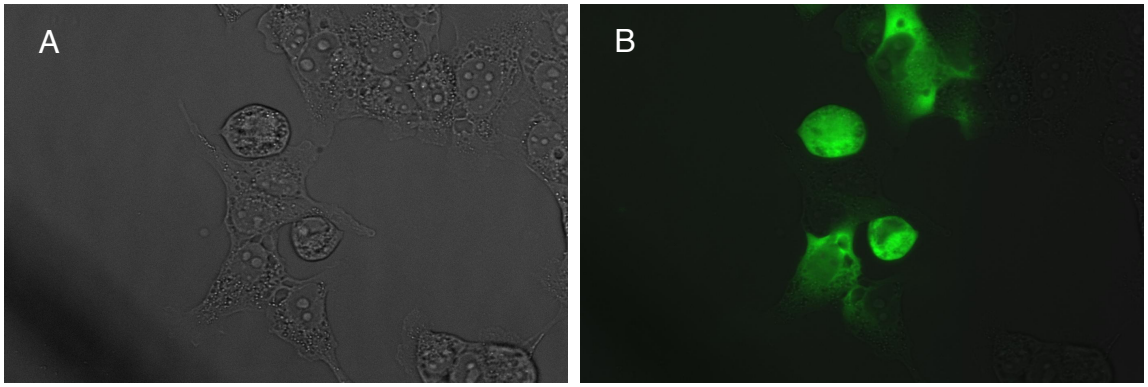

Figure 32. GE in-cell analyser images of PS-EK cells. Cells were transfected with wild-type prME as an example of machine output. Cells were fixed and probed with 3H5 or 4G2, Alexa Fluor 488 and Hoechst. The imager took four fields of view per well and one field is shown as an example of wt prME probed with α-E 4G2 **[A]** Phase contrast microscopy, **[B]** α-E 4G2 and Alexa Fluor 488 immunofluorescence.

5.3 Results: Detection of E protein production with SDS-PAGE and Western immunoblot

PS-EK cells were transfected with wild-type prME along with the ten MPER E mutants to determine protein expression as well as correct conformation with epitopes available for antibody binding. Immunoblot experiments were undertaken to compare wild type with mutant polyprotein expression. Binding of monoclonal antibodies 3H5 and 4G2 was also compared. An infected cell control sample was used (m.o.i. = 1, 24 hour infection). DTT was used in the treatment of samples with monoclonal antibody 3H5, which cross reacts with the linker between domains I and II and thus, requires a linearised protein without disulfide bonds. DTT is not required with 4G2 as it binds with the α-E fusion peptide.

α-E Monoclonal Antibody 4G2

As detected by 4G2 α-E antibody, all mutants except F422A were expressed in PS-EK cells (E protein band at 65kDa, figure 33). Expression levels were variable with F429A and F429Y mutants showing the highest expression. A secondary band appears above 65 kDa with the infected control, mutant F448A, and possibly mutant Y444A. This has been seen with other E protein gels and is thought be a difference in glycosylation of the envelope protein [P. Young communication].

The F448Y band migrated faster than wild-type prME but in line with the infected control sample (figure 33, [B]). It is unclear whether or not this is a gel artifact or true migration difference due to glycosylation.

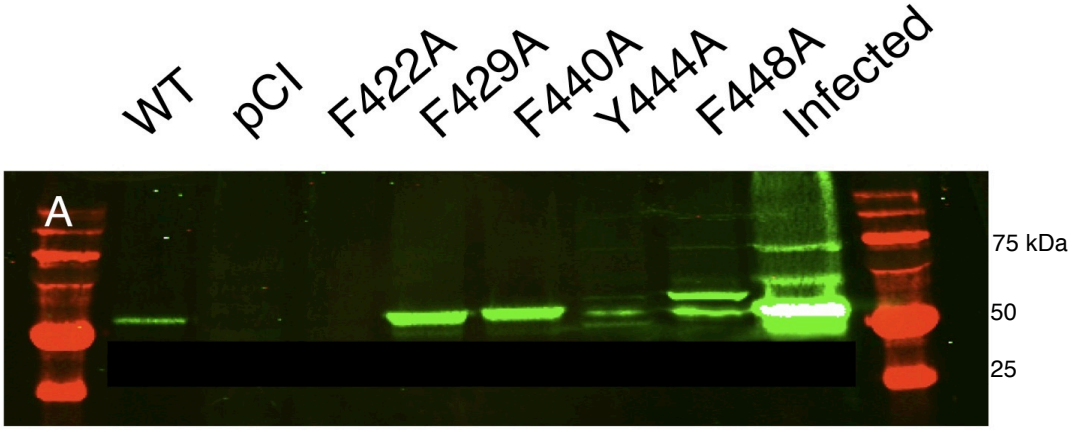

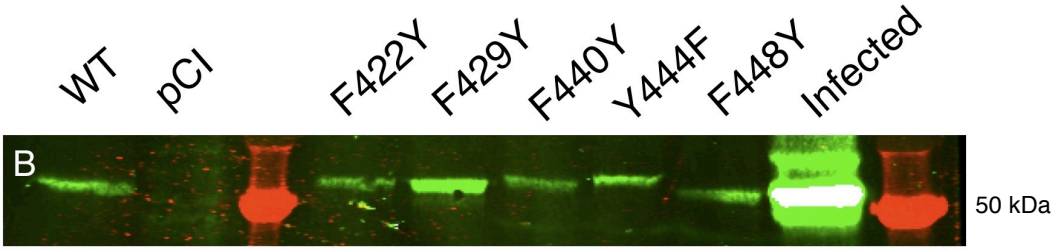

Figure 33. Western immunoblot of transfected PS-EK cell samples. **[A]** All F/Y → A mutants with 4G2 antibody. Distinct E-sized (~50 kDa) bands are shown for wt prME, F429A, F440A, Y444A, F448A (two bands) and infected control. There is no band for F422A. **[B]** All F/Y → Y/F mutants with 4G2 antibody. Distinct E-sized bands are shown for wt prME, F422Y, F440Y, Y444F, F448Y, and infected control. pCI negative control shows no 4G2 binding.

α-E Monoclonal Antibodies 3H5 and 4G2

Transfected cell samples were then incubated in parallel with 4G2 (without DTT) and 3H5 (with DTT). Transfected samples for 3H5 antibody were heat treated with DTT present in the SDS-PAGE loading buffer to break the disulfide bridges present in the secondary structure of E. Epitopes present in wild-type prME and the infected control sample bound 4G2 well (prME shows two E bands, which may be the glycosylated version of E, figure 34, [A]). pCI negative control again did not show 4G2 binding. MPER E mutants F429A, F440A, Y444A, F448A bound 4G2 well while F442A did not, which confirms the results above. Mutant Y444A appears to run faster here than figure 33A; this may be a molecular weight difference due to less glycosylation of the protein. It does migrate in line with wt prME lower band. MPER E mutants F422A (strong binding), F429A and F440A (moderate binding), bound 3H5 while Y444A and F448A showed weak binding (figure 34, [B]).

α-E 4G2, F/Y → A mutants

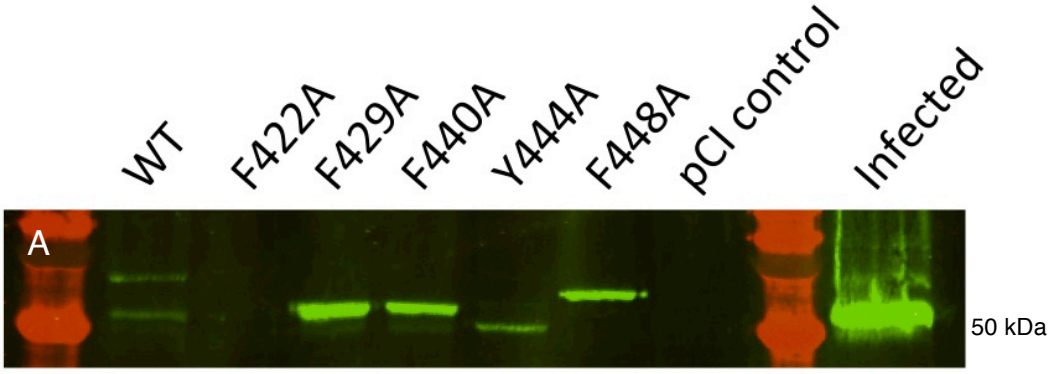

α-E 3H5, F/Y → A mutants, with DTT

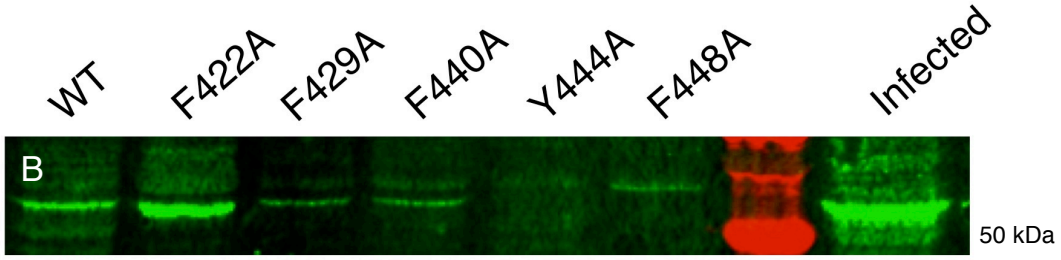

Figure 34. Western immunoblot of transfected PS-EK cell samples, all F/Y → A/F mutants. **[A]** The top gel is of 4G2 detection with bands shown for wt prME (two bands), F429A, F440A, Y444A, F448A and the infected control. No bands are seen for F422A and pCI. **[B]** The bottom gel shows 3H5 detection. There were distinct E-sized bands seen for wt prME (two bands), F422A, and the infected control. There may be weak binding with F429A and F440A.

MPER E mutants F422Y, F429Y, F440Y, Y444F, F448Y bound 4G2 well, which confirmed previous results. When samples were probed with 3H5, MPER E mutants F422Y, F429Y, Y444F and F448Y showed moderate binding while F440Y showed strong binding (figure 35).

α-E 4G2, F/Y → F/Y mutants, without DTT

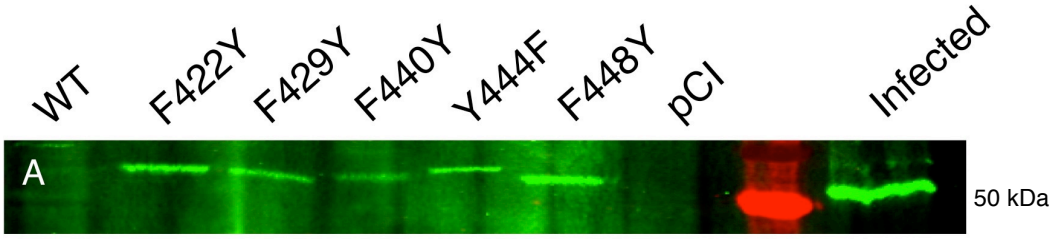

α-E 3H5, F/Y → F/Y mutants, with DTT

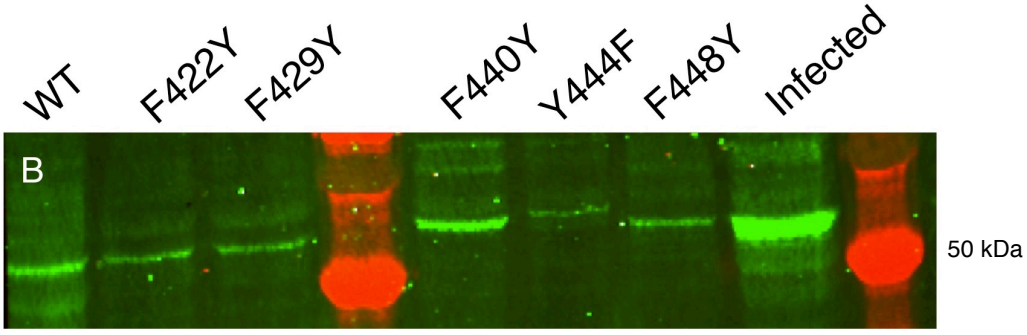

Figure 35. Western immunoblot of transfected PS-EK cell samples, all F/Y → Y/F mutants. **[A]** The top gel is of 4G2 detection with bands shown for F422Y, F429Y, F440Y, Y444F, F448Y and the infected control. The band for wt prME is faint and there is no band for pCI. **[B]** The bottom gel is 3H5 detection showing a distinct band for wt prME and the infected control. There are bands for F422Y, F429A, Y444F and F448Y and a strong band for F440Y.

As this system was optimised for cell lysis (lytic buffers), immunoblot transfer (submerged or semi-dry), and antibody incubation (length and volume), there was some loss during handling of the viscous protein samples and gel artifact shown. To summarize mutant protein expression, MPER E mutants F429A, F440A, Y444A, F448A showed good levels of binding with 4G2 while F442A did not. A secondary band appears above 65 kDa with the infected control and mutant F448A. This is thought to a difference in glycosylation of the envelope protein. MPER E mutants F422Y, F429Y, F440Y, Y444F, and F448Y all showed binding with 4G2, while the F448Y band migrated lower than wt prME but in line with the infected control sample. It is unclear whether or not this is a gel artifact or again, true migration due to glycosylation. To confirm this, protein samples could be standardised to compare identical quantities. With antibody 3H5, F422A showed a high expression level unlike with antibody 4G2. There may be a conformational preference for the 3H5 epitope between DI and DIII, due to F422's position between the E1 and E2 helices. With the alanine substitution, 4G2 binding is reduced either by reduction in protein expression or conformational epitope loss. MPER E mutants F422Y, F429Y, F440Y, Y444F and F448Y all showed good binding with 3H5, while bands for F440Y were stronger than with the other mutants.

5.4. Results: Detection of in-cell and surface expressed E protein production with confocal microscopy

5.4.1. Analysis of cellular and surface expressed E protein production in transfected cells

To track E maturation and progression through the secretory pathway after protein expression was confirmed as above, MPER E mutant plasmids were transfected into PS-EK cells and probed with monoclonal antibodies for immunolocalisation. Cells were seeded on coverslips in 24-well plate format and transfected for confocal microscopy imaging. Twenty-four hours post-transfection, cells were either fixed or fixed and permeabilised. Optimal concentrations of α-E 4G2 (1:400 dilution) and Alexa Fluor 488 (1:400 dilution) were determined by a comparison of 1:200 to 1:800 dilution series. Nuclei were stained with a Hoechst.

PS-EK cells were first transfected with controls wt prME and pCI and all ten MPER E mutants and non-permeabilised, fixed cells were probed with 4G2 (figure 36). Efficiencies of 1 μg plasmid transfected were determined by counting fluorescing cells, subtracting from the total cell population in three visual fields and averaged (one image sample shown). Transfection efficiencies were close to the wild-type prME (92% of cells positive) as detected by 4G2, while mutants ranged from 77 to 85%. F422A was the exception at 49% positive cells. The number of perinuclear foci of E protein fluorescence was also averaged. For wild-type prME this was 33%, while mutants ranged from 7 to 19%, except for F422A, which was zero. The lack of detection of F422A compared with the other mutations is consistent with the Western immunoblot data.

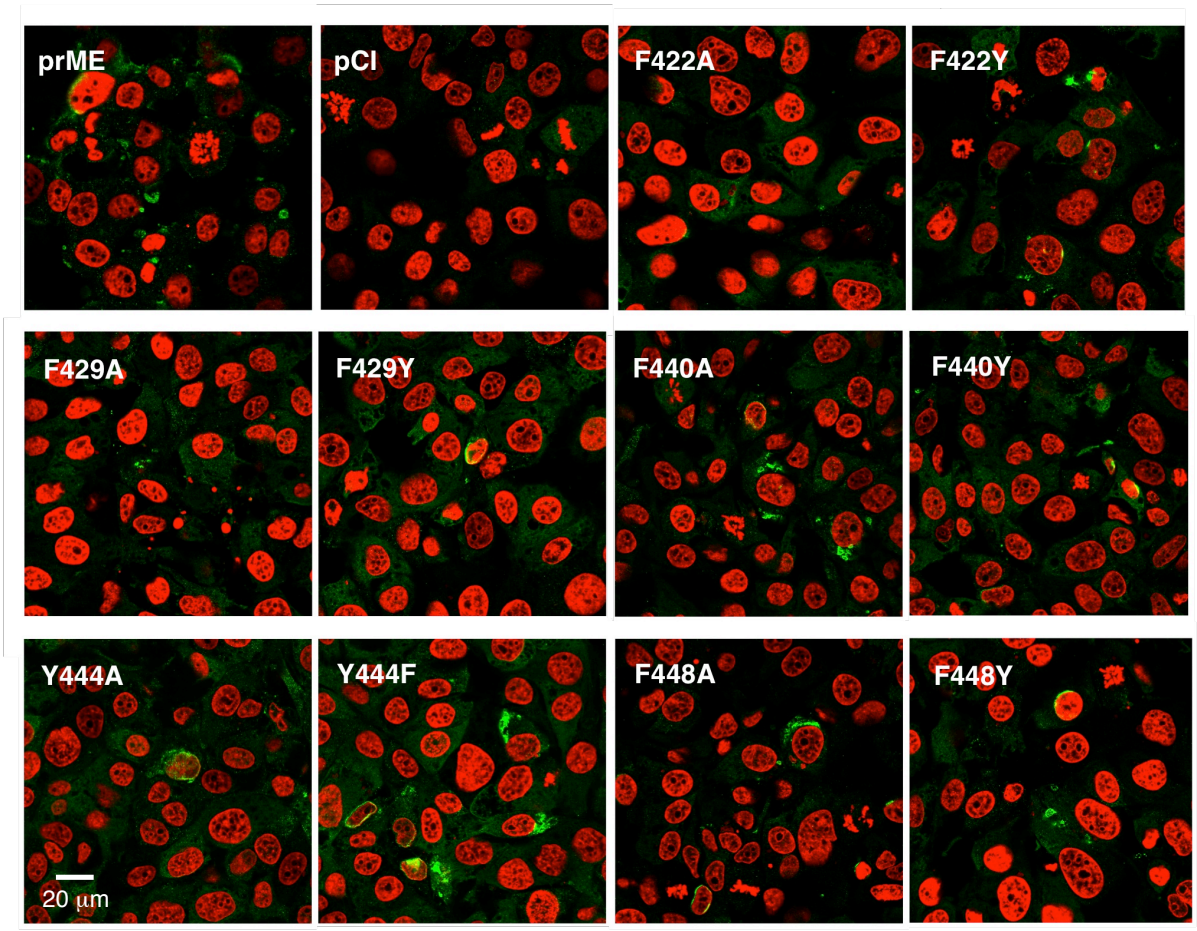

	% positive cells	% perinuclear staining		% positive cells	% perinuclear staining
wt prME	92	33	F440A	77	12
pCI (neg)	5	0	F440Y	85	12
F422A	49	0	Y444A	83	8
F422Y	79	19	Y444F	85	14
F429A	85	7	F448A	77	8
F429Y	84	10	F448Y	82	14

Figure 36. Immunofluorescence confocal microscopy of transfected non-permeabilised PS-EK cells probed 4G2 (green) and Hoechst (1:20,000, red). The transfection efficiency was calculated as an average of three images per sample (all images not shown). Background fluorescence was negligible (pCI, 5%) and wild-type transfection, prME was good (92%) while mutants ranged from 49% (F422A) to 85% (SD = 10.88, mutants only). There was evident perinuclear foci with the wild type prME at 33% and mutants ranging from 7-19%, with none shown for F422A (bottom table).

Transfection of PS-EK cells (non-permeabilised), probed with Cholera toxin

To make sure homogeneous fluorescence was background (Alex Fluor 488), a membrane marker for lipid rafts (Cholera Toxin Subunit B) was tested in conjunction with 4G2/488. With the plasma membrane stained, fluorescence seen outside the cells would not be expression of E. PS-EK cells were transfected with controls wild-type prME and pCI (empty vector) and the MPER E mutants and not permeabilsed. Cells were probed with 4G2/488 (1:400 dilution), Cholera toxin subunit B (Tx-B, (1:500 dilution, 0.5 μg/μl solution), and 1:20,000 Hoechst. Fluorescence of controls and mutants were comparable to figure 36 and there is a clear difference between homogeneous staining of the cytoplasm and perinuclear staining (figure 37). Cholera Tx-B shows inconsistent staining (in blue), likely due to dye precipitation. Mutant F422A did not show 4G2 binding localised to the nuclei while all other mutants did.

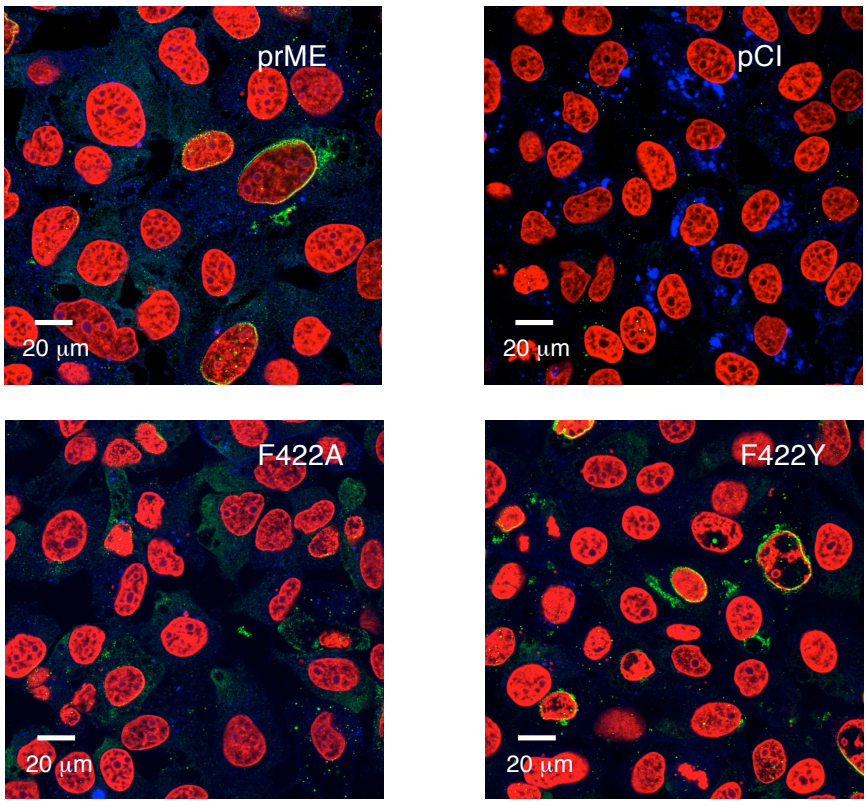

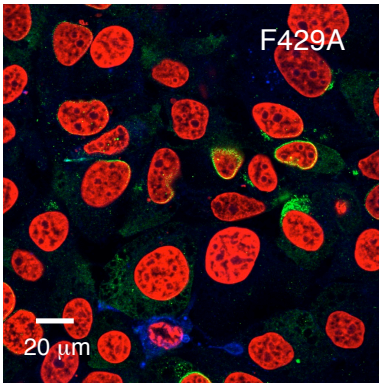
F429A
20 μm

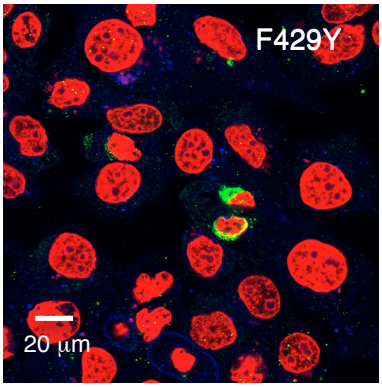
F429Y
20 μm

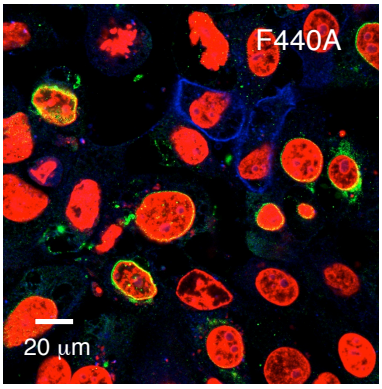
F440A
20 μm

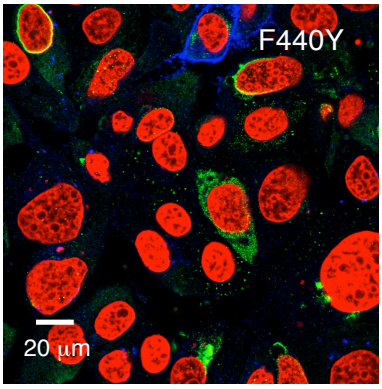
F440Y
20 μm

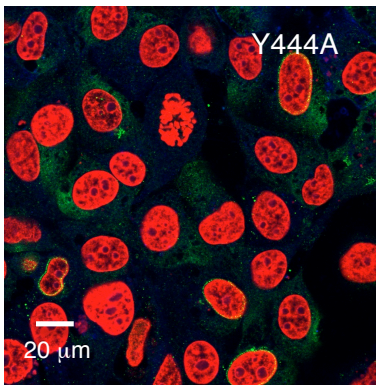
Y444A
20 μm

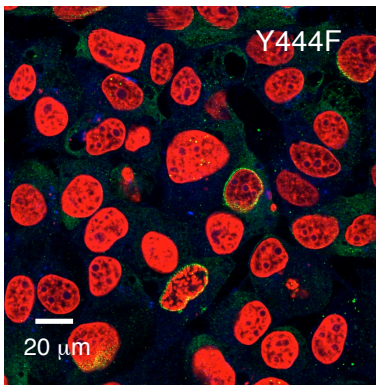
Y444F
20 μm

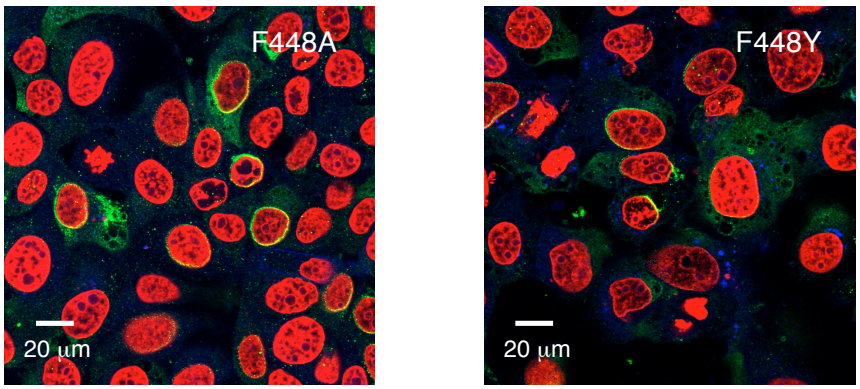

Figure 37. Immunofluorescent confocal microscopy of PS-EK cells transfected with wt prME (positive control), pCI (negative control), and ten mutants. Cells were fixed with 4% PFA, stained with Hoechst (red) and probed with 1:400 4G2/Alexa 488 (green) and 1:500 Cholera Tx-B (blue). Mutants showed good expression levels compared to wt prME except for F422A, which showed no perinuclear binding. Cholera Tx-B showed inconsistent staining, possibly due to the age of this dye.

Transfection of PS-EK cells (permeabilised), probed with Cholera toxin

PS-EK cells were then transfected, permeabilised and probed with 4G2/488 (1:400), Hoechst (1:20,000) and Cholera Tx-B (1:500, 0.5 μg/μl solution) (figure 38). Again, positive fluorescence was high for wild-type prME and all ten MPER E mutants with F422A the exception. For F422A, there are negligible, background patches of fluorescence. Cholera Tx-B staining was seen in certain images (Y444A) was variable probably due to precipitation of the reagent as discussed previously. From the permeabilised and non-permeabilised data, a summary of expression and transfection efficiency averages was determined (table 9). For permeabilised cells, prME showed 59% cells fluorescing while mutants ranged from 34 to 57% with outlying F422A at 8%. For non-permeabilised cells, prME showed 52% cells fluorescing, while mutants ranged from 24 to 43%. F422A again stood out from the other mutants, showing no perinuclear binding. It appears that this mutant, which lies in the conserved sequence (CS) just upstream from E2, does not display the epitope for 4G2 as well as the other mutants or it is not being expressed at the same quantity to allow for similar detection.

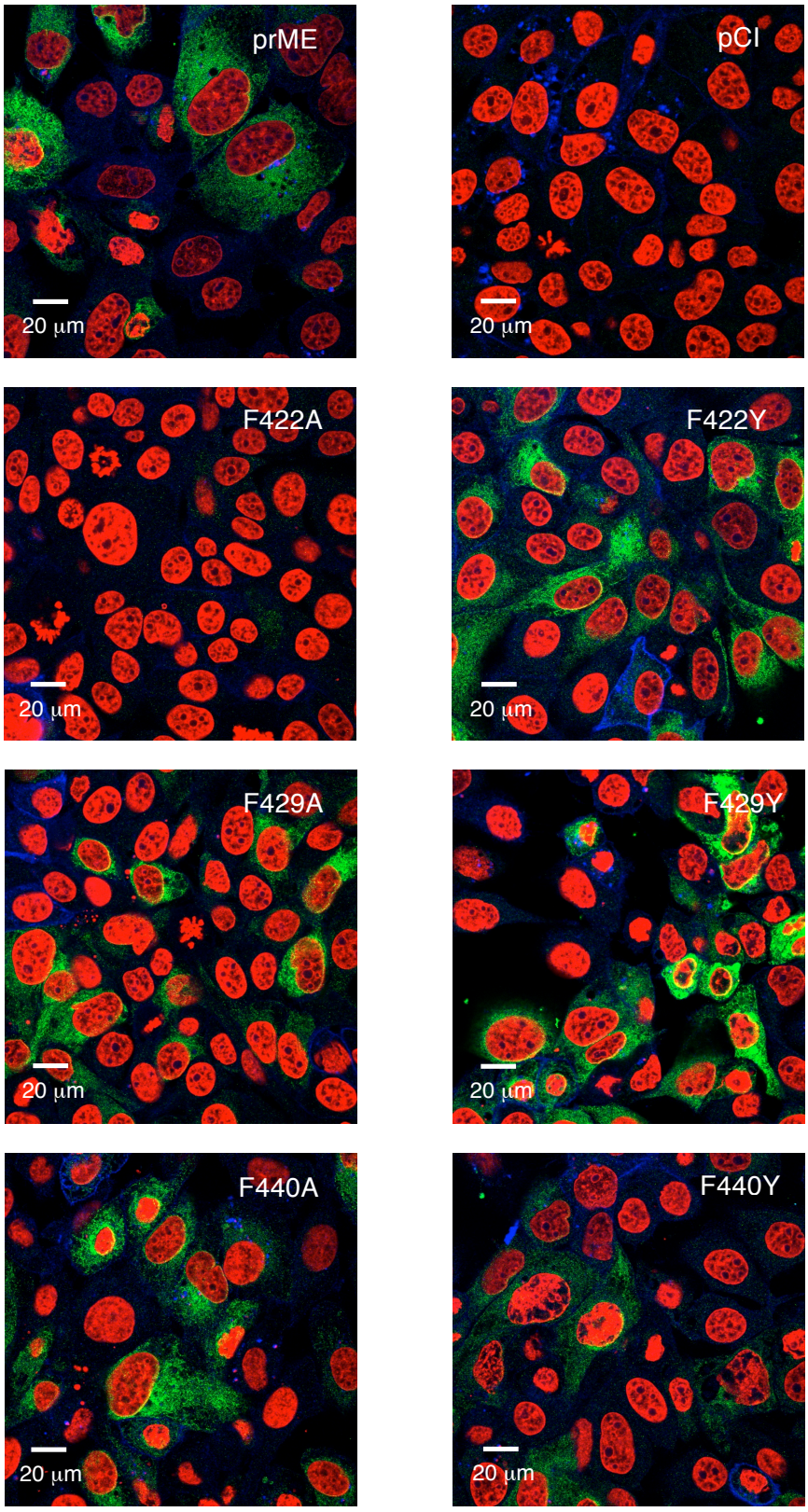
prME
20 μm
pCI
20 μm
F422A
20 μm
F422Y
20 μm
F429A
20 μm
F429Y
20 μm
F440A
20 μm
F440Y
20 μm

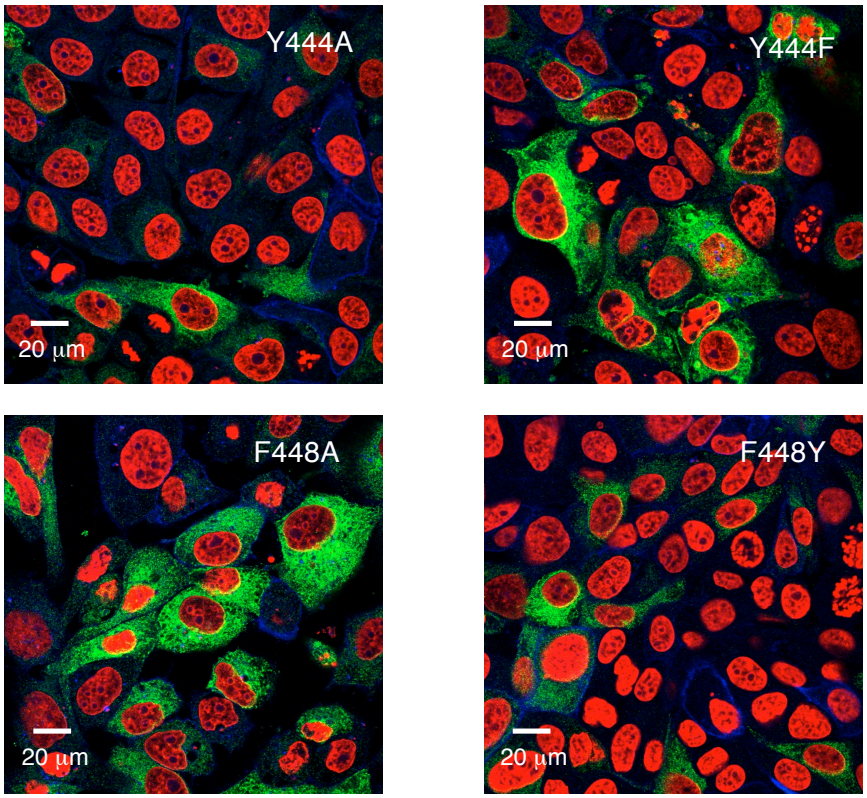

Figure 38. Immunofluorescent confocal microscopy of PS-EK cells transfected with wt prME (positive control), pCI (negative control), and ten mutants. Cells were fixed with 4% PFA, stained with 1:20,000 Hoechst (in red), 1:500 Cholera Tx-B (in blue) and probed with 1:400 4G2/Alexa Fluor 488 (green). Mutants showed good expression levels compared to wild-type prME except, again, with F422A.

Permeabilised PS-EK cells: 4G2, Cholera Tx-B and Hoechst

Plasmid	Avg % of cells, 4G2/Alexa binding	Expression Levels
prME	59%	High and even expression of E
pCI	0%	Negative control
F422A	8%	Low expression
F422Y	54%	High and even expression
F429A	44%	Moderate but variable expression
F429Y	56%	High expression
F440A	53%	High expression
F440Y	44%	Moderate expression
Y444A	42%	Moderate expression
Y444F	48%	High but variable expression
F448A	57%	High expression
F448Y	34%	Moderate expression

Non-Permeabilised PS-EK cells: 4G2, Cholera Tx-B and Hoechst

Plasmid	Avg % of cells, 4G2/Alexa binding	Expression levels
prME	52%	High expression of E
pCI	0%	Negative control
F422A	27%	Moderate expression, no perinuclear
F422Y	29%	Moderate expression
F429A	38%	High expression
F429Y	24%	Moderate expression
F440A	36%	Moderate expression
F440Y	41%	High expression
Y444A	42%	High expression
Y444F	37%	High expression
F448A	38%	High expression
F448Y	43%	High expression

Table 9. Fluorescence levels of transfected PS-EK cells. Immunofluorescent confocal microscopy of cells transfected with wt prME (positive control), pCI (negative control), and ten mutants. Expression levels of E is summarized. For permeabilised cells, prME showed 59% cells fluorescing while mutants ranged from 34 to 57% with outlying F422A at 8%. For non-permeabilised cells, prME showed 52% cells fluorescing, while mutants ranged from 24 to 43%. F422A again stood out from the other mutants, showing no perinuclear binding.

Transfection of PS-EK cells (non-permeabilised), probed with α-E 4G2 or 3H5

To test antibody ∝-E 3H5 (domain I and III linker) in conjunction with antibody 4G2 (fusion peptide), PS-EK cells were probed with 4G2 or 3H5 in parallel. This was to compare a 1:400 dilution of 3H5 with 4G2 in non-permeabilised, transfected cells (seen in figure 36). There was no staining with pCI, and prME showed approximately 30-40% transfection efficiency with either probe (figure 39). All ten mutants were probed with both antibodies but only a subset is shown (F448A and F448Y). These mutants, including F422A, showed consistent binding when comparing 4G2 with 3H5, displaying approximately even fluorescence with both antibodies.

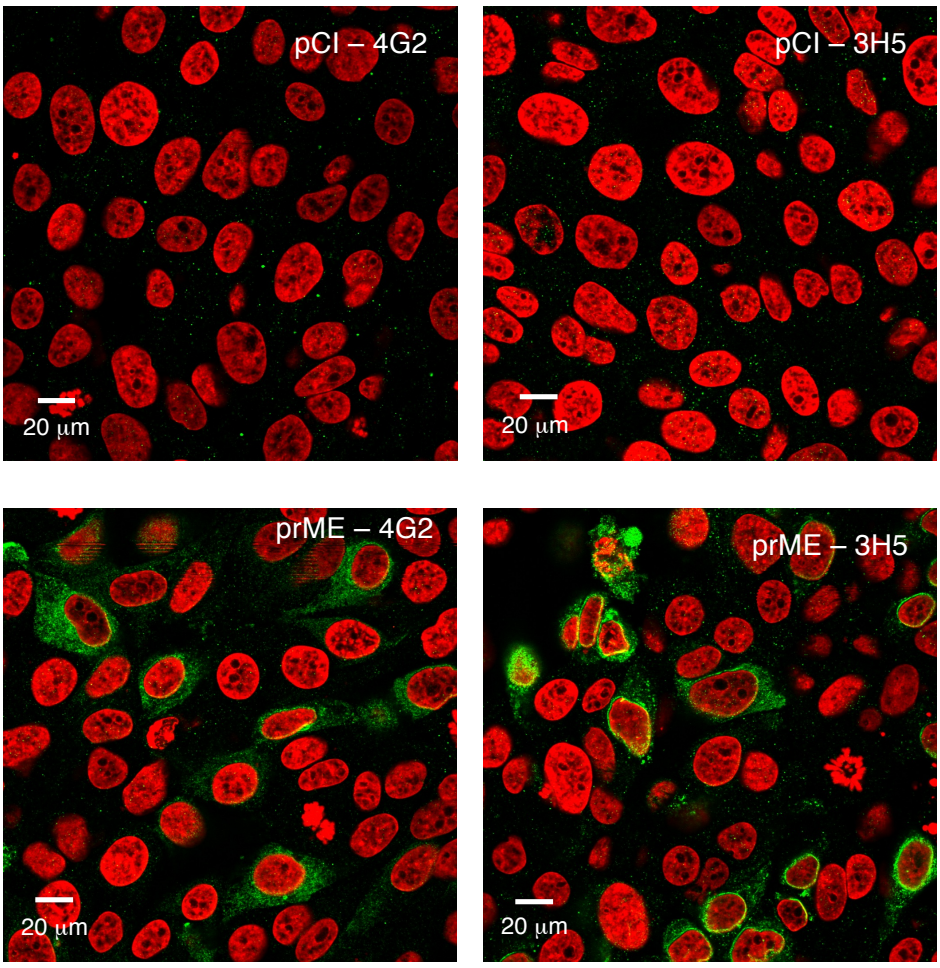

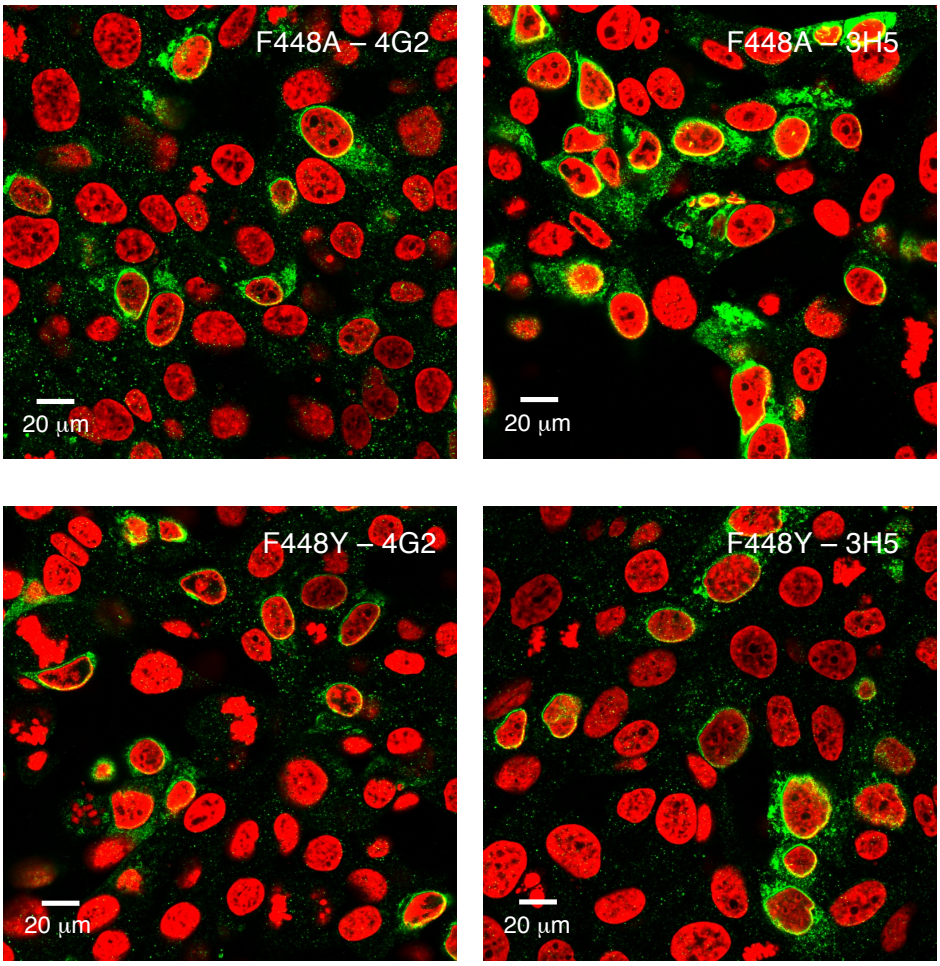

Figure 39. Immunofluorescent confocal microscopy of PS-EK cells transfected with wt prME (positive control), pCI (negative control), and ten mutants. Cells were fixed with 4% PFA, stained with 1:20,000 Hoechst (in red) and probed 4G2 or 3H5 (1:400) and 1:400 Alexa Fluor 488 (in green). Mutants showed good expression levels, comparable to wild-type prME (not all mutants are shown).

Transfection of cells with or without permeabilisation, probed with WGA

After experimentation with molecular dyes (section 5.5) to track the progression of E through the secretory pathway, WGA (Wheat germ agglutinin) was determined to be the best dye to visualise other cellular organelles. It clearly stains the plasma membrane (for cell surface localisation), whilst also partially staining intracellular membranes as it binds with the Golgi apparatus. PS-EK cells were transfected and probed with 4G2, Alexa Fluor 488 (both 1:400), Hoechst (1:10,000), and WGA (1:500). Images shown display the Hoechst signal only (blue, upper left), Alexa/4G2 signal only (green, upper right), WGA only (purple, lower left) and merged (lower right, figure 40). As before, all ten mutants showed fluorescence comparable to wild-type prME upon probing with 4G2.

F422A was again the exception; non-permeabilised cell binding was in line with other mutants but upon permeabilisation, this mutant showed reduced levels of fluorescence in comparison. WGA stained plasma membranes well (PM, in purple), with most membranes evenly fluorescing. E protein is seen aggregating around the cellular surface, possibly favouring E binding receptors. With permeabilisation, a high degree of accumulation of E can be seen in the perinuclear region and diffused throughout the cytoplasm and secretory pathway (Golgi to ER) towards the PM.

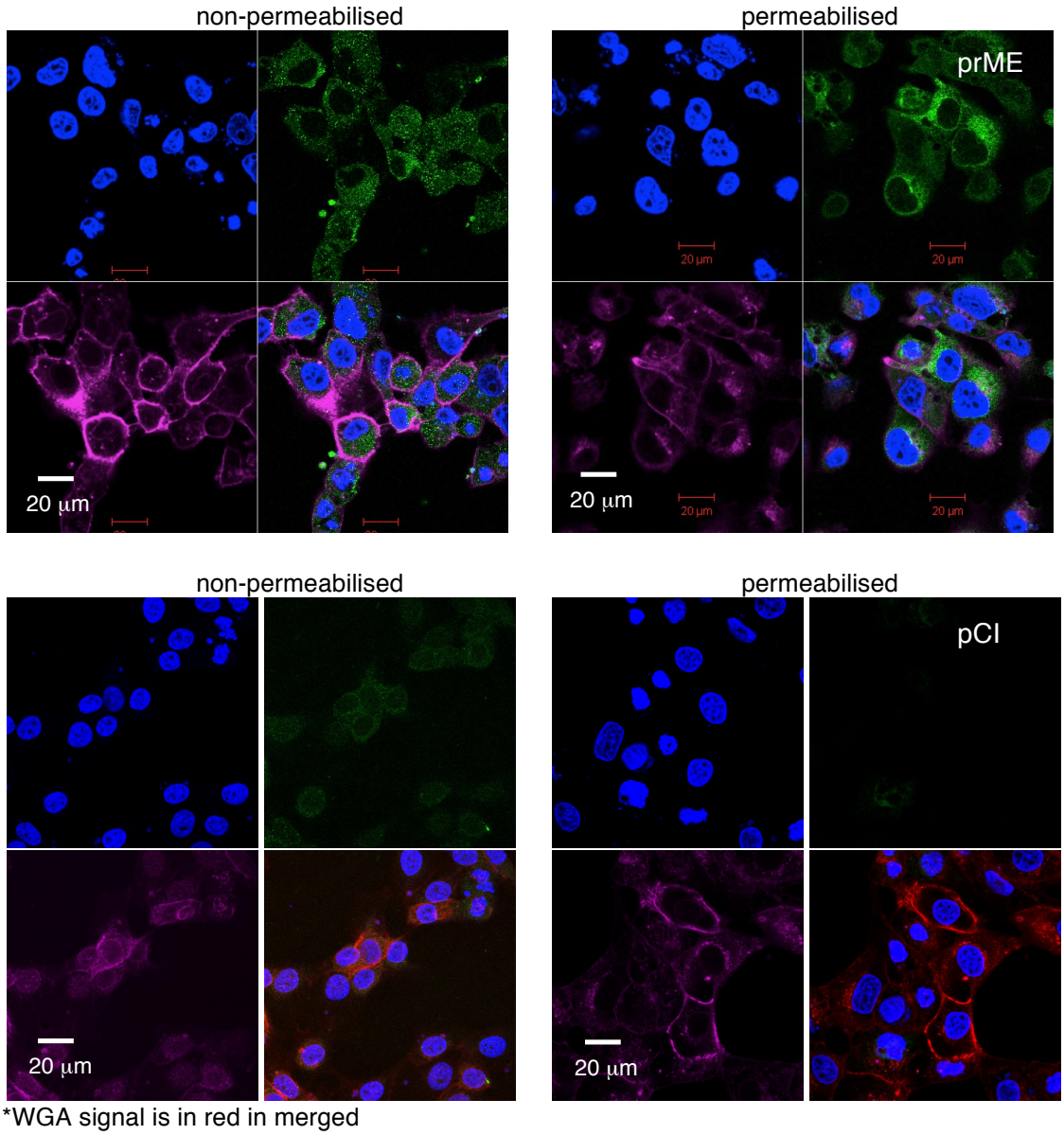

*WGA signal is in red in merged

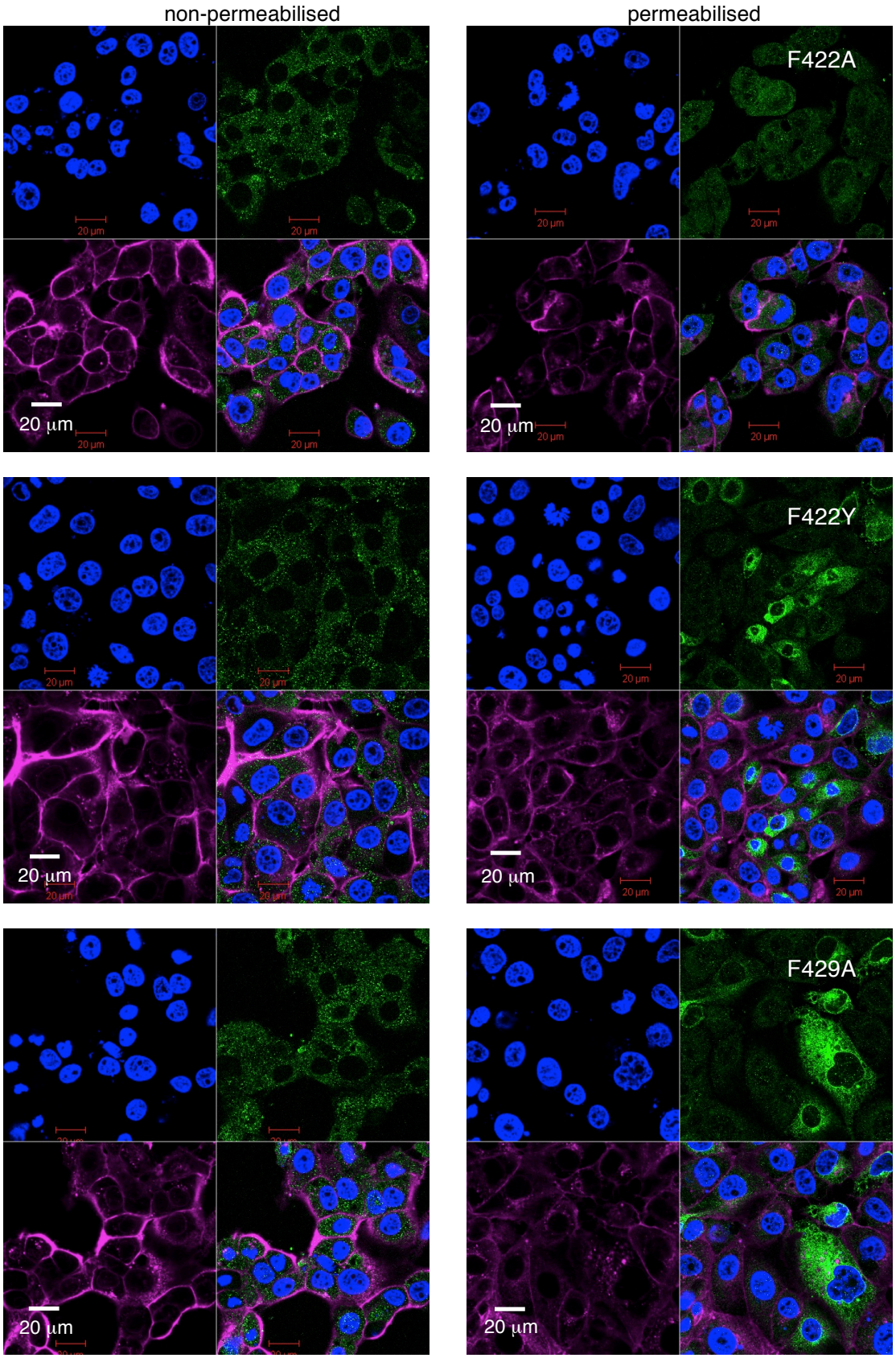
non-permeabilised
permeabilised
F422A
F422Y
F429A
20 µm

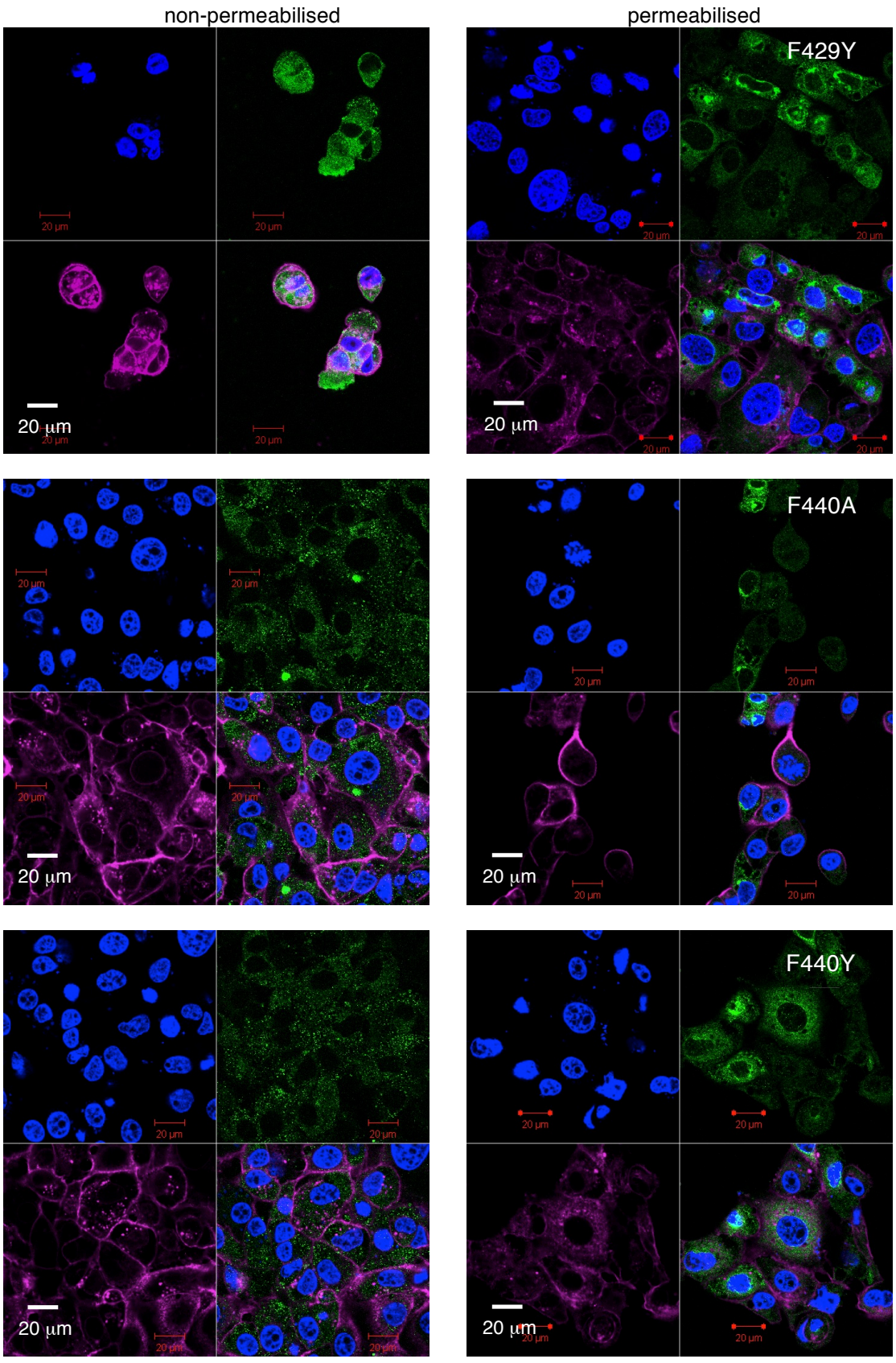
non-permeabilised
permeabilised
F429Y
F440A
F440Y
20 µm

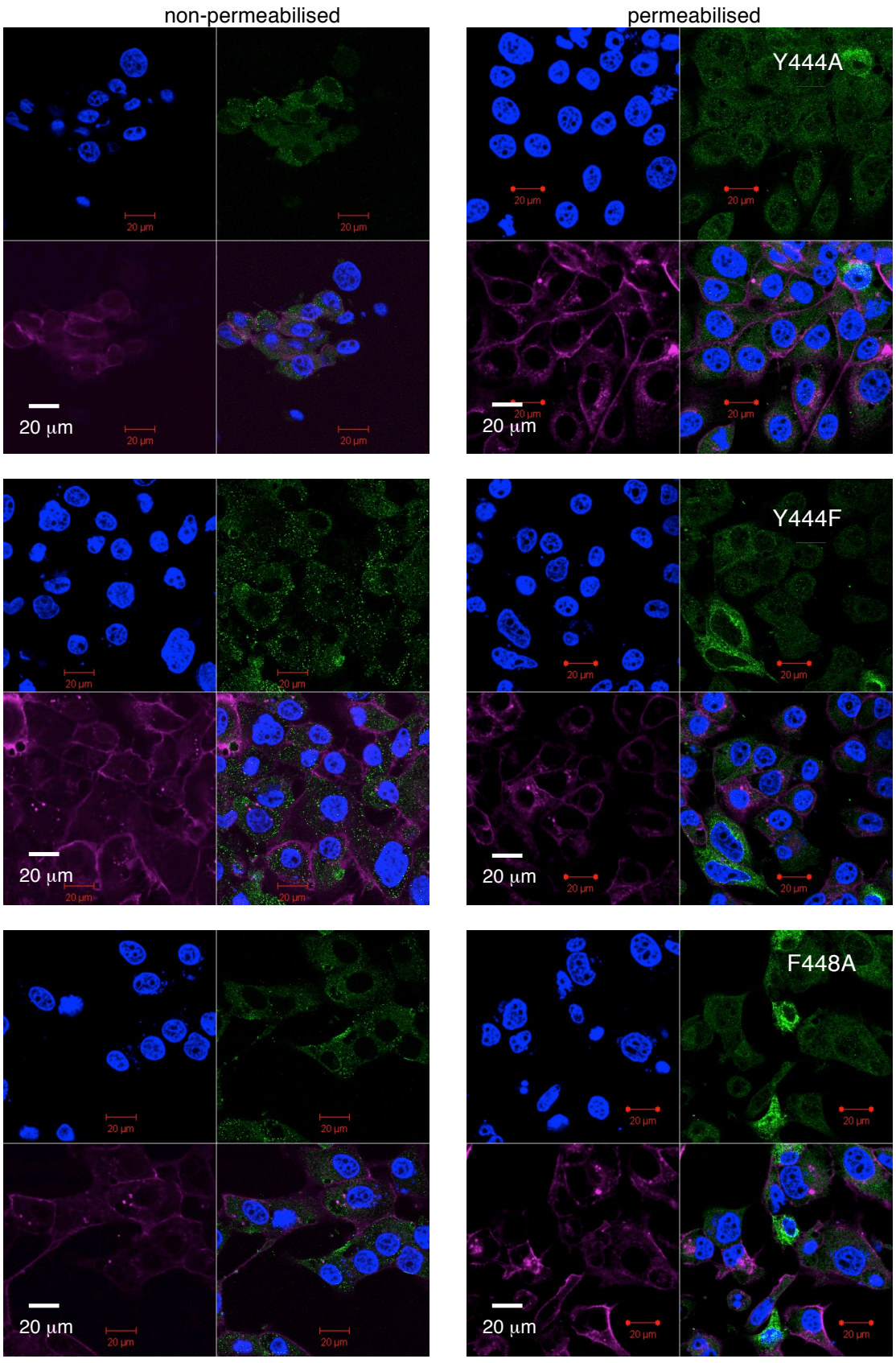
non-permeabilised
permeabilised
Y444A
Y444F
F448A
20 µm

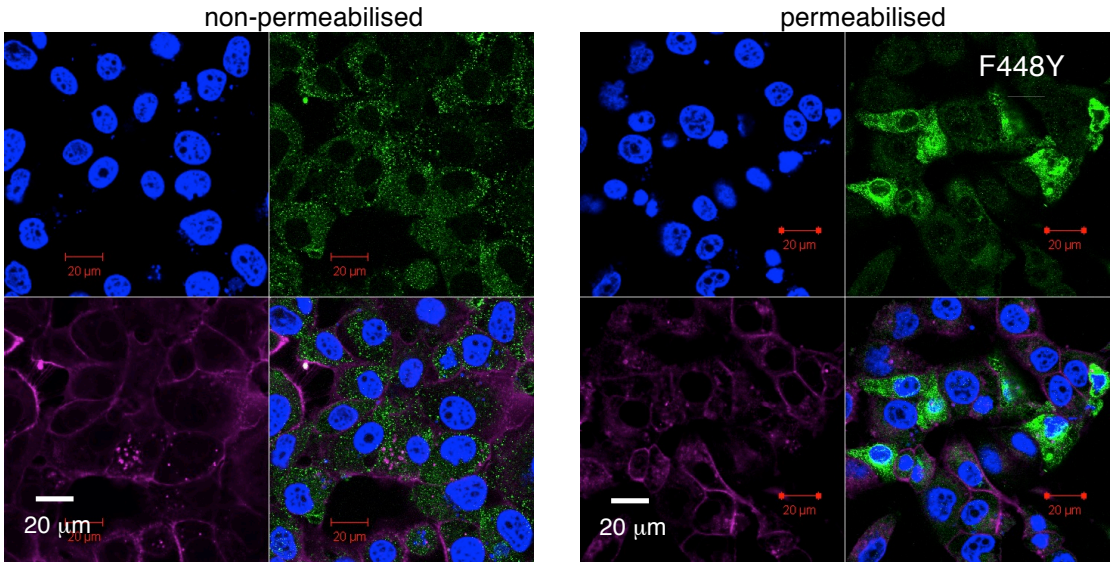

Figure 40. Confocal microscopy of PS-EK cells probed with 4G2 and WGA. Images of PS-EK cells transfected with wild-type prME, negative control pCI and all ten E2 mutants. Cells were fixed or fixed and permeabilised, then probed with 4G2 (1:400), Alexa Fluor 488 (1:400, in green), Hoechst (1:10,000, in blue) and WGA (1:500, in purple). The WGA for pCI is in red due to a different imaging software. All E2 mutants showed decent levels of E protein expression compared to wild-type prME except for F422A, which was detectable but low.

5.4.2. Analysis of cellular and surface expressed prM and E in infected cells

To correlate E expression in transfected cells with that of infected, cells were infected with New Guinea C strain of dengue subtype 2 (NGC DENV-2). Twenty-four hours post-infection, cells were either fixed or fixed and permeabilised. As shown in the following figures, Vero cells were infected at m.o.i. = 0.1 and 1. Dilutions of 4G2 (1:200 and 1:400) and 1:400 Alexa Fluor 488 were tested with m.o.i. = 0.1 (figure 41, top). Cells showed infectivity of around 5%, which was too low for comparison. Either dilution of antibody provided adequate fluorescence. Cells were also infected with m.o.i. = 1, which showed 75% infectivity and good fluorescence with 4G2 at both 1:200 and 1:400 (figure 41, bottom). M.o.i. = 1 and 4G2 dilution of 1:400 was used in proceeding experiments for an infection control. After optimisation with molecular probes (section 5.5), an infection time point series was carried out, which best shows the visualisation of E in infected cells (see page 98).

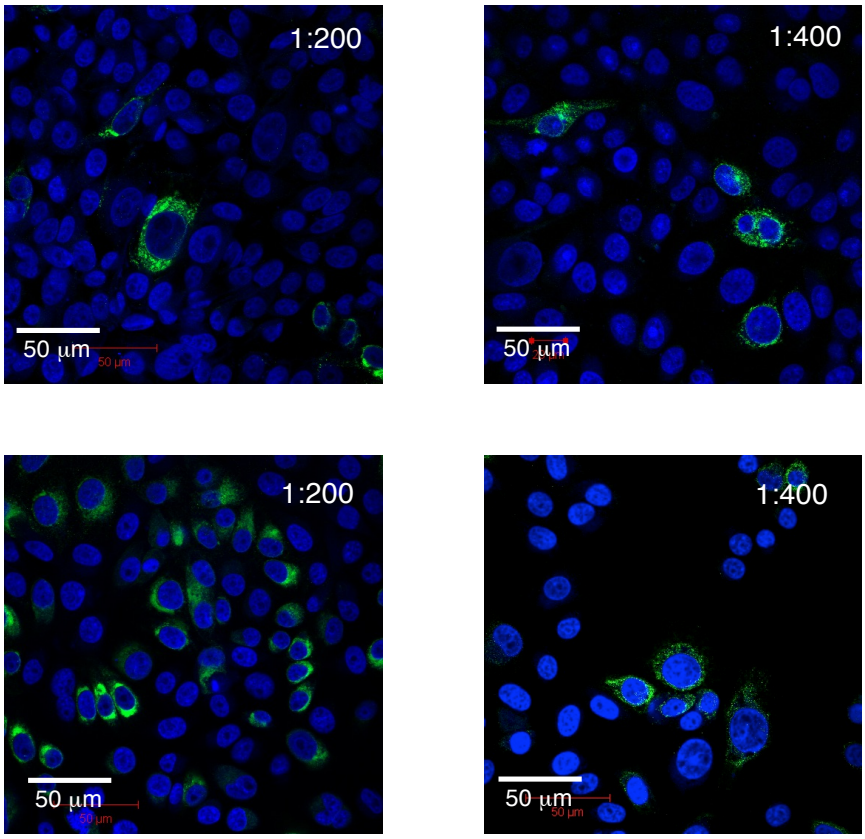

Figure 41. Immunofluorescent confocal microscopy of infected Vero cells with nuclei stain Hoechst (1:20,000), monoclonal antibody α-E 4G2 at 1:200 and 1:400 dilutions and conjugate dye Alexa Fluor 488 at 1:400. **[Top]** With m.o.i. = 0.1 only ~5% of cells are infected suggesting that this m.o.i. is too low. **[Bottom]** At m.o.i. = 1 and 1:200 dilution of 4G2, infectivity is clearly shown (left, approximately 75%). Adequate fluorescence was seen with the 1:400 dilution of 4G2 (right).

5.5. Analysis of the secretory pathway of prM and E

5.5.1. Tracking of the secretory pathway with molecular probes and antibodies

As a possible way of assaying fusion of DENV infected cells and/or tracking the progression of E through its secretory pathway, several molecular probes were tested, which stain an assortment of organelles. The probes tested (Invitrogen) include CM DiI (PM), CMAC and Calcein (cytoplasm), ER Tracker (endoplasmic reticulum), and WGA (Golgi apparatus and PM). Antibodies α-E 4G2 and 3H5 conjugated with Alexa Fluor 488 were used and cells were counterstained with Hoechst or propidium iodide (nuclei).

Un-infected PS-EK cells were seeded in 24-well plate format on to coverslips. Cells were not infected. After overnight incubation, cells were stained separately with cytoplasmic dyes Calcein (and Hoechst) or CMAC (and propidium iodide) or the plasma membrane

dye CM DiI (and Hoechst). Cells were incubated at thirty minutes at 37°C for Calcein and CMAC or fifteen minutes at 4°C incubation for CM DiI. The cells were then fixed, washed, dried and mounted on slides. This first experiment was designed to optimise staining with even coverage on uninfected cells. CMAC was tested in 2.5-fold dilutions from 10 μM to 0.10 μM. Calcein was titrated in two-fold dilutions from 10 to 0.31 μM and CM DiI was tested in two-fold dilutions from 2.5 to 0.08 μM (optimal concentration shown, figure 43). Hoechst was diluted to 0.05 ng/ml and propidium iodide (CMAC only) was used at 10 mg/ml. The optimal concentration for Calcein was 2.5 μM, CMAC at 0.64 μM, and CM DiI at 0.63 μM (figure 42 and 43).

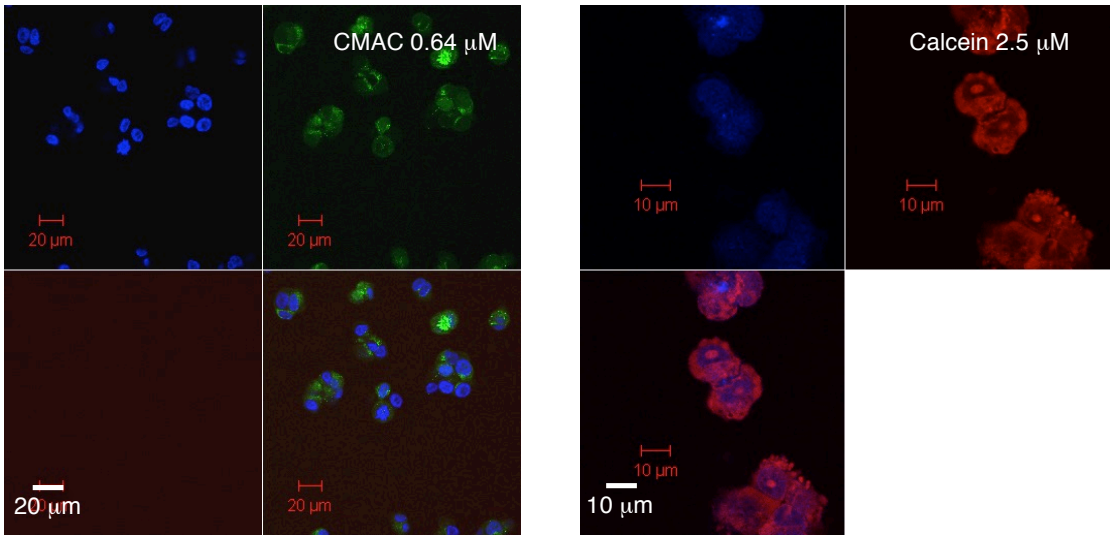

Figure 42. Immunofluorescent confocal microscopy of PS-EK cells stained with CMAC and Calcein. **[Left]** PS-EK cells stained with CMAC (green) at 0.64 μM and Propidium Iodide (blue) at 10 mg/ml. These concentrations show even distribution of the cytoplasmic dyes. **[Right]** Immunofluorescent confocal microscopy of PS-EK cells stained with Calcein at 2.5 μM (red) and Hoechst at 0.05 ng/ml (blue).

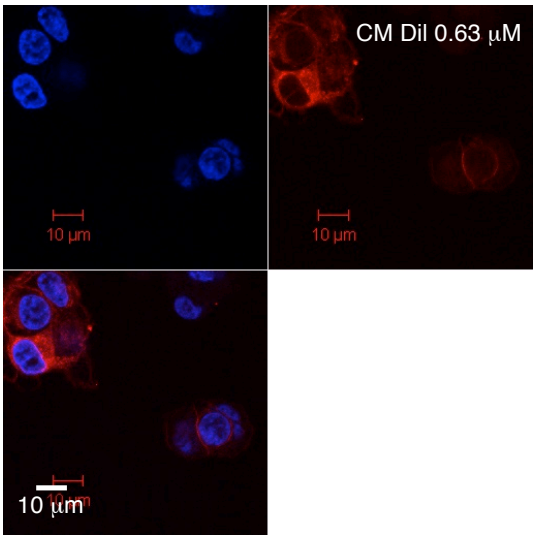

Figure 43. Confocal microscopy of PS-EK cells stained with CM DiI and Hoechst. Non-infected PS-EK cells were stained with CM DiI (red) at 0.63 μM and Hoechst (blue) at 0.05 ng/ml.

An endoplasmic reticulum dye (ER-Tracker) and a Golgi apparatus dye (WGA, wheat germ agglutinin), along with CM DiI and Hoechst were optimised. On fixed and permeabilised or non-permeabilised PS-EK cells, WGA was titrated from 10 μg/ml to 1 μg/ml from a stock concentration of 5 mg/ml; 5 μg/ml appeared to be the best as 10 μg/ml over-stained the cells and 1 μg/ml was not homogenous (optimal concentration shown, figure 44). WGA also appears to stain the PM, which would negate the need for a separate dye, and it distinctly stains the Golgi as seen in permeablised cells.

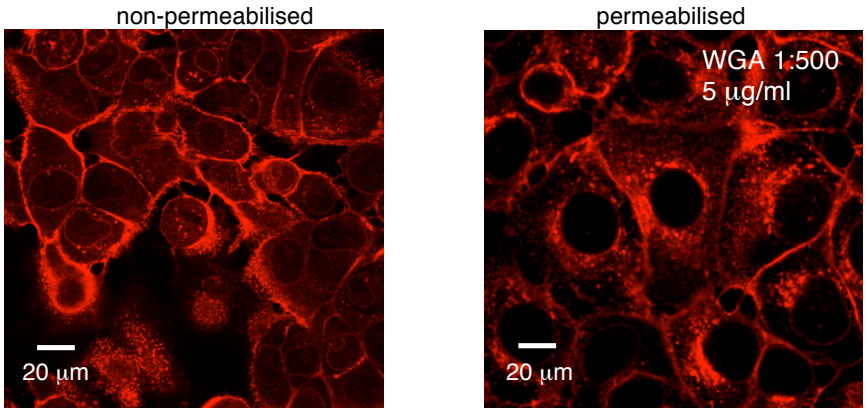

Figure 44. Immunofluorescent confocal microscopy of non-infected PS-EK cells treated with WGA. WGA was titrated from 10 μg/ml to 1 μg/ml from a 5 mg/ml stock. 5 μg/ml appeared to be the best concentration as 10 μg/ml over-stained and 1 μg/ml was not homogenous. Golgi staining was consistent and plasma membrane shows clearly as well.

ER Tracker, which stains the endoplasmic reticulum, was titrated from 250 nM to 1 μM. CM DiI was also titrated again from 0.63 μM to 2.5 μM on permeabilised and non-permeabilised cells. Both of these dyes must be applied prior to fixation. The best concentration for ER Tracker was 1 μM (figure 45). ER Tracker cannot be used in conjunction with Hoechst as they both emit at the same wavelength. At 1 μM ER Tracker, some nuclei are also stained, which is not ideal. CM DiI, at 2.5 μM, proved more consistent at plasma membrane staining when heating this dye up before dilution. CM DiI also stains the cytoplasm along with the PM when cells are permeabilised. This may interfere when visualising the progression of E protein throughout the secretory pathway.

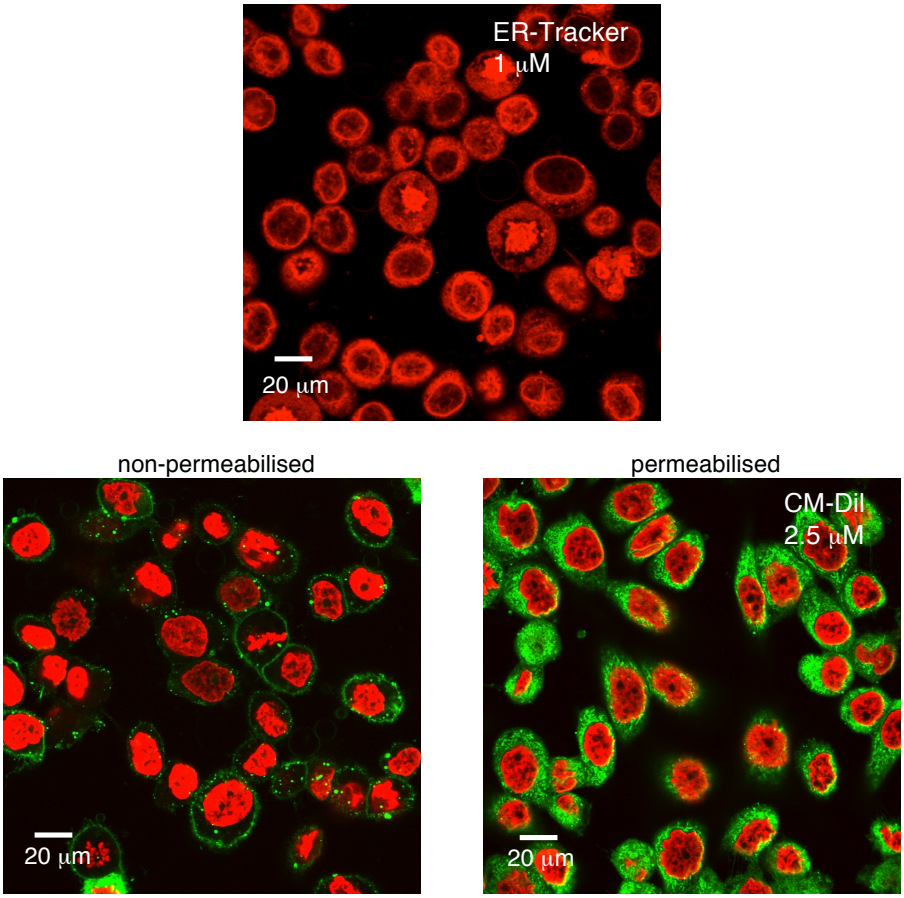

Figure 45. Immunofluorescent confocal microscopy of non-infected PS-EK cells. **[Top]** ER Tracker was titrated from 250 nM to 1 μM with 1 μM the best concentration. The endoplasmic reticulum is seen distinctly although some nuclei are also stained. **[Bottom]** CM DiI was heated before dilutions, with the optimal concentration at 2.5 μM. Once cells are permeabilised, CM DiI displays the cytoplasm as well as the plasma membrane.

Ideally, to track the progression of E protein, CM DiI (PM) with Hoechst (nuclei) or WGA (Golgi and PM) with Hoechst would sufficiently display the relevant organelles. ER Tracker (ER) with propidium iodide (nuclei) could also be used. Because of the possible confusion of cytoplasmic staining with CM DiI upon permeabilisation, WGA with Hoechst seems most ideal in conjunction with α-E 4G2 and Alexa Fluor 488. Unfortunately, there is no molecular dye for endosomes. There are rabbit polyclonal antibodies available for Rab 5 (early endosome) and Rab 7 (late endosome).

5.5.2. Tracking of the secretory pathway with molecular probes and antibodies in infected cells

Continued testing of molecular probes was carried out with infected PS-EK cells and the following optimized dyes: ER Tracker (endoplasmic reticulum), WGA (Golgi apparatus) and CM DiI (PM). These dyes were used on their own or in combination with Hoechst and 4G2 (α-E fusion peptide antibody) in conjunction with Alexa Fluor 488.

PS-EK cells were infected at m.o.i. = 2 for 24 hours and either fixed or fixed and permeabilised. The optimised concentration from previous experiments of WGA was 10 μg/ml, CM DiI was 2.5 μM and ER Tracker was 1 μM. It is recommended that ER Tracker be used prior to fixation, as is CM DiI. WGA may be used either before or after. On fixed and infected cells, all three dyes were tested to determine if the PM and ER could be stained post-fixation. E monoclonal antibody 4G2/488 was tested in combination with the organelle dyes.

ER Tracker stains the endoplasmic reticulum well and can be used post-fixation but it is not distinguishable from Hoechst as they both emit at the same frequency (figure 46). WGA clearly displays the Golgi apparatus and PM in combination with 4G2/488. CM DiI should not be used prior to fixation, as it does not stain the PM well (data not shown).

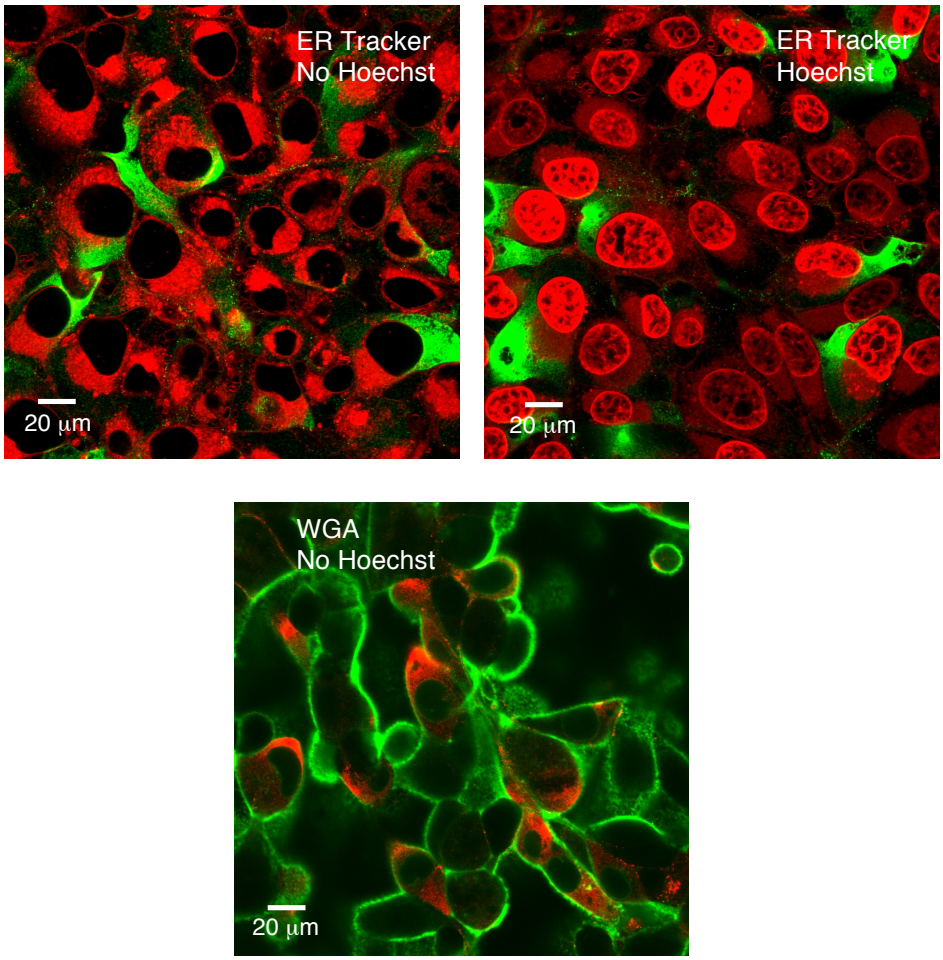

Figure 46. Immunofluorescent confocal microscopy of infected PS-EK cells. Cells are probed with 4G2 and Alexa Fluor 488. **[Top]** ER Tracker stains the ER clearly but it emits at the same wavelength as Hoechst (both in red). **[Bottom]** WGA, shown without Hoechst, clearly displays the Golgi and plasma membrane.

ER Tracker, CM DiI, and WGA were then tested in combination on infected PS-EK cells and applied prior to or post-fixation as recommended. PS-EK cells were infected for 24 hours at m.o.i. = 2. CM DiI (applied after fixation) with 4G2 and Hoechst on non-permeabilised cells stained the PM (blue) and E protein was clearly seen (green, figure 47). CM DiI with ER Tracker and 4G2 applied before fixation with permeabilisation did not work. It is not clear whether this is due to application of the two dyes or that CM DiI does not intercolate well prior to fixation.

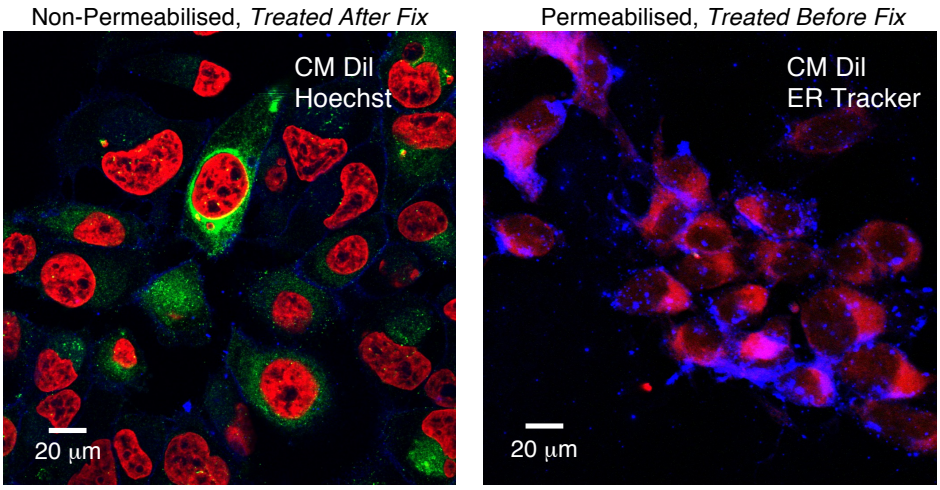

Figure 47. Immunofluorescent confocal microscopy images of infected PS-EK cells, permeabilised or non-permeabilised. Cells were stained with CM DiI (plasma membrane, blue), 4G2/488 (green) and Hoechst (nuclei, red), with or without ER Tracker (endoplasmic reticulum, red). CM DiI stains well with infected cells treated post-fixation. In combination with ER Tracker, the dyes were unclear but this may be due to the application of CM DiI requiring fixation as recommended or the two dyes interfering when applied together.

WGA with 4G2/488 and Hoechst on non-permeabilised cells stained well, clearly displaying the PM (blue, figure 48). Cell surface expression of the protein E in green is seen clearly. With permeabilised cells, the Golgi apparatus can be seen but it is more difficult to see the plasma membrane; E expression throughout the cytoplasm is well visualised. This dye works wells prior to fixation with permeablisation or without.

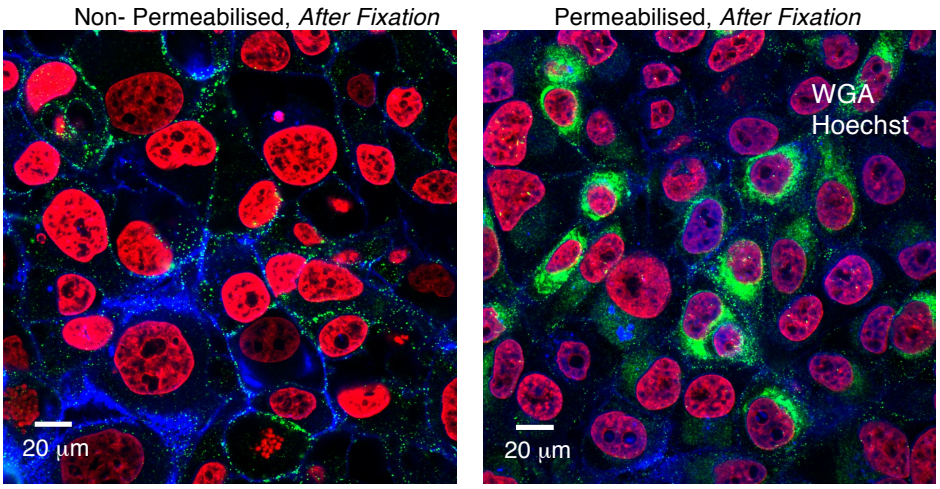

Figure 48. Immunofluorescent confocal microscopy images of infected PS-EK cells, permeabilised or impermeabilised. Cells were stained with WGA (Golgi apparatus, blue), Hoechst (nuclei, red) and α-E 4G2 with Alexa Fluor 488 (green).

WGA with ER Tracker and 4G2/488 on non-permeabilised cells (before fixation) shows a well-detailed view of the plasma membrane and E expression (figure 49, top left). Not seen previously, E is shown expelled from the cell surface. With permeabilisation, ER can be seen relatively well (red) and the PM in blue (WGA). WGA with ER Tracker and 4G2 on permeabilised cells (after fixation) shows a lot of overlapping with the dyes (figure 49, bottom), which deems the combination of dyes not useful.

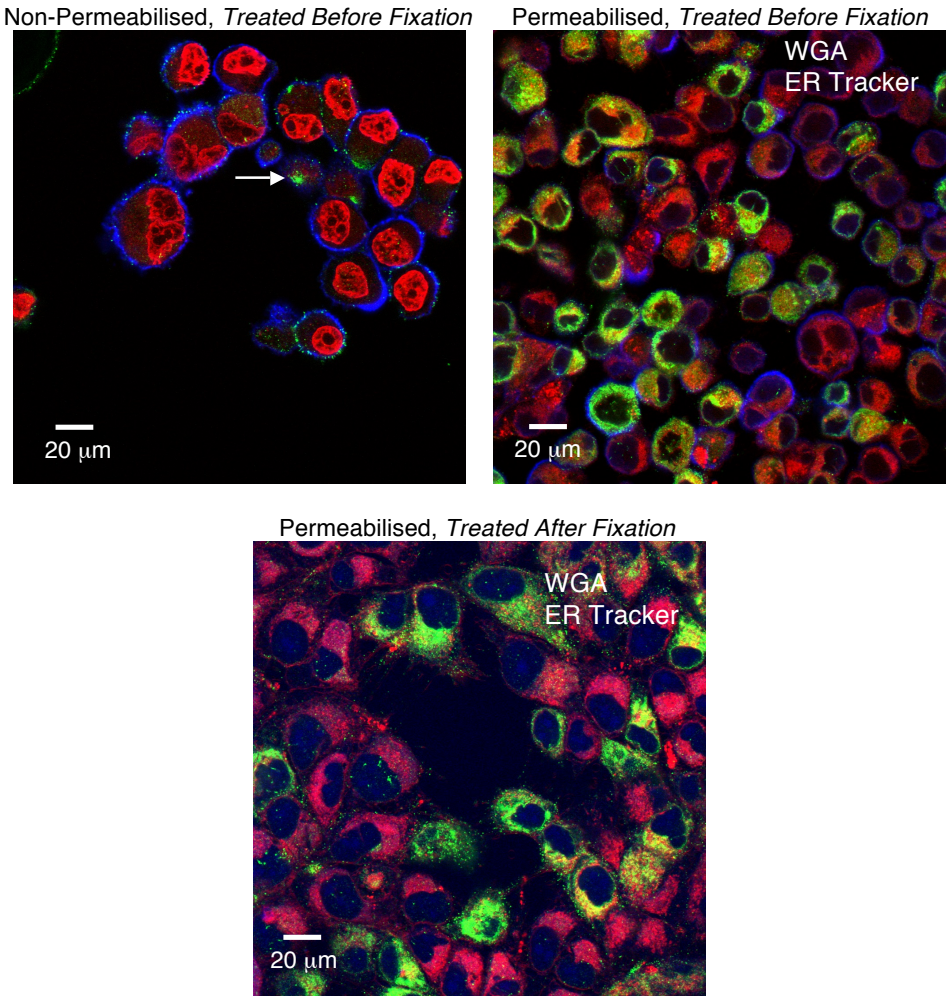

Figure 49. Immunofluorescent confocal microscopy images of infected PS-EK cells, permeabilised or non-permeabilised. **[Top]** Cells were stained with WGA (Golgi apparatus and PM, blue), α-E 4G2 with Alexa Fluor 488 (green) and ER Tracker (red). E protein is clearly detected on the cell surface, the PM is stained well with WGA and the nuclei and ER is stained well with ER Tracker. The arrow shows E protein being expelled from the cell. **[Bottom]** Permeabilised cells were stained with WGA (blue), 4G2 with Alexa Fluor 488 (green) and ER Tracker (red). E protein is clearly detected in the cytoplasm but the nuclei, ER and Golgi staining overlap too much.

In summary, these dyes display organelles well in the presence of α-E antibody 4G2 staining with or without Hoechst. ER Tracker works well with WGA on non-permeabilised cells whereas when the cells are permeabilised, the plasma membrane staining is lost. CM DiI works well with Hoechst but possibly not with ER; this dual stain should be repeated to confirm results. It is better to use CM DiI before cell fixation but ER Tracker and WGA can be used before or after. It would be beneficial to acquire an endosomal dye to complete the E secretory pathway but a single organelle dye is not available. There are rabbit polyclonal antibodies available for Rab 5 (early endosome) and Rab 7 (late endosome). If recombinant infectious particles with wild-type prME and the individual MPER α-helix E2 mutations are made successfully, this system would be useful in tracking DENV E throughout the secretory pathway. In conclusion, these molecular probe experiments showed that the best combination is WGA in conjunction with 4G2 and Alexa Fluor 488 (table 10).

	Organelle	Optimal Combinations
Hoechst	Nuclei	
Propidium Iodide	Nuclei	
Cholera Tx-B	Lipid Rafts/Plasma Membrane	Combine with Hoechst
Calcein	Cytoplasm	
CMAC	Cytoplasm	
CM DiI	Plasma Membrane	Combine with Hoechst
ER-Tracker	Endoplasmic Reticulum	Combine with WGA
WGA	Golgi (and Plasma Membrane)	Combine with ER-Tracker or Hoechst

Table 10. Cellular dyes: target organelle and optimal combinations. In PS-EK cells, these molecular probes target particular cellular components. The optimal combinations targeting multiple organelles, along with 4G2/488, are shown.

5.5.3. Localisation of E in infected cells

Organelle dyes were finally tested on infected PS-EK cells in a time point series with the following dyes: ER Tracker (endoplasmic reticulum), WGA (Golgi apparatus), CM DiI (PM), Hoechst (nuclei), and 4G2 (α-E fusion peptide) in conjunction with Alexa Fluor 488. Previously optimised concentrations of ER Tracker (1 μM), WGA (10 μg/ml) and CM DiI (2.5 μM) were used. PS-EK cells were infected at m.o.i. = 2 and cells fixed at

time points 4, 8, 12, 14, 16 and 24 hours. Some samples were also permeabilised. The best image for each time point is shown (figures 50-53).

In figure 50, CM DiI and Hoechst was used on non-permeabilised PS-EK cells. At 4 hours, E protein can be seen just after translation. It appears to be expressed and migrating to the cell surface by 8 hours. At 16 hours, the arrow shown depicts the accumulation of E at the cell surface. E can be seen extending out from the plasma membrane. In figure 51, WGA and Hoechst stains permeabilised PS-EK cells. At 8 hours, there is some E protein visible outside the nucleus. There are large amounts of E being expressed and migrating through the secretory pathway at 12 hours. This increases at 14 and 16 hours. At 24 hours, E is seen aggregating at the plasma membrane. In figure 52, WGA, ER-Tracker and Hoechst, in combination, is used on non-permeabilised PS-EK cells. At 8 hours, E protein can just be seen after translation. By time point 14 hours, E protein is shown at the perimeter of the cells. There are large amounts of E being generated in the endoplasmic reticulum at 16 hours. E has migrated through the trans-Golgi network to the cell surface by 24 hours. The plasma membrane is well visualised with WGA but the ER-Tracker dye is difficult to see as it is in the same spectrum as Hoechst. In figure 53, the same combination of dyes (WGA, ER-Tracker, and Hoechst) is used on permeabilised PS-EK cells. There is some E protein visible at 4 hours, seen as punctation on the cellular surface. This could be incoming viral particles, which had not been seen previously. At 8 hours, E is visible in the cytoplasm and at 12, it appears E is being translated in the ER. There are large amounts of expression and migration through the secretary pathway at 14 hours, which increases at 16 and 24 hours.

CM DiI, Hoechst with non-permeabilised cells

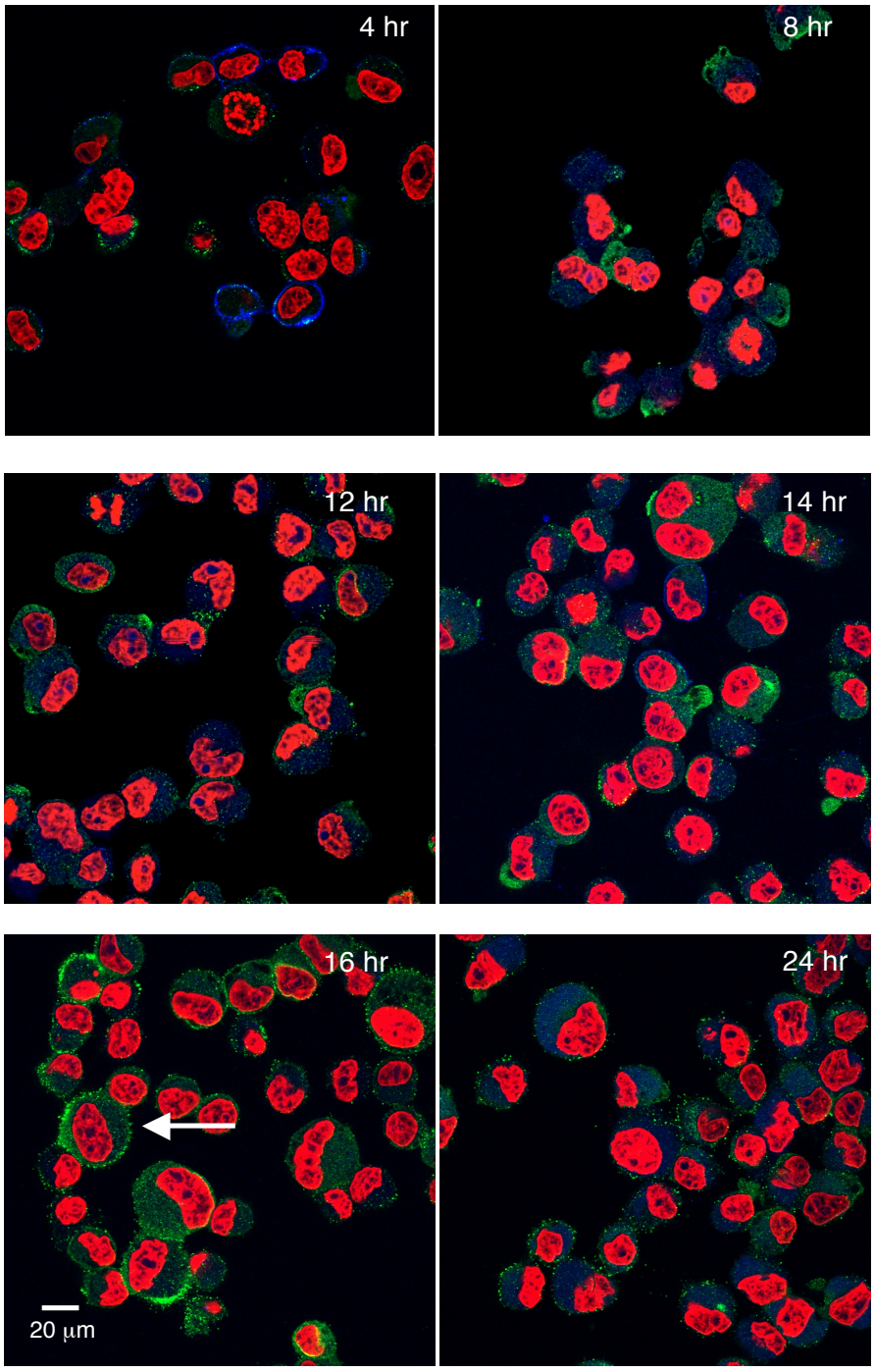

Figure 50. Immunofluorescent confocal microscopy images of infected PS-EK cells non-permeabilised and probed with 4G2/488 (green). Cells are stained with CM DiI (blue, PM) and Hoechst (red). The arrow depicts the accumulation of E at the cell surface and extending out from the plasma membrane.

WGA, Hoechst with permeabilised cells

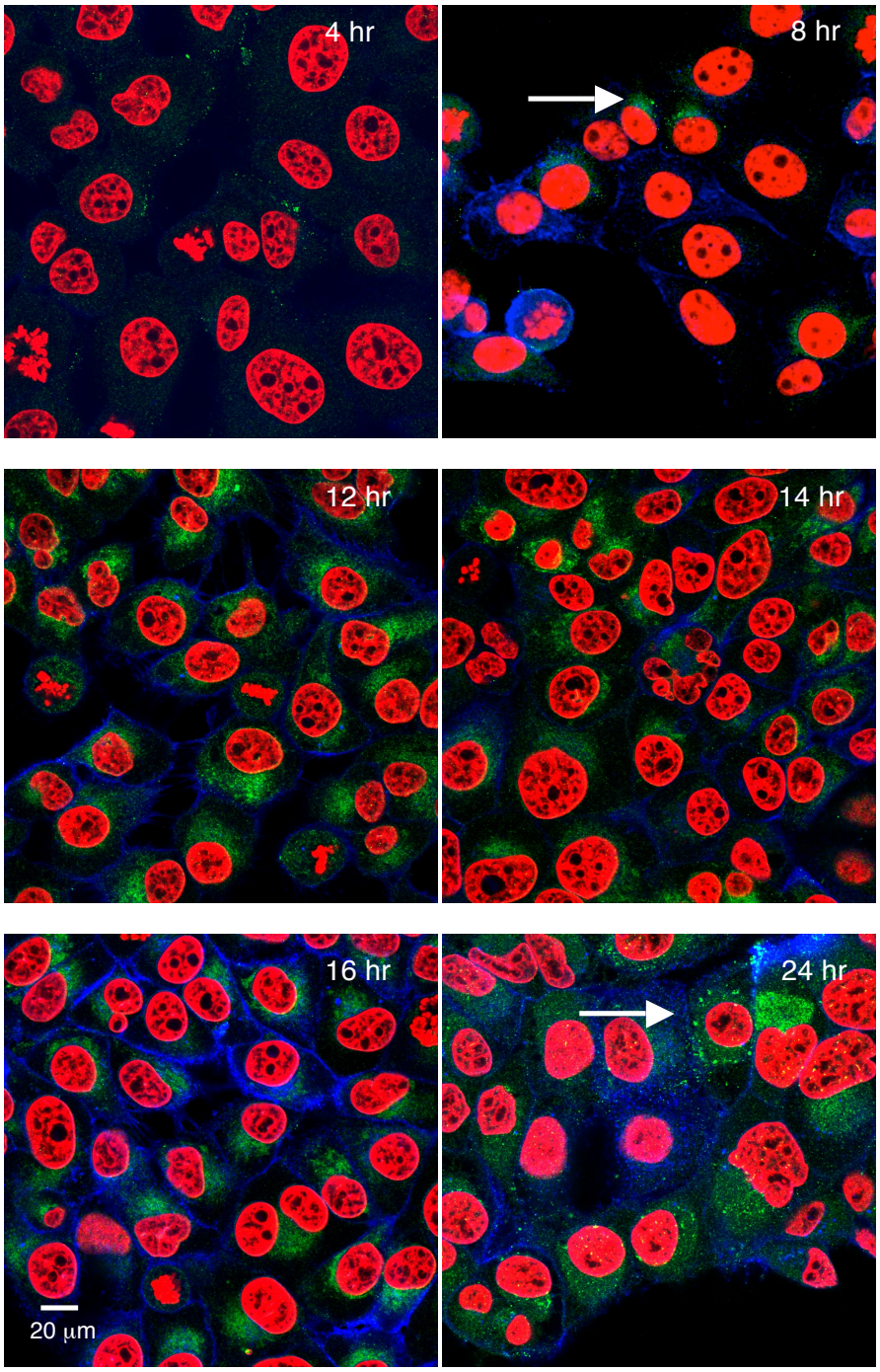

Figure 51. Immunofluorescent confocal microscopy images of infected PS-EK cells permeabilised and probed with 4G2/488 (green). Cells are stained with WGA (blue) and Hoechst (red). The arrow, at 8 hours, shows E after translation around the nuclei. At 24 hours, E is seen aggregating at the cell surface (arrow).

WGA, ER-Tracker, Hoechst with non-permeabilised cells

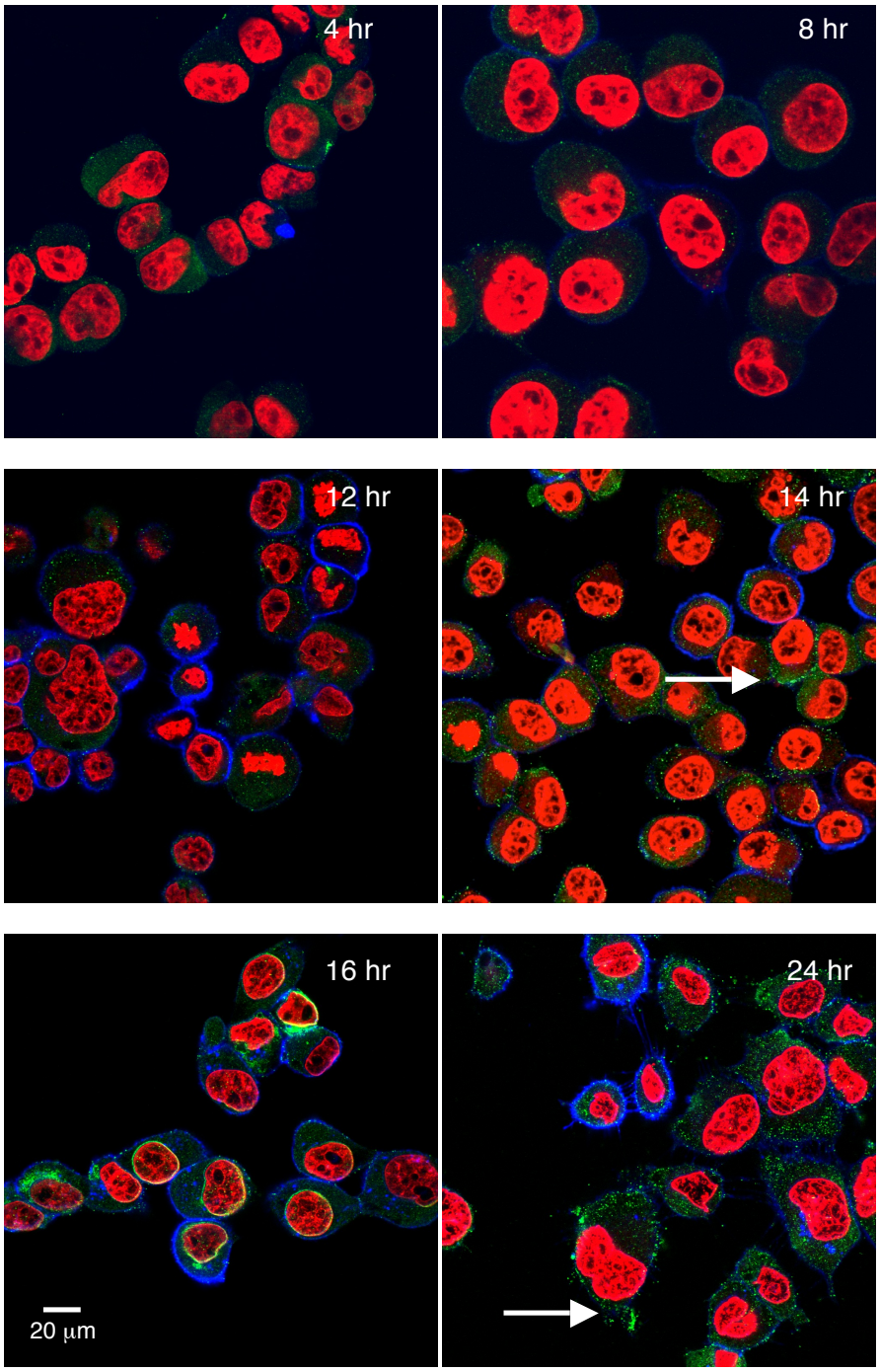

Figure 52. Immunofluorescent confocal microscopy images of infected PS-EK cells non-permeabilised and probed with 4G2/488 (green). Cells are stained with WGA (blue), ER-Tracker (red) and Hoechst (also in red). The arrows depict the migration of E to the cell surface at 14 hours and extending from the PM at 24 hours.

WGA, ER Tracker, Hoechst with permeabilised cells

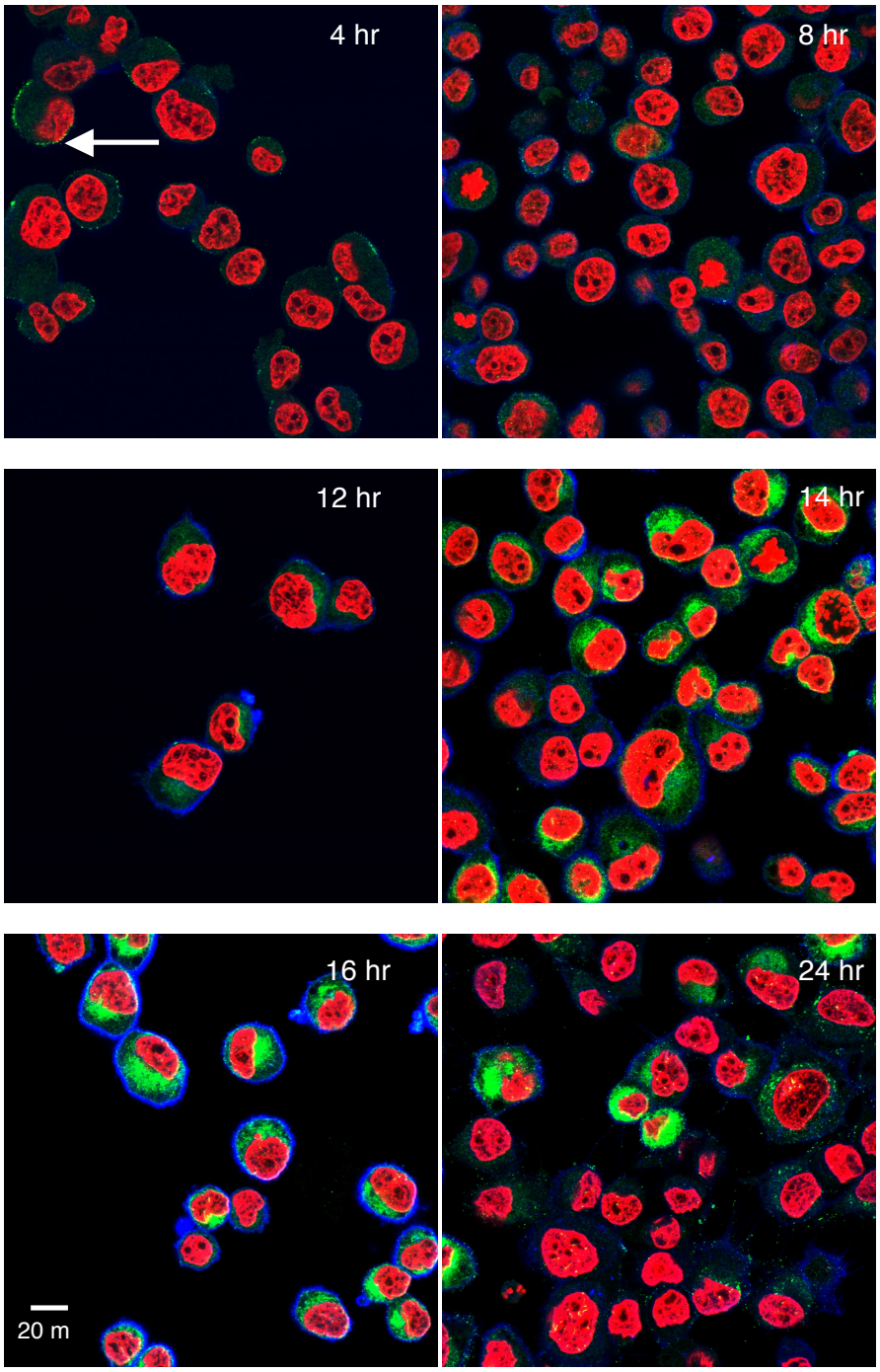

Figure 53. Immunofluorescent confocal microscopy images of infected PS-EK cells permeabilised and probed with 4G2/488 (green). Cells are stained with WGA (blue), ER-Tracker (red) and Hoechst (also in red). The arrow depicts E protein at the cell surface at 4 hours, which could be incoming viral particles.

To summarize this time point series, with permeabilised cells (WGA, ER-Tracker, and Hoechst images, figures 51 and 53), E can be seen at 4 hours, which could be incoming viral particles. After receptor-mediated endocytosis, fusion and release from endosomes, cytoplasmic E appears at 8 hours. Post-synthesis, E can be found in the ER/Golgi apparatus at 12-14 hours. With non-permeabilised cells, E appears at the cell surface by 12-14 hours (CM DiI and Hoechst, figure 50 and WGA, ER-Tracker, and Hoechst, figure 52). Accumulation of translated E protein appears at 14-16 hours. Cell surface appearance and exocytosis occurs at 16-24 hours. The pathway for E localisation, as described, is portrayed in the diagram below (figure 54).

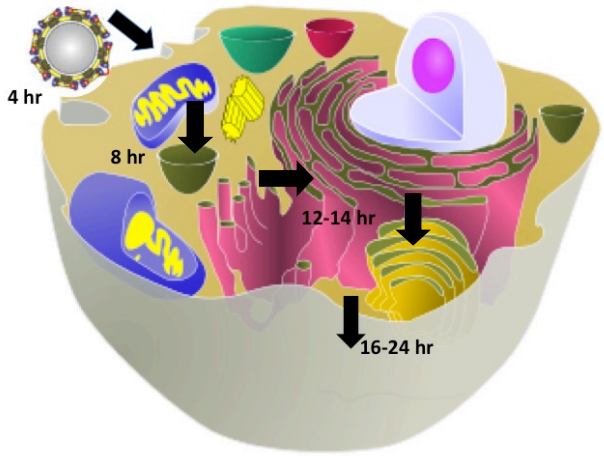

Figure 54. Possible timepoints for the virus pathway [95]. The replication pathway starts with attachment and receptor-mediated endocytosis at 4 hours. Cytoplasmic E appears at 8 hours. After translation, endoplasmic reticulum and Golgi apparatus presence occurs at 12 to 14 hours. Release of viral particles occurs between 16 and 24 hours.

5.6. Discussion

5.5.3. Conclusions of cellular and surface expressed MPER E2 mutant protein

PS-EK cells were transfected and probed with α-E 4G2 (fusion peptide) or 3H5 (DI and DIII linker), 1:400 Alexa Fluor 488, Hoechst and tertiary dyes Cholera Tx-B (lipid rafts) or WGA (Golgi and plasma membrane staining). Transfection efficiencies were 92% as detected by 4G2 with wild-type prME and mutants ranging from 49 to 85%, in the absence of a tertiary dye. The number of cells expressing perinuclear staining of E protein was quantified. For wt prME this was 33%, while mutants ranged from 7 to 19%. Antibody 3H5 was tested in parallel with 4G2 and both showed similar fluorescence. Cholera toxin was tested to confirm homogenous fluorescence was background signal and not E expression. With Cholera Tx-B added and cells permeabilised, 59% of cells were positive for wt prME while mutants ranged from 34 to 57% with outlying F422A at 8%, which agrees with immunoblot conclusions. For non-permeabilised cells, 52% of cells were positive for wt prME, while mutants ranged from 24 to 43%. F422A again was in contrast to the other mutants, showing no perinuclear localisation. In transfected cells stained with WGA and Hoechst, F422A was also the exception; non-permeabilised cell binding was comparable to other mutants but upon permeabilisation, this mutant showed reduced levels of fluorescence. The F422A mutation is just upstream to the conserved sequence (CS) between ∝-helix E1 and E2. The F422A mutants that are cell-surface expressed must be in a favourable conformation for 4G2 binding, in contrast to protein in the cytoplasm. Or alternatively, the binding site for 4G2 may be lost in its tertiary conformation as it is adjacent to the CS. With all other mutants, E protein is seen clearly in the perinuclear region and throughout the secretory pathway (Golgi to ER) en route to the PM.

Several molecular probes were tested, which include CM DiI (PM), Cholera Tx-B, CMAC and Calcein (cytoplasm), ER Tracker (endoplasmic reticulum), and WGA (Golgi apparatus and PM), along with α-E 4G2 and 3H5 conjugated with Alexa Fluor 488. Cells were counterstained with Hoechst or propidium iodide (nuclei). The optimal concentration for Calcein was 2.5 μM, CMAC at 0.64 μM and CM DiI at 0.63 μM. CM DiI, Hoechst and 4G2/488 can be used together to visualise the plasma membrane and E expression in infected PS-EK cells. CM DiI also stains the cytoplasm with permeabilised

cells, which can interfere with tracking E, while CMAC can be used to stain the cytoplasm with 4G2/488 and without Hoechst. The best concentration for WGA was 5 μg/ml and whilst it stains the Golgi it also stains the PM, which would negate the need for a separate dye. Cholera Tx-B was tested to display lipid rafts and its optimal concentration appeared to be 1:500 although this dye was precipitating. CM DiI (PM) was titrated from 0.63 μM to 2.5 μM along with ER Tracker (ER) from 250 nM to 1 uM. The best concentration for this combination was 2.5 μM for CM DiI and 1 μM for ER Tracker. Interference occurs with CM DiI staining both the cytoplasm and PM when permeabilised and ER Tracker cannot be used with Hoechst as they both emit at the same wavelength.

Ideally, to track the progression of E protein, CM DiI (PM) with Hoechst (nuclei) or WGA (Golgi and PM) with Hoechst would sufficiently identify the relevant organelles. ER Tracker (ER) with propidium iodide (nuclei) could also be used. Because of the possible confusion of cytoplasmic staining with CM DiI upon permeabilisation, WGA with Hoechst seems most ideal in conjunction with α-E 4G2 or 3H5 and Alexa Fluor 488. It is the most useful tertiary dye as it stains both the Golgi apparatus and the plasma membrane.

PS-EK cells were infected with DENV-2 and probed with 4G2 and Alexa Fluor 488 at a 1:400 optimal dilution. The cells were stained at various time points with the following dyes: ER Tracker, WGA, CM DiI, Hoechst, and 4G2/488. Cells were infected at m.o.i. = 2 and fixed at time points 4, 8, 12, 14, 16 and 24 hours. Upon permeabilisation, E is seen as incoming viral particles at the cell surface at four hours. After translation, E appears in the cytoplasm at eight hours, followed by ER/Golgi apparatus presence at twelve to fourteen hours post-polyprotein processing. Without permeabilisation, accumulation of translated E protein appears at fourteen to sixteen hours. This is followed by PM appearance and exocytosis at sixteen to twenty-four hours (table 11). To see E internally, cells should be fixed at fourteen and sixteen hours (permeabilised and non-permeabilised, respectively). To track E to the cell surface, cells should be fixed at a minimum of sixteen hours.

Dye	Compartment Labeled	Co-Localisation with E (Hours)				
		4	8	12-14	14-16	24
WGA, CM DiI	Plasma Membrane (Endocytosis)	+	+	-	-	-
ER-Tracker, WGA	ER and Golgi Apparatus	-	+	+	+	+
WGA, CM DiI	Cytoplasm and Cellular Surface	+	+	+	+	+
WGA, CM DiI	Plasma Membrane (Exocytosis)	-	-	-	+	+

Table 11. Localisation of E with 4G2/488 and cellular dyes. In combination with α-E 4G2/488, these molecular probes are the best choice to visualise listed organelles.

CHAPTER 6

RESULTS: INSECT CELL LINE EXPRESSION OF prM AND E

6.1. Introduction and design of pSFV-prME vector

To compare the results of MPER E2 mutant expression in a mammalian cell line with insect-derived E protein, a plasmid was created to transfect C6/36 cells. A cassette system was developed to insert wild-type and mutant prME segments into a second vector, pSFV (Semliki Forest Virus replicon) for insect cell expression. pSFV (Invitrogen) is a cDNA clone containing non-structural proteins, 26S subgenomic RNA promoter, 5' and 3' UTRs, ampicillin resistance and MCS (figure 20). The plasmid pSFV was stripped of all but the AmpR gene and MCS sequences and these were ligated to a linker containing unique restriction sites for cloning. This linker contains the sites *Not I* and *Xho I*, allowing for insertion of the prME gene. This ligation generates the pSFVprME "cassette" vector, which is 5.2 kB in length (figure 55). This vector, along with wt pSFV was then digested with *Spe I* and *BamH I*, which produced two products, a 10172 bp product from pSFV and a 2917 bp product from the pSFVprMEcassette. These products were then ligated together to make a 13 kB full-length pSFVprME clone. Purified plasmid was transformed into competent cells. Figure 56 shows twenty-four of these transformants, one of which was the correct length.

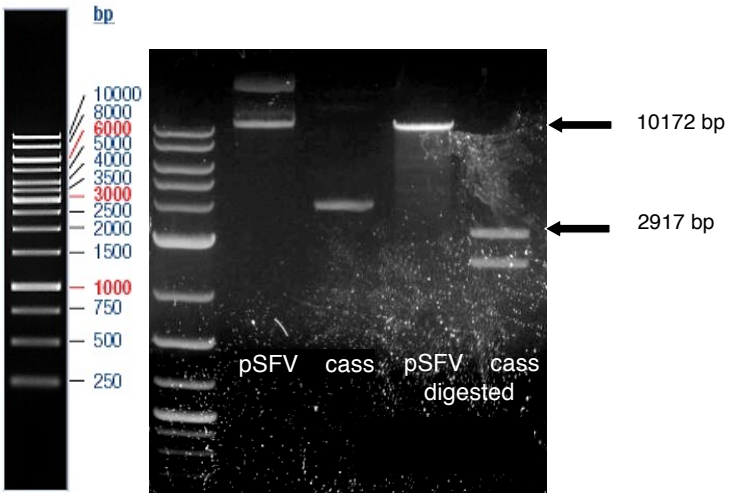

Figure 55. Agarose gel of pSFV cloning products. Lane 1 is wt pSFV followed by pSFVprMEcassette (cass), pSFV digested with *Spe I* and *BamH I*, and pSFVprMEcassette digested with *Spe I* and *BamH I*. pSFVprME cassette is 5.2 kB in length and cut with these two enzymes results in two bands, 2342 and 2917 bp in length. Wild type pSFV cut results in 861 and 10172 bp bands. The 10172 bp band ligated to the 2917 bp of pSFVprMEcassette (arrows point bands) results in the new 13 kB pSFVprME vector.

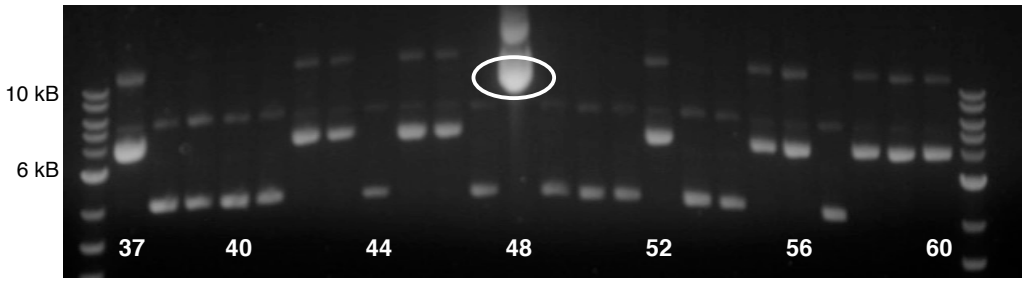

Figure 56. Agarose gel of transformants from the ligation of wt pSFV and pSFVprMEcassette (*Spe I* and *BamH I*). There are twenty-four transformants shown (Samples 37-60) and Clone 48 is positive for the correct length of 13 kB (circled). This pSFVprME (wild-type) plasmid will be used as the control against mutant pSFVprME plasmids.

Four of these transformants were digested with *EcoR I*, which cuts at several sites (figure 57). The correct 13 kB plasmid will be cut at bases 2185, 3763, 7390, 7411 resulting in 1578, 3627, 21 and 7861 bp bands. In contrast wt pSFV has three cut sites at bases 2185, 3763, 7390 resulting in 1578, 3627 and 5828 bp bands and pSFVprMEcassette has one at base 3214, which linearises the plasmid. Wild-type prME also only has one site, which linearises the plasmid to 7485 bp. Clone 48 resulted in the correct-sized bands; it was subsequently sequenced and shown to be correct.

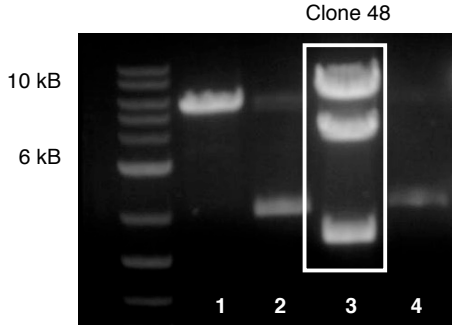

Figure 57. Agarose gel of pSFVprME clones 37, 38, 48 and 49 diagnostic digest. Clones were digested with *EcoR I* to test correct restriction enzyme cut sites. The correct 13 kB plasmid cuts at 2185, 3763, 7390, 7411 resulting in 1578, 3627, **21 and 7861** bands (the 21 bp band is not visible). Clone 48 was subsequently sequenced and shown to be the correct plasmid (boxed).

Lane	Sample	Results
1	Clone 37 Eco	Linearised to 7485 (prME wt)
2	Clone 38 Eco	Linearised to 3214 (pSFVprMEcassette)
3	Clone 48 Eco	*Possible positive for* pSFVprME – 7861, 3627, 1578
4	Clone 49 Eco	Linearised to 3214 (pSFVprMEcassette)

The pSFVprMEcassette vector was then used as the backbone for cloning all ten MPER E2 mutations. pCI_NGCprME mutants were digested with *Not I* and *Xho I* and the band

containing prME was excised and purified from agarose (figure 58). This was then ligated with pSFV (*Not I*/*Xho I*) to create pSFVprMEcassette mutant plasmids. After transformation, several clones were again digested with *Not I* and *Xho I* to select for correct-sized bands. Three of these mutants (F429A, F448A, and Y444A) that had the correct-sized bands are shown in figure 59. All ten cassette vectors were made and confirmed by diagnostic restriction digests. It was intended that these cassette mutants would be then digested to clone mutant prME back into full-length pSFV, however due to time constraints this last cloning step was not completed.

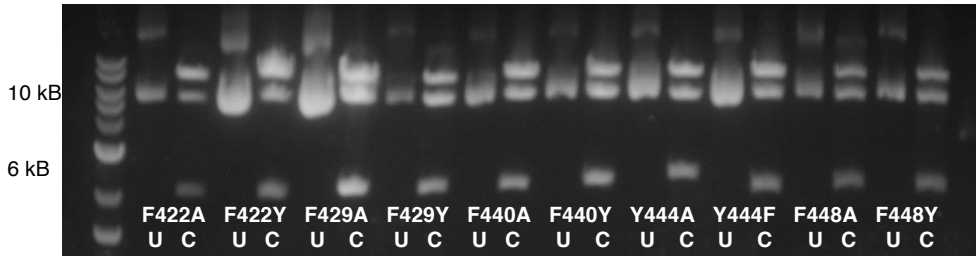

Figure 58. Agarose gel of pCI_NGCprME E2 mutants. Plasmids were digested with *Not I* and *Xho I* to obtain the 2917 bp prME mutant segment. Samples are as follows: F422A, F422Y, F429A, F429Y, F440A, F440Y, Y444A, Y444F, F448A, F448Y uncut (U) followed by digested plasmid (C). The bottom bands were gel extracted and purified. These mutant prME segments were subsequently ligated with digested pSFVprME cassette (*Not I*/*Xho I*). Ligations were transformed into Top ten cells and tested for presence of prME insertion by diagnostic colony PCR.

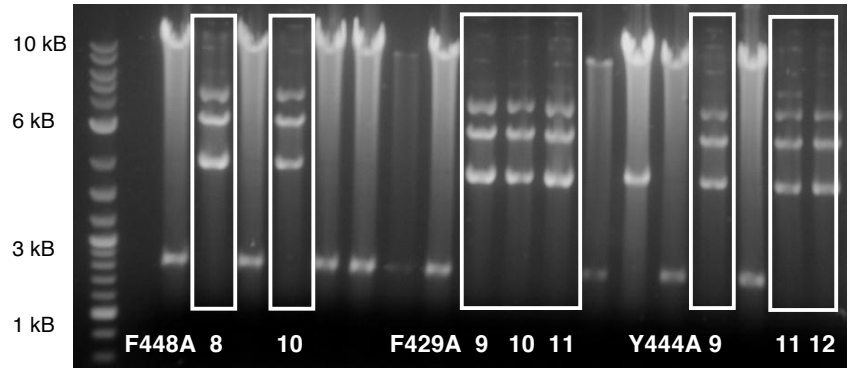

Figure 59. Agarose gel of possible pSFVprMEcassette mutant clones. Plasmids were digested with *Not I* and *Xho I* to diagnose presence of the prME E2 mutant gene. The first set of samples numbered 7-12, are F448A, the second F429A and the third, Y444A. The correct sized plasmid should be 5.2 kB, which when cut with *Not I* and *Xho I* results in two bands 3.2 and 2 kB. Clones F448A 8 and 10, F429A 9, 10 and 11, and Y444A 9, 11 and 12 had the correct sized digestion products. This is an example of selection of pSFVprMEcassette mutant plasmids; the other mutants are not shown.

6.2. Results: Transfection of wt pSFVprME with C6/36 cells to test expression of prM and E

RNA was transcribed from the cloned wild-type pSFV-prME plasmid and appears to be expressing with a preliminary test of transfected C6/36 cells. Wild-type pSFV-prME was linearised, purified and transcribed with SP6 RNA polymerase according to the procedure described in Materials and Methods. C6/36 cells were transfected immediately following transcription, with 1.6, 3.2 and 6.4 μg of wt pSFV-prME RNA. Cells were fixed twenty-four hours post-transfection. Samples were then blocked and probed with 4G2/488 and Hoechst. Cells were visualised with confocal microscopy and positive fluorescence was seen (green, figure 60). The majority of cells appear to show expression of prME and protein can be seen throughout the cytoplasm. There is a small degree of background fluorescence with the mock-transfection (bottom left image) due to Alexa Fluor 488 at this concentration.

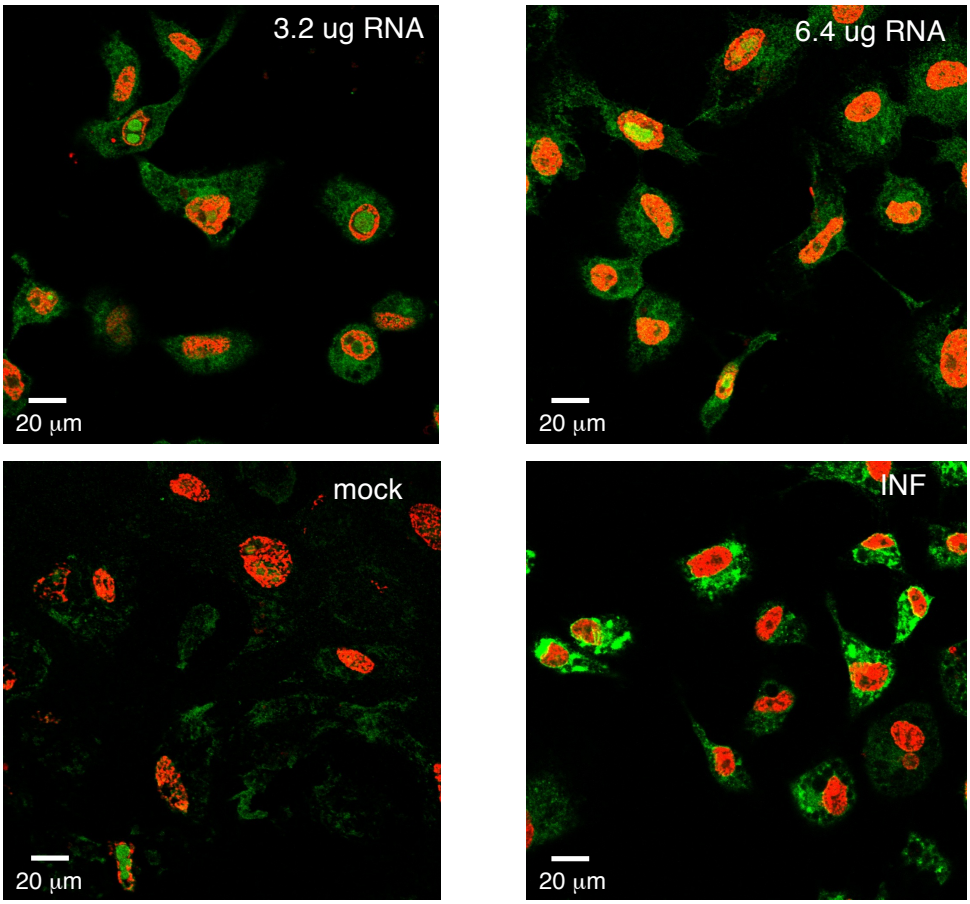

Figure 60. Test transfection with RNA pSFV-prME in C6/36 cells. **[Top]** Cells were probed with 1:400 4G2/488 and 1:10,000 Hoechst. **[Bottom]** The left image is a mock transfection, which shows a small degree of background fluorescence with Alexa Flour 488. The right image is a control sample with cells infected with DENV-2.

6.3. Discussion

6.3.1. Further work on expression of prM and E in C6/36 cells

After all ten E2 mutant pSFVprME vectors are made, these plasmids would be transcribed and transfected into C6/36 cells. These cells would then be analysed similarly to mammalian cells, including expression of prME mutant protein, trafficking and maturation along the secretory pathway. Instead of analysis with FACS on RNA transfected C6/36 cells, in-cell analysis could be used to quantify cell surface and cytoplasmic expression (section 5.2.2.). FACS analysis provides inconsistent results with the conditions used in previous experiments with mammalian cell lines. In-cell analysis appeared promising and may be a more consistent detection method for quantifying expression of prME. It also has the advantage of assaying 384 samples at a time, in microtiter plates. SDS-PAGE and Western immunoblots should be completed to confirm protein expression of prME in C6/36 cells and E epitope display. Immunofluorescent confocal microscopy images should then be obtained to view prME secretory trafficking, cell surface and cytoplasmic expression, along with calculation of transfection efficiencies to compare with mammalian cells. Transfected C6/36 cells would be probed with 3H5 and 4G2 in combination with Hoechst and WGA.

CHAPTER 7

GENERAL DISCUSSION

The aim of this research project was to determine the structural significance of the membrane-proximal (MPER) E2 α-helix in Dengue's E protein in pH-activated conformational change and its role in membrane fusion. To begin this structural analysis, single-point mutations (F422A/Y, F429A/Y, F440A/Y, Y444A/Y, F448A/Y) were inserted into ten separate NGC_prME_opt_neo plasmids, by site-directed mutagenesis. These amino acid mutants were then available to investigate the role of each of these residues in the structural changes of E, including prME heterodimeric formation and protein maturation.

For the second aim of this project, a lentiviral system was developed to assay these mutations. Pseudotyped retroviral particles were constructed to provide a method of measuring fusion by successful entry of prME lentivirus into target cells. There are several challenges with this system. After transfection, cells must take up all four plasmids and expression must be sufficient for infectious particles to assemble. The harvested supernatant must be concentrated, providing sufficient virus for transduction. There was low efficiency of lentiviral particle formation with prME, subsequently leading to low rates of infection. This could be due to prME's ER-retention signal and/or catalytic cleavage of prM. A long harvest is also necessary for an effective level of virus. To overcome these problems, it might be possible to design a three-plasmid, luciferase reporter system, similar to assays currently in use for HCV. This would result in a higher transfection efficiency with one less plasmid needing to be incorporated and thus, larger amounts of lentivirus generated [91]. These pseudotyped lentiviral particles could then be assayed using the sensitive luciferase detection system.

The third aim of this project was to investigate the structural character of MPER E2 mutants by localising E within the cell and cellular compartments in a mammalian cell line. To quantify cell surface expression, cells were transfected, fixed and probed with antibodies 3H5 (anti-E domain I and III linker) and 4G2 (anti-E fusion peptide) and analysed by flow cytometry. Preliminary results showed positive fluorescence but subsequent experiments showed variability, with a lack of sensitivity similar to the drawbacks of lentiviral pseudotype particle system. This method of quantification may have benefitted from harvesting cells at three days instead of one day post-transfection, as with lentivirus. There was a low level of E expressed at the surface, since it could be

detected in non-permeabilised cells. In contrast, in permeabilised cells, E levels were significantly higher. A longer harvest would allow for E to migrate to the cell surface, thus increasing surface expression.

Western immunoblots were performed to confirm the expression and stability of mutant E proteins. This system was optimised for cell lysis (lytic buffer), immunoblot transfer (semi-dry and submerged), and antibody incubation (time and volume). 4G2 recognises the E2 mutants F429A, F440A, Y444A, F448A well but not F442A. An additional band appears above 65 kDa with the infected control and mutant F448A. This could be a difference in glycosylation of the envelope protein, causing a change in migration patterns. MPER E2 mutants F422Y, F429Y, F440Y, Y444F, and F448Y were all detected by 4G2 while F448Y migrated lower than wt prME but in line with the infected control sample. It is unclear whether or not this was gel artifact as F448Y was run next to the infected control. 3H5 recognised all alanine mutants, with F442A detected most readily by this antibody. There may be a conformational preference for the 3H5 epitope between DI and DIII, due to F422's position between the E1 and E2 helices. E2 mutants F422Y, F429Y, F440Y, Y444F and F448Y were all recognised by 3H5.

To track E progression through the secretory pathway, its cell-surface expression and to calculate transfection efficiencies, mammalian PS-EK cells were transfected and analysed by immunofluorescent confocal microscopy. Cells were probed with 4G2 or 3H5 with Hoechst and tertiary dye WGA (Golgi/PM staining). With both antibodies, E protein localised into perinuclear foci, appearing throughout the cytoplasm and expressed on the cell surface. As with Western immunoblot data, F422A showed consistent differences, displaying low to no fluorescence when probed with 4G2 in permeabilised cells. In non-permeabilised cells, F422A showed reduced but comparable levels of fluorescence with the other mutants. The F422A mutation is just upstream from E2, within the conserved sequence between ∝-helix E1 and E2. It is possible that F422A mutants that are present on the cell surface are in a favourable conformation for 4G2 binding, in contrast to protein within the cytoplasm.

Several cellular dyes were optimised for concentration and incubation times, including CM DiI (PM), CMAC and Calcein (cytoplasm), ER Tracker (endoplasmic reticulum), and WGA (Golgi apparatus and PM) along with 4G2 and 3H5 antibodies. Cells were counterstained with Hoechst or propidium iodide (nuclei). While CM DiI and ER-Tracker were useful probes to track the progression of E, the combination of WGA and Hoechst

was the most suitable, in conjunction with 4G2 or 3H5, as it stains both the Golgi apparatus and the plasma membrane. There is a new pH-sensitive molecular dye available specifically for endocytosis called pHrodo™ (Molecular Probes) [96]. This dye is non-fluorescent at neutral pH and fluoresces bright red in acidic environments. The minimal dye fluorescence at neutral pH also eliminates the need for wash steps and quencher dyes, which reduces handling, timing, and loss of samples. It can also be multiplexed with other dyes such as eGFP, CM DiI, or WGA. This dye could be tested in conjunction with WGA, 4G2/488, and Hoechst to track fusion between E and the endosome/lysosome.

PS-EK cells were also infected and probed with 4G2/488 and tested with cellular dyes in an infection time point series. CM DiI (PM) was tested on its own and WGA (Golgi apparatus/PM) was used with or without ER Tracker. Cells were infected at m.o.i. = 2 and fixed at time points 4, 8, 12, 14, 16, and 24 hours. With permeabilised cells, E can be detected at four hours, seen as punctation on the cellular surface. This could be incoming viral particles undergoing receptor-mediated endocytosis. Cytoplasmic E appears at eight hours, which could be release of the nucelocapsid after low-pH lysosome fusion. After translation of prM and E, viral assembly begins in the ER and Golgi, seen at twelve to fourteen hours. With non-permeabilised cells, accumulation of translated E appears at the cell surface and exocytosis occurs at sixteen to twenty-four hours. To see internal E, cells should be fixed at fourteen and sixteen hours (permeabilised and non-permeabilised respectively). To track E expression to the cell surface, cells should be infected for a minimum of sixteen hours prior to fixing.

It is now known that residues F422 and F448 do not lie strictly in the α-helix E2 but do correlate with the membrane-proximal external region (MPER). F422 is located in the conserved (CS) region between the two helices. F429 is in the α-helix E2, along with F440 and F444. F448 is part of the four amino acid C-terminus of E2 [97]. For DENV-2, the N-terminus of the stem region is thus G395-S397, α-helix E1 is I398-L415, the CS is G416-S424, α-helix E2 is L425-A447 and the C-terminus is F448-V491 [69, 70] (figure 61).

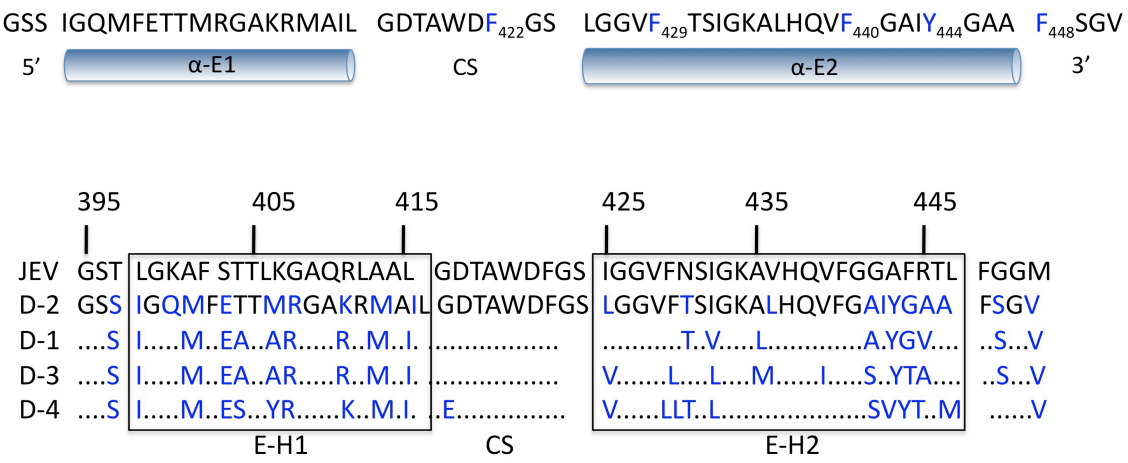

Figure 61. Diagram of Dengue MPER ∝-helices E1 and E2. **[Top]** Revised position of E1, CS, and E2 for DENV-2. The location of the five hydrophobic mutations are shown in blue. The location of F422 is in the CS region and not E2 while F448 is in the C-terminus. **[Bottom]** Multiple sequence alignment of JEV and DENV-1 through 4 showing the non-conservative residues (adapted from [97]).

Previously, F429 has been proven to be crucial in the formation of virus-like particles (VLPs), heterodimerisation and protein production [68]. When mutated to proline (to disrupt the ∝-helix) in a pSFV system, a lower rate of infectivity occurred, as well as low levels of protein expression and viral RNA production. With this mammalian system, F429A does not show reduced protein expression as seen with the Western immunoblot data and confocal immunofluorescent images of transfected PS-EK cells. F422 has also been mutated to proline, resulting in reduced viral assembly and membrane binding [68]. With F422 substituted for alanine in this series of mutations, epitope binding to 4G2 was unsuccessful. Expression of prME, as assessed by immunofluorescence imaging, was reduced but trafficking and localisation to the cytoplasm was detected. Since F448 resides outside the E2 ∝-helix, it is unlikely to disrupt conformation while the removal of side groups for F440A and Y444A mutations may not interfere with helix formation. It is likely that F429Y, F440Y, and Y444F are helix-retaining conservative mutations.

To properly view fusion and syncticial formation, mutants should be tested within an insect system in contrast with this mammalian system. Infection with dengue in mammalian cell lines does not produce multi-nucleated cells, while in *A. albopictus* cell lines, it is well-demonstrated [98, 99]. In C6/36 cell lines, fusion can be seen with high m.o.i. [100] or with low-pH culture media [101]. To complete the structural analysis of all

ten MPER ∝-helix E2 mutants, these mutations were introduced into a pSFV vector for transfection into C6/36 cells. The wild-type prME clone was transfected by *in vitro* transcription of RNA under the control of the pSFV vector. PrME expression was clearly detected. Eight of the MPER ∝-helix E2 mutants (discarding F448A/Y) need to be cloned into the full-length pSFV vector and transcribed. For comparative analysis, SDS-PAGE and Western immunoblots with expressed wt prME and mutant proteins should be run with standardized quantities. In-cell analysis with transfected C6/36 cells should be completed to quantify cell surface and cytoplasmic expression. Mutants would be imaged with immunofluorescent confocal microscopy to confirm protein expression, localisation of E and cell surface trafficking. Cells should be probed with Hoechst, WGA and 4G2/488. The molecular dye for endocytosis, pHrodo™, could also be tested. Transfection efficiencies should be calculated to compare with mammalian cells. And finally, these mutants could be tested in a C6/36-based fusion assay. A functional syncytial assay has previously been developed in the Young laboratory (J. Robinson, P. Campbell) to analyse recombinant prM and E proteins. Cells are treated with a low-pH media change for several hours to induce the E protein conformational changes that lead to fusion. After confocal microscopy image acquisition, a fusion index can be determined. The number of infected cells, the number of nuclei and syncytia are counted to calculate the fusion index (FI = 1- No of infected cells/No. of nuclei). If this fusion assay system is deployed, wild-type pSFV-prME can be compared with the MPER mutants in C6/36 cells. These results can then be related to results obtained with mammalian transfection and infection in PS-EK cells (pCI_NGCprME and NGC DENV-2).

REFERENCES

1. Brett D. Lindenbach, H.-J.T., and Charles M. Rice, *Flaviviridae: the viruses and their replication*. Fields Virology, 2007. **5th edition**: p. 1101-1152.
2. Raja Mazumder, Z.-Z.H., C. R. Vinayaka, Jose-Luis Sagripanti, Simon D. W. Frost, Sergei L. Kosakovsky Pond, Cathy H. Wu, *Computational analysis and identification of amino acid sites in dengue E proteins relevant to development of diagnostics and vaccines*. Virus Genes, 2007. **35**: p. 175-186.
3. CDC. *Epidemiology of Dengue*. [Website] 2012; Available from: http://www.cdc.gov/dengue/epidemiology/index.html.
4. Kouri, M.G.G.a.G., *Dengue: an update*. Lancet Infectious Diseases, 2002. **33**: p. 33-42.
5. Takasaki, I.K.a.T., *Dengue fever and dengue haemorrhagic fever: challenges of controlling an enemy still at large*. Reviews in Medical Virology, 2001. **11**(5): p. 301-311.
6. Kanakatte Raviprakash, G.D., Timothy Burgess and Kevin Porter, *Advances in dengue vaccine development*. Human Vaccines, 2009. **5**(8): p. 1-9.
7. Richard C Russell, B.J.C., Michael D Lindsay, John S Mackenzie, Scott A Ritchie and Peter I Whelan, *Dengue and climate change in Australia: predictions for the future should incorporate knowledge from the past*. The Medical Journal of Australia, 2009. **190**(5): p. 265-268.
8. WHO. *World Health Organisation: Dengue Fever*. 2007 January 16, 2007.
9. digest, P.-m., *Pro-med digest: Dengue*, in *Pro-Med Digest*2011.
10. Samir Bhatt, P.W.G., Oliver Brady, Jane P. Messina, Andrew W. Farlow, Catherine L. Moyes, John M. Drake, John S. Brownstein, Anne G. Hoen, Osman Sankoh, Monica F. Myers, Dylan B. George, Thaomas Jaenisch, G. R. William Wint, Cameron P. Simmons, Thomas W. Scott, Jeremy J. Farrar, & Simon I. Hay *The Global distribution and burden of Dengue*. Nature, 2013. **496**: p. 504-507.
11. Daniel P. Webster, J.F., and Sarah Rowland-Jones, *Progress towards a dengue vaccine*. Lancet Infectious Diseases, 2009. **9**: p. 678-687.
12. Scott B. Halstead, F.X.H., A. D. T. Barrett, John T. Roehrig, *Dengue virus: molecular basis of cell entry and pathogenesis, 25-27 June 2003, Vienna, Austria*. Vaccine, 2005. **23**: p. 849-856.
13. Fauci, D.M.M.a.A.S., *Emerging infectious diseases: threats to human health and global stability*. PlOS Pathogens, 2013. **9**(7): p. 1-3.
14. DVI. *Dengue Vaccine Initiative*. 2013 [cited 2013 October 11, 2013]; Available from: http://www.denguevaccines.org/vaccine-development.
15. Lauren E. Yauch, R.l.M.Z., Maya F. Kotturi, Afrina Qutubuddin, John Sidney, Bjoern Peters, Tyler R. Prestwood, Alessandro Sette, and Sujan Shresta2, *A protective role for Dengue Virus-specific CD8 T cells*. Journal of Immunology, 2009: p. 4865-4873.
16. Snowden, F.M., *Emerging and reemerging diseases: a historical perspective*. Immunological Reviews, 2008. **225**: p. 9-26.
17. Bruno Guy, M.S.a.J.L., *Development of Sanofi Pasteur tetravalant dengue vaccine*. Human Vaccines, 2010. **6**(9): p. 696-705.
18. Joseph E. Blaney, J.M.M., Brian R. Murphy, and Stephen S. Whitehead, *Recombinant, live-attenuated tetravalent dengue virus vaccine formulations*

induce a balanced, broad, and protective neutralizing antibody response against each of the four serotypes in rhesus monkeys. Journal of Virology, 2005. **79**(9): p. 5516-5528.
19. Umareddy, I., Pluquet, O., Wang, Q. Y., Vasudevan, S. G., Chevet, E., and Gu, F., *Dengue virus serotype infection specifies the activation of the unfolded protein response*. Virology, 2007. **4**: p. 91-101.
20. Schneider-Schaulies, J., *Cellular receptors for viruses: links to tropism and pathogenesis*. Journal of General Virology, 2000. **81**: p. 1413-1429.
21. Yorgo Modis, S.O., David Clements, and Stephen C. Harrison, *Structure of the dengue virus envelope protein after membrane fusion*. Nature, 2004. **427**: p. 313-319.
22. J. M. Wahlberg, R.B., J. Wilschut, and H. Garoff, *Membrane fusion of Semliki Forest virus involves homotrimers of the fusion protein*. Journal of Virology, 1992. **66**(12): p. 7309-7318.
23. Yorgo Modis, S.O., David Clements, and Stephen C. Harrison, *A ligand-binding pocket in the dengue virus envelope glycoprotein*. Proceedings of the National Academy of Science, 2003. **100**(12): p. 6986-6991.
24. Karin Stiasny, F.X.H., *Review: Flavivirus membrane fusion*. Journal of General Virology, 2006. **87**: p. 2755-2766.
25. S. L. Allison, J.S., K. Stiasny, C. W. Mandl, C. Kunz, and F. X. Heinz, *Oligomeric rearrangement of Tick-Borne Encephalitis Virus envelope proteins induced by an acidic pH*. JOURNAL OF VIROLOGY, 1995. **69**(2): p. 695-700.
26. Franz X. Heinz, S.L.A., *The machinery for flavivirus fusion with host cell membranes*. Current Opinion in Microbiology, 2001. **4**: p. 450-455.
27. Richard J. Kuhn, W.Z., Michael G. Rossmann, Sergei V. Pletnev, Jeroen Corver, Edith Lenches, Christopher T. Jones, Suchetana Mukhopadhyay, Paul R. Chipman, Ellen G. Strauss, Timothy S. Baker, and James H. Strauss, *Structure of Dengue Virus: implications for flavivirus organization, maturation, and fusion*. Cell, 2002. **108**: p. 717-725.
28. Hilde M. van der Schaar, M.J.R., Barry-Lee Waarts, , *Characterization of the early events in dengue virus cell entry by biochemical assays and single-virus tracking*. Journal of Virology, 2007. **81**(21): p. 12019-12028.
29. Suchetana Mukhopadhyay, R.K., and Michael G. Rossman, *A structural perspective of the flavivirus life cycle (review)*. Nature Reviews: Microbiology, 2005. **3**: p. 13-22.
30. Jolanda M. Smit, B.M., Izabela Rodenhuis-Zybert and Jan Wilschut, *Flavivirus cell entry and membrane fusion*. Viruses, 2011. **3**: p. 160-171.
31. Ying Zhang, W.Z., Steven Ogata, David Clements, James H. Strauss, Tomothy S. Baker, Richard J. Kuhn, and Michael G. Rossmann, *Conformational Changes of the Flavivirus E Glycoprotein*. Structure, 2004. **12**: p. 1607-1618.
32. Stephen J. Seligman, D.J.B., *The importance of being outer: consequences of the distinction between the outer and inner surfaces of flavivirus glycoprotein E*. Trends in Microbiology, 2003. **11**(3): p. 108-110.
33. Yorgo Modis, S.O., David Clements, and Stephen C. Harrison, *Variable surface epitopes in the crystal structure of Dengue Virus type 3 envelope glycoprotein*. Journal of Virology, 2005. **79**(2): p. 1223-1231.

34. Wei Zhang, P.R.C., Jeroen Corver, Peter R. Johnson, Ying Zhang, Suchetana Mukhopadhyay, Timothy S. Baker, James H. Strauss, Michael G. Rossmann and Richard J. Kuhn, *Visualization of membrane protein domains by cryo-electron microscopy of dengue virus*. Nature Structural Biology, 2003. **10**(11): p. 907-912.
35. Srinivasan, R.A.G.a.N., *Prediction of protein-protein interactions in dengue virus coat proteins guided by low resolution cryoEM structures*. BMC Structural Biology, 2010. **10**(17): p. 1-13.
36. Heidi E. Drummer, P.P., *Hepatitis C virus glycoprotein E2 contains a membrane-proximal heptad repeat sequence that is essential for E1E2 glycoprotein heterodimerization and viral entry*. The Journal of Biological Chemistry, 2004. **279**(29): p. 30066-30072.
37. Karin Stiasny, S.L.A., Juliane Schalich, and Franz X. Heinz, *Membrane interactions of the tick-borne encephalitis virus fusion protein E at low pH*. Journal of Virology, 2002. **76**(8): p. 3784-3790.
38. Kuhn, R.P.a.R.J., *Structural proteomics of dengue virus*. Current Opinion in Microbiology, 2008. **11**: p. 369-377.
39. Edwin G. Westaway, A.A.K., and Jason M. Mackenzie, *Nascent flavivirus RNA colocalized in situ with double-stranded RNA in stable replication complexes*. Virology, 1999. **258**(1): p. 108-117.
40. Marie Flamand, F.M., Magali Mathieu, Jean Lepault, Felix A. Rey, and Vincent Deubel, *Dengue virus type 1 nonstructural glycoprotein NS1 is secreted from mammalian cells as a soluble hexamer in a glycosylation-dependent fashion*. Journal of Virology, 1999. **73**(7): p. 6104-6110.
41. Jason M. Mackenzie, M.K.J., and Paul R. Young, *Immunolocalization of the Dengue Virus nonstructural glycoprotein NS1 suggests a role in viral RNA replication*. Virology, 1996. **220**(1): p. 232-240.
42. Thomas J. Chambers, D.W.M., and Charles M. Rice, *Yellow fever virus proteins NS2A, NS213, and NS4B: Identification and partial N-terminal amino acid sequence analysis*. Virology, 1989. **169**(1): p. 100-109.
43. Sven Miller, S.K., Jacomine Krijinse-Locker, Sandra Buhler, and Ralf Bartenschlager, *The non-structural protein 4A of dengue virus is an integral membrane protein inducing membrane alterations in a 2K-regulated manner*. Journal of Biological Chemistry, 2007. **282**(12): p. 8873-8882.
44. Indira Umareddy, A.C., Aruna Sampath, Feng Gu, and Subhash G. Vasudevan, *Dengue virus NS4B interacts with NS3 and dissociates it from single-stranded RNA*. Journal of General Virology, 2006. **87**: p. 2605-2614.
45. Jorge L. Muñoz-Jordán, G.G.S.-B., Maudry Laurent-Rolle, and Adolfo García-Sastre, *Inhibition of interferon signalling by dengue virus*. PNAS Microbiology 2003. **100**(24): p. 14333-14338.
46. Weissenhorn, D.J.S.a.W., *Class I and class II viral fusion protein structures reveal similar principles in membrane fusion (Review)*. Molecular Membrane Biology, 2004. **21**: p. 361-371.
47. Isabel Munoz-Barroso, K.S., Eric Hunter, and Robert Blumenthal, *Role of membrane-proximal domain in the initial stages of human immunodeficiency virus type 1 envelope glycoprotein-mediated membrane fusion*. Journal of Virology, 1999. **73**(7): p. 6089-6092.

48. J. J. Skehel, K.C., D. Steinhauer and D. C. Wiley, *Influenza fusion peptides*. Biochemical Society Transactions, 2001. **29**: p. 623-626.
49. Lukas K. Tamm, X.H., Yinling Li, and Alex L. Lai, *Structure and function of membrane fusion peptides*. Biopolymers, 2002. **66**(249-260): p. 249.
50. D. C. Wiley, J.J.S., *The structure and functions of the hemagglutinin membrane glycoprotein of influenza virus*. Annual Review Biochemistry, 1987. **56**: p. 365-394.
51. Lukas K. Tamm, J.C., and Volker Kiessling, *Membrane fusion: a structural perspective on the interplay of lipids and proteins*. Current Opinion in Structural Biology, 2003. **13**: p. 453-466.
52. Felix A. Rey, F.X.H., Christian Mandl, Christian Kunz, and Stephen C. Harrison, *The envelope glycoprotein from tick-borne encephalitis virus at 2 Å resolution*. Nature, 1995. **375**: p. 291-298.
53. Harrison, S.C., *The pH sensor for flavivirus membrane fusion*. Journal of Cell Biology, 2008. **183**(2): p. 177-179.
54. Claudia Sa´nchez-San Martı´n, C.Y.L.a.M.K., *Dealing with low pH: entry and exit of alphaviruses and flaviviruses*. Trends in Microbiology, 2009. **17**(11): p. 514-521.
55. Karin Stiasny, R.F., Karen Pangerl, Franz X. Heinz and Steven L. Allison, *Molecular mechanisms of flavivirus membrane fusion*. Amino Acids, 2009: p. 1-5.
56. Richard Fritz, K.S., and Franz X. Heinz, *Identification of specific histidines as pH sensors in flavivirus membrane fusion*. The Journal of Cell Biology, 2008. **183**(2): p. 353-361.
57. Thorsten Kampmann, D.S.M., Alan E. Mark, Paul R. Young, *The role of histidine residues in hypothesis low-pH-mediated viral membrane fusion*. Structure, 2006. **14**: p. 1481-1487.
58. Elena Zaitseva, S.-T.Y., Kamran Melikov, Sergei Pourmal, Leonid V. Chernomordik, *Dengue virus ensures its fusion in late endosomes using compartment-specific lipids*. PLOS Pathogens, 2010. **6**(10): p. 1-14.
59. Ste ´phane Bressanelli, K.S., Steven L Allison, Enrico A Stura, Stephane Duquerroy, Julien Lescar, Franz X Heinz , and Fe ´lix A Rey, *Structure of a flavivirus envelope glycoprotein in its low-pH-induced membrane fusion conformation*. The EMBO Journal, 2004. **23**: p. 728-738.
60. Aihua Zhang, M.U., Margaret Kielian, *In vitro and in vivo stuies identify important features of Dengue Virus pr-E protein interactions*. PLOS Pathogens, 2010. **6**(10): p. 1-12.
61. Karin Stiasny, C.K., Jean Lepault, Felix A. Rey, Franz X. Heinz, *Characterization of a structural internediate of flavivirus membrane fusion*. Public Library of Science Pathogens, 2007. **2**(2): p. 0191.
62. Annarita Falanga, M.C., Carlo Pedone and Stefania Galdiero, *Membrane fusion and fission: enveloped viruses*. Protein and Peptide Letters, 2009. **16**: p. 751-759.
63. Spear, A.C.S.a.P.G., *Viral glycoproteins and an evolutionary conundrum*. Science, 2006. **313**(5784): p. 177-178.
64. Jardetzky, M.B.a.T.S., *Class III viral membrane fusion proteins*. Current Opinion in Structural Biology, 2009. **19**: p. 189-196.

65. Karin Stiasny, S.L.A., Aron Marchler-Bauer, Christian Kunz, and Franz X. Heinz, *Structural requirements for low-pH-induced rearrangements in the envelope glycoprotein of tick-borne encephalitis virus* Journal of Virology, 1996. **70**(11): p. 8142-8147.
66. Nerea Huartea, M.L., Renate Kunert, José L. Nieva, *Lipid modulation of membrane-bound epitope recognition and blocking by HIV-1 neutralizing antibodies*. FEBS Letters, 2008. **582**: p. 3798-3804.
67. Robinson, J.R., *Functional Analysis of key domains of the dengue virus prM and E proteins in membrane fusion*, in *School of Chemistry and Molecular Biosciences*2003, University of Queensland, St. Lucia.
68. Su-Ru Lin, G.Z., Szu-Chia Hsieh, Min Qing, Wen-Yang Tsai, Pei-Yong Shi, and Wei-Kung Wang, *The helical domains of the stem region of dengue virus envelope protein are involved in both virus assembly and entry*. Journal of Virology, 2011. **85**(10): p. 5159-5171.
69. Aaron G. Schmidt, P.L.Y., Stephen C. Harrison, *Peptide inhibitors of Dengue-Virus entry target a late-stage fusion intermediate*. PLOS Pathogens, 2010. **6**(4): p. 1-11.
70. Aaron G. Schmidt, P.L.Y.a.S.C.H., *Peptide inhibitors of Flavivirus entry derived from the E protein stem*. Journal of Virology, 2010. **84**(24): p. 12549-12554.
71. Aaron G. Schmidt, K.L., Priscilla L. Yang, Stephen C. Harrison, *Small molecular inhibitors of dengue-virus entry*. PLOS Pathogens, 2012. **8**(4): p. 1-10.
72. Heidi E. Drummer, I.B., Anne L. Maerz, and Pantelis Poumbouris, *A conserved Gly436-Trp-Leu-Ala-Gly-Leu-Phe-Tyr motif in hepatitis C virus glycoprotein E2 is a determinant of CD81 binding and viral entry*. Journal of Virology, 2006. **80**(16): p. 7844-7853.
73. Bartosch, B., Dubuisson, J., Cosset, F., *Infectious Hepatitis C virus pseudo-particles containing functional E1–E2 envelope protein complexes*. The Journal of Experimental Medicine, 2003. **197**(5): p. 633-642.
74. Bates, R.J.W.-L.a.P., *Characterization of Ebola virus entry by using pseudotyped viruses: identification of receptor-deficient cell lines*. Journal of Virology, 1998. **72**(4): p. 3155-3160.
75. Tanja Schnell, P.F., Melanie Wirth, Jan Munch, and Klaus Uberla, *Development of a self-inactivating, minimal lentivirus vector based on simian immunodeficiency virus*. Human Gene Therapy, 2000. **11**: p. 439-447.
76. Tsanan Giroglou, J.C.J., Holger Rabenau, Christian Drosten, Harald Schwalbe, Hans Wilhelm Doerr, and Dorothee von Laer, *Retroviral Vectors Pseudotyped with Severe Acute Respiratory Syndrome Coronavirus S Protein*. JOURNAL OF VIROLOGY, 2008. **78**(17): p. 9007-9015.
77. Barbara Mitta, M.R., Martin Fussenegger, *Detailed design and comparative analysis of protocols for optimized production of high-performance HIV-1 derived lentiviral particles*. Metabolic Engineering, 2005. **7**: p. 426-436.
78. Hiroyuki Miyochi, U.B., Masayo Takahashi, Fred H. Gage, and Inder M. Verma, *Development of a self-inactivating lentivirus vector*. Journal of Virology, 1998. **72**(10): p. 8150-8157.
79. Ekaterina Klimatcheva, J.D.R.a.V.P., *Lentiviral vectors and gene therapy*. Frontiers in Bioscience, 1999. **4**: p. 481-496.

80. Natacha Klages, R.Z., and Didier Trono, *A stable system for the high-titer production of multiply attenuated lentiviral vectors*. Molecular Therapy, 2000. **2**(2): p. 170-176.
81. Znamenskiy, P. *Packaging and infection by a lentiviral vector*. 2006 [cited 2012 2 May 2012]; Available from: http://en.wikipedia.org/wiki/File:Lentiviral_vector.png.
82. Malcolm, W.W.a.B.A., *Two-Stage PCR protocol allowing introduction of multiple mutations, deletions and insertions using QuikChange site-directed mutagenesis*. Biotechniques, 1999. **26**: p. 680-682.
83. Heidi E. Drummer, I.B., Pantelis Poumbouris, *Mutagenesis of a conserved fusion peptide-like motif and membrane-proximal heptad-repeat region of hepatitis C virus glycoprotein E1*. Journal of General Virology, 2007. **88**: p. 1144-1148.
84. Sharookh B. Kapadia, H.B., Thomas Baumert, Jane A. McKeating and Francis V. Chisari, *Initiation of Hepatitis C virus infection is dependent on cholesterol and cooperativity between CD81 and scavenger receptor B type I*. Journal of Virology, 2007. **81**(1): p. 374-383.
85. Yann Ciczora, N.C., Franc¸ois Penin, Eve-Isabelle Pe´cheur, and Jean Dubuisson, *Transmembrane domains of Hepatitis C virus envelope glycoproteins: residues involved in E1E2 heterodimerization and involvement of these domains in virus entry*. Journal of Virology, 2007. **81**(5): p. 2372-2381.
86. Hsiao-Fen Li, C.-H.H., Li-Shuang Ai, Chin-Kai Chuang and Steve SL Chen, *Mutagenesis of the fusion peptide-like domain of hepatitis C virus E1 glycoprotein: involvement in cell fusion and virus entry*. Journal of Biomedical Science, 2009. **16**(89): p. 1-18.
87. Anna Albecka, R.M., Thomas Krey, Alexander W. Tarr, Eric Diesis, Jonathan K. Ball, Ve´ronique Descamps, Gilles Duverlie, Felix Rey, Franc¸ois Penin, Jean Dubuisson, *Identification of new functional regions in Hepatitis C Virus envelope glycoprotein E2*. Journal of Virology, 2010. **85**(4): p. 1777-1792.
88. Kathleen McCaffrey, I.B., Kevin Tewierek, Mark L. Edmunds, Pantelis Poumbourios and Heidi E. Drummer, *Role of conserved cysteine residues in Hepatitis C Virus glycoprotein E2 folding and function*. Journal of Virology, 2012. **86**(7): p. 3961-3974.
89. Kathleen McCaffrey, H.G., Irene Boo, Pantelis Poumbourios, Heidi E. Drummer, *The variable regions of Hepatitis C Virus glycoprotein E2 have an essential structural role in glycoprotein assembly and virion infectivity*. Journal of General Virology, 2010. **92**: p. 112-121.
90. R. Liu, R., Tewari, M., Kong, R., Zhang, R., Ingravalloa, P. and Ralston R., *A peptide derived from Hepatitis C virus E2 envelope protein inhibits a post-binding step in HCV entry*. Antiviral Research, 2010: p. XX.
91. Heidi E. Drummer, A.L.M., and Pantelis Poumbouris, *Cell surface expression of functional hepatitis C virus E1 and E2 glycoproteins*. Federation of European Biochemical Societies, 2003. **546**: p. 385-390.
92. Mariko Kobayashi, M.C.B., Theodore Bercot, and Ila R. Singh, *Functional analysis of hepatitis C virus envelope proteins, using a cell-cell fusion assay*. Journal of Virology, 2006. **80**(4): p. 1817-1825.

93. Anne Op De Beeck, C.c.V., Birke Bartosch, Yann Ciczora, Laurence Cocquerel, Zhenyong Keck, Steven Foung, Francois-Loïc Cosset, and Jean Dubuisson, *Characterization of Functional Hepatitis C Virus Envelope Glycoproteins*. Journal of Virology, 2004. **78**(6): p. 2994-3002.
94. M. M. F. Alen, S.J.F.K., T. D. Burghgraeve, J. Balzarini, J. Neyts, and D. Schols, *Antiviral activity of carbohydrate-binding agents and the role of DC-SIGN in dengue virus infection*. Virology, 2009. **387**(1): p. 67-75.
95. MesserWoland. *Biological Cell*. [Website] 2006; 15 October 2006:[Available from: http://commons.wikimedia.org/wiki/File:Biological_cell.svg.
96. Invitrogen. *pHrodo™ Indicators for Phagocytosis, Endocytosis, and Internalization*. 2013 [cited 2013 29 March 2013]; Available from: http://www.invitrogen.com/site/us/en/home/brands/Molecular-Probes/Key-Molecular-Probes-Products/pHrodo-indicators.html.
97. Chang, D.E.P.a.G.-J.J., *Secretion of noninfectious dengue virus-like particles and identification of amino acids in the stem region involved in intracellular retention of envelope protein*. Virology, 2005. **333**: p. 239-250.
98. Olson, P.S.a.L.C., *Replication of Dengue Virus Type 2 in Aedes albopictus Cell Culture*. Journal of Virology, 1973. **12**(2): p. 275-283.
99. Paul, E.C.S.J.a.F.J., *Syncytia formation of mosquito cell cultures mediated by type 2 dengue virus*. Virology, 1969. **38**(3): p. 482-485.
100. Peter L. Summers, W.H.C., Maria M. Ruiz, Tatsuo Hase, and Kenneth H. Eckels, *Flaviviruses can mediate fusion from without in Aedes albopictus mosquito cell cultures*. Virus Research, 1989. **12**(4): p. 383-392.
101. Stollar, V.B.R.a.V., *Low pH-induced cell fusion in flavivirus-infected Aedes albopictus cell cultures*. Journal of General Virology, 1990. **71**: p. 1845-1885.

APPENDIX 1.